A Szilikátipari Tudományos Egyesület lapja

építőanyag

Journal of Silicate Based and Composite Materials

A TARTALOMBÓL:

- The effects of partially replacing cement by glass waste powder on concrete properties
- Evaluation of chloride resistance of silica fume and glass waste MWCNT-geopolymer composite
- Thermal conductivity of wood-plastic composites as insulation panels: theoretical and experimental analysis
- Effect of organoclay reinforcement on the mechanical and thermal properties of unsaturated polyester resin composites
- Rheological properties of a slip based on synthesized slavsonite and properties of ceramic materials based on it
- Shear behaviour of silicate-based structural adhesives for timber

2021/2

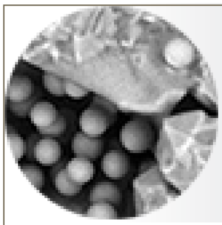

We are pleased to announce the organization of

ec-siliconf2

THE 2ND EUROPEAN CONFERENCE ON SILICON AND SILICA BASED MATERIALS

to be held in Hotel Palota in Miskolc-Lillafüred, Hungary, in October 4-8, 2021

The **ec-siliconf2** conference will be held in the wonderful palace of **Hotel Palota** in the exceptionally beautiful environment of **Beech Mountain** in **Miskolc-Lillafüred** in **Hungary**. In 2019 in the previous conference scientists had participated from **21** countries of **Asia, Europe, North- and South America** and **Africa**.

THE CONFERENCE SESSIONS

SESSION 1: Silicon and silica in inorganic and molecular chemistry
SESSION 2: Metallic silicon and silicon as an alloying agent
SESSION 3: Silicon (Si) and silica (SiO2) in medicine, therapy and health
SESSION 4: Silicon in micro and nanoelectronics and devices
SESSION 5: Silicon and silica in functional materials
SESSION 6: Silicon and silica in polymers
SESSION 7: Silicon and silica in ceramics and composites
SESSION 8: Silicon and silica in construction materials and glass
SESSION 9: Silicon and silica in biological systems and technologies
SESSION 10: Silicon and silica in smart materials and technologies
SESSION 11: Silicon and silica in minerals and rocks
SESSION 12: Testing and characterization methods, tools and errors
SESSION 13: Other results in research and development of silicon and silica and materials contain of them
SESSION 14: Other results in processing and application of silicon and silica and materials contain of them
SESSION 15: Miscellaneous in silicon and silica materials science

Registration abstract submission, and further information are available in:
www.ec-siliconf.eu

építőanyag

2021/2

Journal of Silicate Based and Composite Materials

TARTALOM

CONTENT

A finomkerámia-, üveg-, cement-, mész-, beton-, tégla- és cserép-, kő- és kavics-, tűzállóanyag-, szigetelőanyag-iparágak szakmai lapja
Scientific journal of ceramics, glass, cement, concrete, clay products, stone and gravel, insulating and fireproof materials and composites

Szerkesztőbizottság ▪ Editorial board
Prof. Dr. GÖMZE A. László – elnök/president
GYURKÓ Zoltán – főszerkesztő/editor-in-chief
Dr. habil. BOROSNYÓI Adorján – vezető szerkesztő/senior editor
WOJNÁROVITSNÉ Dr. HRAPKA Ilona – örökös tiszteletbeli felelős szerkesztő/honorary editor-in-chief
TÓTH-ASZTALOS Réka – tervezőszerkesztő/design editor

Tagok ▪ Members
Prof. Dr. Parvin ALIZADEH, Dr. Benchaa BENABED, BOCSKAY Balázs, Prof. Dr. CSŐKE Barnabás, Prof. Dr. Emad M. M. EWAIS, Prof. Dr. Katherine T. FABER, Prof. Dr. Saverio FIORE, Prof. Dr. David HUI, Prof. Dr. GÁLOS Miklós, Dr. Viktor GRIBNIAK, Prof. Dr. Kozo ISHIZAKI, Dr. JÓZSA Zsuzsanna, KÁRPÁTI László, Dr. KOCSERHA István, Dr. KOVÁCS Kristóf, Prof. Dr. Sergey N. KULKOV, Dr. habil. LUBLÓY Éva, MATTYASOVSZKY ZSOLNAY Eszter, Dr. MUCSI Gábor, Dr. Salem G. NEHME, Dr. PÁLVÖLGYI Tamás,Prof. Dr. Tomasz SADOWSKI, Prof. Dr. Tohru SEKINO, Prof. Dr. David S. SMITH, Prof. Dr. Bojja SREEDHAR, Prof. Dr. SZÉPVÖLGYI János, Prof. Dr. SZŰCS István, Prof. Dr. Yasunori TAGA, Dr. Zhifang ZHANG

Tanácsadó Testület ▪ Advisory board
FINTA Ferenc, KISS Róbert, Dr. MIZSER János

A folyóiratot referálja · The journal is referred by:

A folyóiratban lektorált cikkek jelennek meg.
All published papers are peer-reviewed.
Kiadó · Publisher: Szilikátipari Tudományos Egyesület (SZTE)
Elnök · President: ASZTALOS István
1034 Budapest, Bécsi út 120.
Tel.: +36-1/201-9360 ▪ E-mail: epitoanyag@szte.org.hu
Tördelő szerkesztő · Layout editor: NÉMETH Hajnalka
Címlapfotó · Cover photo: GYURKÓ Zoltán

Hirdetési árak 2021 ▪ ADVERTISING RATES 2021:

B2 borító színes · cover colour	76 000 Ft	304 EUR
B3 borító színes · cover colour	70 000 Ft	280 EUR
B4 borító színes · cover colour	85 000 Ft	340 EUR
1/1 oldal színes · page colour	64 000 Ft	256 EUR
1/1 oldal fekete-fehér · page b&w	32 000 Ft	128 EUR
1/2 oldal színes · page colour	32 000 Ft	128 EUR
1/2 oldal fekete-fehér · page b&w	16 000 Ft	64 EUR
1/4 oldal színes · page colour	16 000 Ft	64 EUR
1/4 oldal fekete-fehér · page b&w	8 000 Ft	32 EUR

Az árak az áfát nem tartalmazzák. · Without VAT.

A hirdetési megrendelő letölthető a folyóirat honlapjáról.
Order-form for advertisement is avaliable on the website of the journal.

WWW.EPITOANYAG.ORG.HU
EN.EPITOANYAG.ORG.HU

Online ISSN: 2064-4477
Print ISSN: 0013-970x
INDEX: 2 52 50 ▪ 73 (2021) 39–82

Az SZTE támogató tagvállalatai
Supporting companies of SZTE

3B Hungária Kft. ▪ Akadémiai Kiadó Zrt. ▪ ANZO Kft.
Baranya-Tégla Kft. ▪ Berényi Téglaipari Kft.
Beton Technológia Centrum Kft. ▪ Budai Tégla Zrt.
Budapest Keramia Kft. ▪ CERLUX Kft.
COLAS-ÉSZAKKŐ Bányászati Kft. ▪ Daniella Ipari Park Kft.
Electro-Coord Magyarország Nonprofit Kft.
Fátyolüveg Gyártó és Kereskedelmi Kft.
Fehérvári Téglaipari Kft.
Geoteam Kutatási és Vállalkozási Kft.
Guardian Orosháza Kft. ▪ Interkerám Kft.
KK Kavics Beton Kft. ▪ KŐKA Kő- és Kavicsbányászati Kft.
KTI Nonprofit Kft. ▪ Kvarc Ásvány Bányászati Ipari Kft.
Lighttech Lámpatechnológiai Kft.
Maltha Hungary Kft. ▪ Messer Hungarogáz Kft.
MINERALHOLDING Kft. ▪ MOTIM Kádkő Kft.
MTA Természetíudományi Kutatóközpont
O-I Hungary Kft. ▪ Pápateszéri Téglaipari Kft.
Perlit-92 Kft. ▪ Q & L Tervező és Tanácsadó Kft.
QM System Kft. ▪ Rákosy Glass Kft.
RATH Hungária Tűzálló Kft. ▪ Rockwool Hungary Kft.
Speciálbau Kft. ▪ SZIKKTI Labor Kft.
Taurus Techno Kft. ▪ Tungsram Operations Kft.
Witeg-Kőporc Kft. ▪ Zalakerámia Zrt.

Vol. 73, No. 2

The effects of partially replacing cement by glass waste powder on concrete properties

Antonio BOUTY ▪ City University, POB. 676, Muhieddine Makkouk Boulevard, Tripoli, Lebanon ▪ Antonio.bouty@outlook.com
Farah HOMSI ▪ ESIB, Université Saint-Joseph De Beirut Mar Roukos, POB. 11-154, Riad El Solh, Beyrouth, Lebanon ▪ farah.homsi@usj.edu.lb

Érkezett: 2020. 07. 21. ▪ Received: 21. 07. 2021. ▪ https://doi.org/10.14382/epitoanyag-jsbcm.2021.7

Abstract

The cement production causes different types of pollution in addition to the high amount of energy needed for the manufacturing process, starting by the site extraction and ending by the factory production; at the same time millions of tons of glass waste are dumped yearly at landfills. This research verifies the possibility of partially replacing cement by glass waste powder (GWP) in new concrete mixes. For this purpose, two different concrete mixes having compressive strengths of 25 MPa and 32 MPa were made with 0%, 10%, 15%, 20% and 25% of GWP as a partial replacement of cement. The properties of fresh concrete mixes were determined by the slump, air content and flow table tests. Concerning the tests on hardened concrete, the compressive strength test was carried out on cylindrical specimens at 7, 14 and 28 days in addition to the water absorption and the tensile strength tests at 28 days. As a result, the partial replacement of cement by GWP showed no clear effect on the properties of the fresh concrete mixes. Whereas, 10% GWP in 25MPa concrete mix gave higher compressive and tensile strengths at 28 days and increased the moisture content; and 15% GWP in 32 MPa concrete mix gave the higher compressive strength at 28 days but decreased the tensile strength and the moisture content.

Keywords: recycled glass, environment, compressive strength, fresh concrete properties, cement production, sustainability
Kulcsszavak: újrahasznosított üveg, környezet, nyomószilárdság, friss beton tulajdonságok, cementgyártás, fenntarthatóság

Farah HOMSI
was born in 1984, she received a diploma in Civil Engineering from the Lebanese University in 2007, a Master's degree in Geological, Civil and Environmental Engineering from Bordeaux 1 University in 2008 and a Ph.D. degree in civil Engineering from Ecole Centrale de Nantes in 2011. From September 2019, she is a Full-time Assistant Professor at the department of Civil and Environmental Engineering at the Higher School of Engineering at Saint Joseph's University, teaching Construction Materials, General Construction Procedures, Traffic Engineering, Road and Pavement Engineering. Between February 2017 and August 2019, she was an Assistant Professor at the Civil Engineering Department at City University and the Lebanese American University. From September 2012 till January 2017, she was a Full-time Assistant Professor at the Department of Civil and Environmental Engineering in Beirut Arab University, teaching Transportation Planning and Traffic Engineering, Highway Engineering, Elementary Structural Analysis, Construction Materials and Mechanics of Materials. She was also the Coordinator of the Civil and Environmental Engineering Department, and the Academic Coordinator of the Faculty of Engineering. From September 2011 to August 2012, she was a Full-time Assistant Professor at the Department of Civil and Environmental Engineering in Mechanics and Engineering Institute (I2M), Bordeaux I University in France, teaching Pavement Design, Computer Aided Design, Soil mechanics and Construction Materials. She received the Young Researchers' prize: René Houpert, from the French Academic Association of Civil Engineering (AUGC), in 2011.

Antonio BOUTY
was born in 1995, he received a Master's degree in Civil and Environmental Engineering from City University in 2019. From March 2020, he is enrolling in the master's program of Building's Retrofitting at the department of Civil Engineering at Università degli Study di Genova (Genova, Italy).Between October 2019, and February 2020, he was a Part-time University Instructor at the department of Civil and Environmental Engineering at City University, teaching Construction Materials, and examining graduating students' projects.

1. Introduction

Lebanon suffers from specific and deep-rooted problems affecting waste collection, waste treatment and disposal of municipal solid waste. Since 1997, the waste sector in Lebanon has operated under an emergency municipal solid waste management plan, which ended in July 2015. This culmination in the current national trash crisis was mainly triggered by the premature closure of Lebanon's largest sanitary landfill located in Naameh in July 2015. These problems have led to significant social, economic, and environmental difficulties. In Lebanon, open dumping, and open burning of municipal waste is a common and widely accepted practice. As the case of Lebanon, most of the developing countries are facing shortage of post consumer's disposal waste sites that is becoming a very serious problem. For this reason, regenerating and using waste products as resources is necessary to prevent environmental pollution. According to GMI (Green Med Initiative), Lebanon produces around 2.04 million tons of municipal solid waste per year and glass represents 3.5% of this amount [1].

In Lebanon, the cement industry is the largest source of carbon dioxide emission; in addition, cement factories are also responsible for the emission of Nitrogen Oxide, Sulfur Monoxide, and Carbon Monoxide in the atmosphere. High concentrations of these pollutants in the atmosphere have detrimental effects on the human body and also cause environmental problems such as ozone depletion, water quality deterioration and acid rain [2].

One of the possible solutions that might minimize the environmental impacts of cement production and glass waste dumped at landfills, is to partially replace cement by glass waste powder in new concrete mixtures. On the one hand, it helps reducing the toxic gases resulting from the manufacturing process of cement and on the other hand, it valorizes glass waste instead of being dumped in landfills. Since glass is mainly composed of silica, when it is milled down into micro size particles, it is expected to undergo pozzolanic reactions with cement hydrates, forming secondary Calcium Silicate Hydrate (C-S-H) that provide strength for the concrete mix.

To study the mechanical properties of concrete when neon glass, brown glass, and green glass partially replace cement, [3] chose a design compressive strength of 35 MPa to be achieved at 28 days, with three different replacement ratios of cement by each type of glass (11%, 13% and 15%). Their results have pointed out that the compressive strength increases proportionally with curing process because the hydration process is continuous until getting the full strength of concrete; the highest compressive strength that appeared at 28 days was

31.75 MPa with 13% replacement of cement by neon glass. The results of splitting tensile strength tests showed that the splitting tensile strengths of the three different types of glass were greater than that of the control concrete mix, especially for green glass where the higher value was recorded at 13% replacement. The results also showed that the splitting tensile strength increased gradually at 11% and 13% for neon, green, and brown glass but decreased at 15% for all the three types of glass.

[4] tested four different replacement ratios of cement by glass waste powder (5%, 10%, 15%, 20% and 25%) in order to achieve a target compressive strength of 35 MPa. The difference in compressive strengths between the control mix and the mix with 25% glass replacing cement at 180 and 365 days were further reduced and provided similar mean compressive strengths. At the age of 180 and 365 days, the 20% replacement of cement by glass gave 10% and 14% respectively higher strengths than the control concrete mix. The results revealed that an increase in the replacement ratio of glass resulted in a slight increase in the mortar flow while a minor effect on concrete workability was noted. In addition, the results have shown that the compressive strength was decreasing with the addition of glass powder in recycled glass mortar and concrete, but gave better strength compared to control samples at later age.

[5] took the waste bear bottles and soda lime glass and transformed them into powder of 75 μm diameter to study the pozzolanic reaction of glass powder for up to 60% cement replacement and its influence on the microstructure of cement paste, which has not been investigated before. The design compressive strength in this study was 48 MPa and four percentages of cement were replaced by glass waste powder (15%, 30%, 45% and 60 % by weight of cement). As a result, the rate and the total heat generated during the hydration consistently decreased with higher glass powder content due to the dilution of cement in the mix. Concerning the compressive strength at 28 days, the 30% replacement of cement by glass waste powder gave 49 MPa (the highest compressive strength), whereas its compressive strength was 55 MPa at 91 days. The results have revealed that this increase in later age strength was not observed for concrete in which more than 30% cement is replaced by glass waste powder. Therefore, there is an upper limit for cement replacement level, beyond which no further pozzolanic reaction of Glass Waste Powder (GWP) can occur; this replacement level is lower than 30%.

[6] has summarized in her research entitled "Performance of lamp glass waste powder (LGWP) as supplementary cementitious material (SCM) – viscosity and electrical conductivity" the experimental results of a laboratory test series carried out on cement mortar specimens, in which two different lamp glass waste powders were used as cement component: the incandescent light bulb borosilicate glass waste cullet powder (LGWP1) and the fluorescent lamp tube glass waste cullet powder (LGWP2). Patricia had demonstrated that Portland cement substitution with lamp glass waste powders at a level of 30% is possible without any strength loss, moreover, the addition of superplasticizer admixture led to an increase in compressive strength by 15-17% in comparison to the control mortars.

[7] substituted the cement with waste glass powder at levels of 20% or 30% per mass. It was demonstrated that the waste glass powder addition improves the workability of fresh pastes and can be effectively used as cement replacement for compressive strength. It was also demonstrated that the particle size of the waste glass powder (specific surface area) has a stronger influence on the effectiveness of the cement replacement than the chemical composition. The effectiveness of the cement replacement increases as the specific surface area increases.

The results in the literature review showed promising results in terms of the effect of partial replacing the cement by glass waste powder in new concrete mixes and motivated the researchers to undergo an experimental study to analyze the GWP generated in Lebanon and evaluate its effects on the fresh and hardened properties of concrete.

2. Experimental plan

In this study, two different concrete mixes having compressive strengths of 25 MPa and 32 MPa were performed with different replacement ratios of cement by glass waste powder, with reference to the absolute volume method [8]. These two compressive strengths were taken in order to try if possible to not limit our uses only by the 25 MPa concrete mix in all the structural elements of a real life project, especially in high-rise buildings where there is a need to increase the compressive strength of some beams and columns in some stories instead of enlarging there sections, which the architect might not agree on. The different percentages of cement that were replaced by the glass waste powder were the following: 0%, 10%, 15%, 20% and 25%. This resulted in 10 different concrete mixes that were prepared and tested in the laboratory. The maximum replacement ratio was limited by 25% due to the crushing method of the glass that takes a lot of time to give the wanted particles size.

The tests conducted on fresh concrete included the slump test, flow table test, and the air content test. Concerning the hardened concrete tests, the compressive strength test was performed to obtain the compressive strength; the concrete specimens were crushed at 7, 14 and 28 days with three specimens at each age; therefore, nine specimens were tested for the compressive strength [9], and one additional specimen was tested for the indirect tensile strength test [10]. In total 50 cylinders of 150 mm diameter and 300 mm height were prepared for each concrete mix. Furthermore, the water absorption test was conducted to evaluate the effect of inclusion of glass powder on the porosity of concrete [11].

3. Materials

3.1 Cement

The ordinary Portland cement used is fabricated by Holcim (Liban) S.A.L, according to the Lebanese specifications LIBNOR (NL 53:1999) for the cement PA-L, 42.5. The specific gravity and the density were found to be 3.15 and 1551 kg/m^3 respectively [8].

3.2 Glass

The chemical analysis by Energy Dispersive X- Ray Fluorescence Spectrometer (ARL-9800 XP) of the glass waste powder and Portland cement showed in *Fig. 1*, indicates that the waste glass collected from Golden Glass Company located at Al-Badawi / North Lebanon, has a high percentage of silica and has almost the same content of ordinary Portland cement but with different percentages. The glass was crushed using the Los Angeles machine in order to minimize the particles size to less than 75 µm (see *Fig. 2*). Crushing 8 kg of glass waste into the Los Angeles machine took six hours and resulted in approximately 3 kg of glass powder of less than 75 µm particles size.

The density of the GWP was determined to be 1200 kg/m^3, by dividing the mass of the glass powder filled in a cylinder by its volume; in addition, using the Chatelier apparatus, the specific gravity of the GWP was calculated to be 2.75 [8].

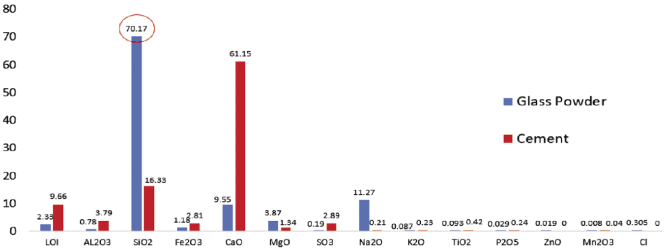

Fig. 1 Comparison between the chemical composition of the glass waste powder and Portland cement
1. ábra Az üveghulladék por és a portlandcement kémiai összetételének összehasonlítása

Fig. 2 Glass particles reduced from 30 mm to less than 75 µm
2. ábra Üveg részecskék porítása 30 mm-es méretről kevesebb mint 75 µm-re

3.3 Aggregates

The used fine aggregates (sand) have a fineness modulus of 2.89, specific gravity of 2.77, and water absorption of 3.09%. While the coarse aggregates used have a specific gravity and absorption of 2.46 and 2.41 respectively [8].

4. Experimental results and discussion

4.1 Fresh concrete properties

The partial replacement of cement with glass powder showed no clear effect on the results of the slump test in both, 25 MPa and 32 MPa concrete mixes. The slump results were very close and within the target values (25 mm-75 mm). The 20% GWP in 25 MPa concrete mix, resulted in the highest level of slump (75 mm), showing an advantage of improving the workability when partially replacing cement with waste glass powder. This partial replacement was however not efficient for the compressive strength (*Fig. 3*). On the other hand, the results represented in *Fig. 4* show that the GWP at 10% and 15% resulted in the highest slump in the concrete mix of 32 MPa (75 mm).

Similarly, the results of the air content test showed no clear effect of the glass powder on the air content in fresh concrete for both concrete grades, as the obtained results were close to the calculated air content for non-air entrained concrete, and within the percentage of air calculated for the control mixes see *Fig. 3* and *Fig. 4*.

The results of the flow table test showed an increase in the flow percentage when the percentage of glass waste powder increase in the 25 MPa concrete mix (*Fig. 3*), while as shown in *Fig. 4*, no clear effect was recorded for 32 MPa concrete mix.

Fig. 3 Results of slump, flow table and air content tests (25MPa Concrete Mix)
3. ábra Roskadás-, terülés- és légtartalom vizsgálat eredményei (25 MPa beton keverék)

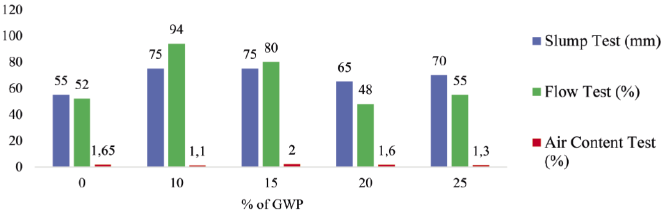

Fig.4 Results of slump, flow table and air content tests (32MPa Concrete Mix)
4. ábra Roskadás-, terülés- és légtartalom vizsgálat eredményei (32 MPa beton keverék)

4.2 Hardened concrete properties

For the 25 MPa concrete mix, the results show that the compressive strength of the concrete cylinders at 7, 14 and 28 days decrease with the increase of the % of GWP. However, for a replacement ratio of 10%, an average compressive strength of 25.6 MPa was achieved, exceeding by that the designed compressive strength at 28 days (*Fig. 5*). For the 32 MPa concrete grade, the results showed similar trends, except that a higher compressive strength was observed with a replacement ratio of 15% compared to 10%.Therefore, the use of 15% GWP as a replacement of cement represent the optimal replacement ratio without affecting the compressive strength of the design mix at the age of 28 days (*Fig. 6*).

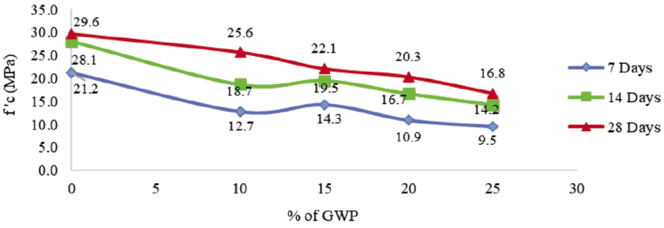

Fig. 5 Evolution of the compressive strength of 25 MPa concrete mix for 7, 14 and 28 days
5. ábra 25 MPa-os betonkeverék nyomószilárdságának alakulása 7, 14 és 28 napos korban

Concerning the tensile strength test, the 10% replacement of cement by GWP in 25 MPa concrete mix increased the tensile strength of the control mix by 0.4 MPa (from 2.4 MPa to 2.8 MPa). In contrary, the tensile strength test of 32 MPa concrete mix, showed no values above 3 MPa (the tensile strength of the control mix), where the results obtained showed a decrease in the tensile strength when the percentage of replacement of cement by GWP increased (see *Fig. 7*).

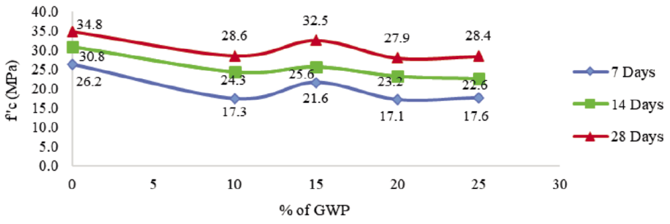

Fig. 6 Evolution of the compressive strength of 32 MPa concrete mix for 7, 14 and 28 days
6. ábra 32 MPa-os betonkeverék nyomószilárdságának alakulása 7, 14 és 28 napos korban

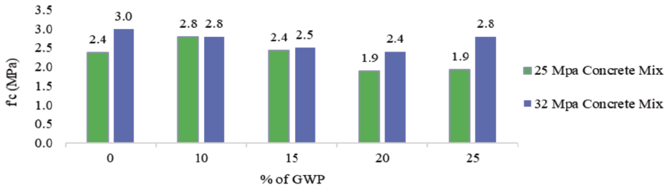

Fig. 7 Results of the tensile strength test of 25 and 32 MPa concrete mixes
7. ábra A 25 és 32 MPa-os beton keverékek húzószilárdság vizsgálatának eredményei

In terms of durability, the water absorption of the 25 MPa concrete mix with 10% GWP increased by 17.8% compared to the control mix. Consequently, construction in cold regions are not encouraged for such concrete use. On the contrary, for the 32 MPa concrete mixes, the water absorption increased when GWP content increased; the concrete mix with 15% GWP has lowered the water absorption of the control mix (32 MPa) from 2.69% to 2.64%, whereas 10% GWP increased this percentage to 3.18% (*Fig. 8*).

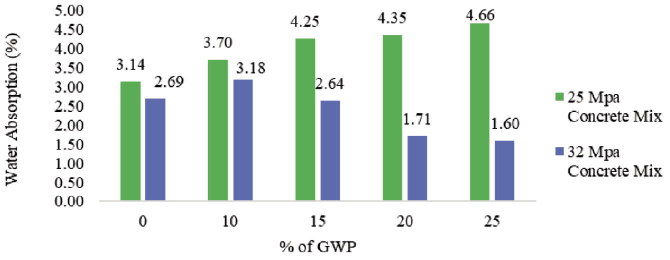

Fig. 8 Results of water absorption test of 25 and 32 MPa concrete mixes
8. ábra A 25 és 32 MPa-os beton keverékek vízfelvétel vizsgálatának eredményei

5. Conclusions and outlook

In conclusion, this research had revealed that reusing 10% and 15% of Glass Waste Powder in 25 MPa and 32 MPa concrete grades respectively has no clear effect on the air content in fresh concrete, but provides a very good workability, as the given slump values were within the target range that was 25mm-75mm in both concrete mixes. Concerning the flow table test, the flow percentage increased from 68% to 84% and from 52% to 80% in 25 MPa and 32 MPa concrete grades respectively.

In term of strength, the results showed that the concrete with Glass Waste Powder averagely has lower compressive strength compared to the control mix at 7, 14 and 28 days in both concrete grades. However, the 10% and 15% of Glass Waste Powder that replaced the cement in 25 MPa and 32 MPa concrete mixes respectively, exceeded the target compressive strength of 25 MPa by 2.4% and 32 MPa by 1.6%.

Therefore, reusing waste materials such glass in new concrete mixes could be a possible solution to save thousands of tons of waste glass from being dumped yearly at landfills and to minimize the environmental effects of cement production and solid waste crisis that Lebanon is suffering from.

However, to standardize the usage of GWP in concrete, there is a need to additionally conduct microscopic and hydration studies for the qualitative assessment and quantitative analysis of hydration and pore fillers according to the physical properties and the chemical compositions of waste glass powder.

Acknowledgments

The first author would like to express his sincere thanks to the Department of Civil and Environmental Engineering at City University for funding this research.

In addition, the authors acknowledge Al-Sabeh Laboratories who conducted the chemical analysis of the glass powder using the Energy Dispersive X- Ray Fluorescence Spectrometer (ARL-9800 XP).

Furthermore, the first author thanks the head of maintenance department of City University, Eng. Wassim Tarraf, and his team who have facilitated the laboratory experimentation.

References

[1] Initiative, G. T. (2014): Country Report on the Solid Waste Management in Lebanon. Deutsche Gesellschaft für Internationale Zusammenarbeit (GIZ) GmbH. Retrieved from www.moe.gov.lb

[2] Ecocentra (2016): The cement import "ban" and pollution. ecocentra word press. Retrieved 7 4, 2016, from https://www.google.com/url?sa=t&source=web&rct=j&url=https://ecocentra.wordpress.com/2016/08/04/the-cement-import-ban-and-pollution/amp/&ved=2ahUKEwjNi_a6tYntAhW8TxUIHZt-A3QQFjAAegQIBBAB&usg=AOvVaw30o_xEkklmROPN13E7wCP7&ampcf=1

[3] Aseel B. AL-Zubaid a, K. M. (2017): Study The Effect of Recycled Glass on The Mechanical Properties of Green Concrete. International Conference on Technologies and Materials for Renewable Energy, Environment and Sustainability. Beirut. https://doi.org/10.1016/j.egypro.2017.07.095

[4] G. M. Sadiqul Islam, M. H. (2016): Waste glass powder as partial replacement of cement for sustainable concrete practice. International Journal of Sustainable Built Environment, 37-41. https://doi.org/10.1016/j.ijsbe.2016.10.005

[5] Hongjian Du, K. H. (2014): Waste Glass Powder as Cement Replacement in Concrete. Advanced Concrete Technology, 12. https://doi.org/10.3151/jact.12.468

[6] Kara, P. (2015): Performance of lamp glass waste powder (LGWP) as supplementary cementitious material (SCM) – viscosity and electrical conductivity. Építőanyag – Journal of Silicate Based and Composite Materials, 67(1), 12-18. http://dx.doi.org/10.14382/epitoanyag-jsbcm.2015.3

[7] Kara, P. – Borosnyói, A. – Fenyvesi, O. (2014): Performance of waste glass powder (WGP) supplementary cementitious material (SCM) – Drying shrinkage and early age shrinkage cracking. Építőanyag – Journal of Silicate Based and Composite Materials, 66(1), 18-22. http://dx.doi.org/10.14382/epitoanyag-jsbcm.2014.4

[8] Steven H. Kosmatka, B. K. (2002): Design and Control of Concrete Mixtures Fourteenth Edition (FOURTEENTH EDITION ed.). United States of America. Retrieved from https://www.google.com/url?sa=t&source=web&rct=j&url=https://www.amazon.com/Design-Control-Concrete-Mixtures-Kosmatka/dp

[9] ASTM, C. (2003): Standard Test Method for Compressive Strength of Cylindrical Concrete Specimens. Retrieved from www.astm.org

[10] ASTM, C. (2004): Standard Test Method for Splitting Tensile Strength of Cylindrical Concrete Specimens. Retrieved from www.astm.org

[11] ASTM, C. (1997): Standard Test Method for Density, Absorption, and Voids in Hardened Concrete. Retrieved from www.astm.org

Ref.:
Bouty, Antonio – **Homsi**, Farah: *The effects of partially replacing cement by glass waste powder on concrete properties*
Építőanyag – Journal of Silicate Based and Composite Materials, Vol. 73, No. 2 (2021), 40–43. p.
https://doi.org/10.14382/epitoanyag-jsbcm.2021.7

Evaluation of chloride resistance of silica fume and glass waste MWCNT- geopolymer composite

H. M. KHATER
Professor of cement chemistry at Raw Building Materials Technology and Processing Research Institute, Housing and Building National Research Center (HBRC). Supervisor of XRF laboratory for the chemical analysis of all type of raw building materials.

Abdeen EL NAGAR
Researcher in the field of geology at Raw Building Materials Technology and Processing Research Institute, Housing and Building National Research Center (HBRC).

H. M. KHATER ▪ Housing and Building National Research Centre (HBNRC), Cairo ▪ Hkhater4@yahoo.com
Abdeen EL NAGAR ▪ Housing and Building National Research Centre (HBNRC), Cairo

Érkezett: 2020. 08. 30. ▪ Received: 30. 08. 2021. ▪ https://doi.org/10.14382/epitoanyag-jsbcm.2021.8

Abstract

The target of the present paper is to study the enhancement effect of MWCNT on alkali activated composites resistivity to chloride attack. Geopolymer composites were made from metakaolin and ground granulated blast furnace slag and to either 10 % silica fume or glass waste. The added MWCNT were in the ratio of 0.01% up to 0.09 % by weight. Results revealed the high resistivity and stability against magnesium chloride solution; in addition glass waste mixes acquired high mechanical strength as compared with silica fume mixes as related to the high amorphous structure as well as high finesty of glass waste as compared with silica fume. The results revealed an increased enhancement in characteristics of activated composites with MWCNT up to 0.07% in both matrices.

Keywords: MWCNT, alkali activation, glass waste, silica fume
Kulcsszavak: MWCNT, alkáli aktiválás, üveghulladék, szilikapor

1. Introduction

Interest in the development of alternative building materials such as alkali-activated binders has been promoted by growing development in building industry and the need for materials with high superior properties with high sustainable properties. Alkali-activated binders represent an attractive alternative for the partial or almost complete substitution of cement in construction industry as they offer durable, high performance in addition to low production cost [1], low greenhouse gas emissions [2,3]. There is a general agreement that alkali-activated cements can offer cradle-to-gate greenhouse emission savings approaching 40–80% compared to Portland cement for a performance-equivalent material.

Alkali activated composites are inorganic polymer binder that processed at room temperature upon activation of alumino-silicate sources using alkali metal oxides. Metakaolin-based geopolymer is one of the most abundant and applicable alumino-silicate polymers worldwide [4]. The synthesis of geopolymer proceeds via polycondensation reactions of metakaolinite (kaolinite calcined at 600–800°C) or other natural and industrial aluminosilicate reach materials as water cooled slag, silica fume fly ash with alkaline solution [5]. In spite metakaolin-based geopolymers possess interesting properties; they have not enough high strength and show brittle behavior. These make the products unsuitable for structural and infrastructural applications; thus, it is necessary to improve the fracture properties of metakaolin-based geopolymers [6]. Many previous studies investigated their reinforcing with various macrofiber as steel, polypropylene (PP), poly vinyl chloride (PVC), and basalt fibers [7,8]. The addition of these fibers increased the flexural strength, fracture energy, and controlled the crack propagation. Multiwall carbon nanotubes (MWCNTs) are being considered as a potential reinforcement in composites because they have mechanical properties superior to those of traditional fibers and possess a Young's modulus of 1 TPa, a yield stress of 100–300 GPa, and a tensile strength of 63 GPa [9]. However, the higher mechanical properties of MWCNTs alone do not ensure a mechanically superior nanocomposites geopolymer. It is clear that the dispersion of the MWCNTs within the metakaolin-based geopolymers and the bonding properties between the surface of the MWCNTs and the metakaolin-based geopolymers around them are the main challenges in the fabrication of metakaolin/MWCNTs composites [10, 11].

Maeva et al., [12] showed that using nanodispersed carbon additives as a modifier in anhydrite compositions provided a dense, low-defect structure of crystalline hydrates, leading to the increased mechanical strength and water resistance of the material. However, the effective application of multi-walled carbon nanotube dispersions required the solution of the problem connected with partial separation of carbon nanotubes into individual particles in the aqueous dispersion medium as well as the problem of stabilizing nanostructures in dispersion while being stored. The solution of the problem of stabilizing suspensions is adsorbing and solvent layer on the surface of nanotubes which prevents their approximation. The best variant to limit coagulation is to use surfactants [13].

Previous studies have shown that sodium hydroxide (NaOH) acts as a surfactant and removes oxidation debris from the surface of the MWCNTs, consequently allowing them to de-bundle and form well-dispersed nanotubes within geopolymer matrix [11]. Recently, Khater and Abdel Gawwad [14, 15] investigated the effect of various ratios of MWCNTs dispersed with carboxylate based superplasticizer on the properties of slag geopolymeric mortar and found that the enhancement in mechanical strength with MWCNT as the high stability against firing up to 500 °C. Also Farag et al., [16] studied the

Oxide content/%	SiO_2	Al_2O_3	Fe_2O_3	CaO	MgO	SO_3	K_2O	Na_2O	TiO_2	MnO	P_2O_5	Cl-	L.O.I	BaO	SrO	Total
Water – Cooled Slag (GGBFS)	36.67	10.31	0.50	38.82	1.70	2.17	1.03	0.48	0.57	4.04	0.04	0.050	0.12	3.28	0.18	99.96
Kaolin	56.38	27. 61	1.32	0.18	0.06	0.06	0.04	0.08	3.73	–	0.13	0.05	10.17	–	–	99.76
MK (fired kaolin at 800 degree for 2hrs)	57.50	35.10	1.59	0.64	0.17	0.25	0.15	0.12	2.85	0.00	0.13	0.06	1.14	–	–	99.70
Silica fume	94.92	0.02	1.28	0.03	0.01	0.02	0.15	0.28	–	–	–	–	3.28	–	–	99.99
Glass waste	72.00	1.19	0.39	9.17	3.98	0.44	0.23	11.10	0.08	0.05	–	–	1.09	–	0.01	99.73

Table 1 Chemical composition of starting materials
1. táblázat A kiindulási anyagok kémiai összetétele

enhancement of water cooled slag geopolymer by multiwall carbon nanotube and studied their effects on their mechanical and microstructure characteristics**.**

Morsy et al. [17] have investigated also the effect of different concentrations of MWCNTs with nanoclay particles on the compressive strength of cement mortar and they noticed that the nanoclay particles improved the dispersion of CNTs within the mortar. Lio et al. [18] studied also the influence of MWCNTs mixed with silica fume (SF) on the mechanical property of cement-based composites. Hunashyal et al. [19] on the other hand fabricated hybrid composites of plain cement by integrating both carbon micro-fibers (CMFs) and MWCNTs.

As known that the immersion in chloride solution resulted in rapid deterioration and softening to the concrete structure, this can be related to the corrosive action depends on the concentration of chloride solution and the kind of cation linked to the chloride ion as reported by Barnes and Bensted[20]. The chloride ions penetration is dependent not only on the porosity of the matrix, but also on the paste composition and the ion-exchange capacity of the system. The damage influence of chloride is either chemical by interaction with liberated lime from the hydration reaction forming what is known as Friedel's salt or hydrocalumite ($C_3A{\cdot}CaCl_2{\cdot}10H_2O$) causing softening to the composition.

Jun et al. [21] investigated the chloride-binding capacity of alkali-activated fly ash and slag samples and their synthesized Cl-bearing phases, which are capable of binding and immobilizing chloride when seawater is used as the mixing water.

In the current work, we aim to examine the stability of the alkali activated composites enhanced with MWCNT against immersion in magnesium chloride solution up to 6 months and trace the formed structures using XRD, FTIR, and DTG as well as study the mechanical stability up on immersion in the solution.

2. Experimental

2.1 Materials

The materials, which used in this investigation, are ground granulated blast furnace slag (GGBFS), sourced from Iron and Steel Factory - Helwan, Egypt. Kaolinite collected from El-Dehesa, South Sinai, Egypt, which was thermally treated at 800 °C for 2 hrs with a heating rate of 5 °C/min to produce metakaolin (Mk) [22,23]. Silica fume sourced from Suez Cement Company (Helwan plant) also known as micro-silica is a by-product of the reduction of high-purity quartz with coal in electric furnaces in the production of silicon and ferrosilicon alloys; it was in the powder form with 95% SiO_2, where about 90% of particles are of 200 µm diameter, while glass waste powder prepared by grinding glass up to fine structure with an average particle size of 38 µm as measured by laser particle size distribution.

Chemical compositions of the starting raw materials are given in *Table 1*. The activators used in the activation process are potassium hydroxide (KOH) bought from Fisher scientific company with 99% purity in the ratio of 10% from the total weight. Whereas liquid sodium silicate (LSS, Na_2SiO_3. $9H_2O$) from Fisher company consists of 32% SiO_2 and 17% Na_2O with silica modulus SiO_2/Na_2O equal 1.88 and its density is 1.46 g/cm^3 used as another source of alkali activators in the ratio of 5%. Magnesium chloride with purity of 99% used as aggressive solution and was brought from Aldrich Company.

Mineralogical compositions of starting raw materials are represented in *Fig. 1*; where ground granulated blast furnace slag known also as water cooled slag composed of amorphous materials and kaolinite material mostly diminished upon thermal treatment at 800 °C for 2 hrs forming amorphous metakaolin. Silica fume and glass waste are nearly composed of amorphous materials, whereas the glass waste structure acquire more amorphous constituents than silica fume.

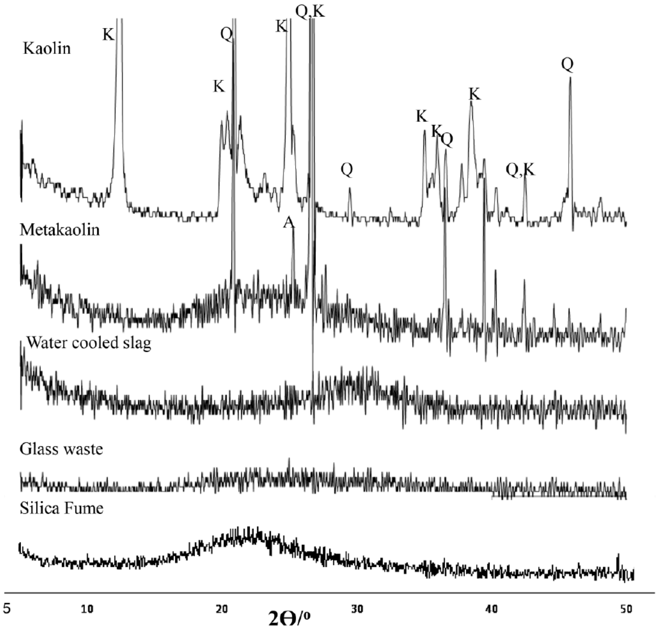

Fig. 1 X-Ray diffraction pattern of the starting raw materials (K: Kaolin, Q:Quartz:, A: Anatase)
1. ábra A kiindulás anyagok röntgendiffrakciós mintája (K: Kaolin, Q: kvarc, A: Anatáz)

Multi-walled carbon nanotubes used in this study were synthesized using a Co/MgO based catalyst using CVD instrument (housing and building national research center, Egypt), the physical properties of the MWCNTs used in the study are given in *Table 2*.

Amorphous carbon [%]	Surface area [$m^2 \cdot g^{-1}$]	Purity [%]	Ash [%]	Length [µm]	Inner diameter [nm]	Aspect ratio [%]
0	> 300	97	3	1-5	20-30	120

Table 2 Properties of CNTs synthesized by using CVD apparatus
2. táblázat A karbon-nanocsövek tulajdonságai CVD készülékkel meghatározva

2.2 Dispersion of MWCNTs

MWCNTs were first mixed with Gelenium Ace 30-polycarboxylate-based superplasticizer and 50% of the added water. This Polycarboxylate-based superplasticizer has been proven to be effective for CNTs dispersion [24,25]. The solution was sonicated using a Fritish 450 Sonifier Analog Cell distributor for 15 min [26]. Solutions with concentration of 0.01, 0.03, 0.05, 0.07 and 0.09 wt% of the total weight of the matrix were used to identify the MWCNT optimum concentrations and their resistivity to aggressive medium.

2.3 Alkali activation, curing and casting

Activation and curing are processed according to the following steps:

1. First activators prepared 24 hrs prior to casting, whereas binder reinforced with MWCNT concentrations: 0.0 (control), 0.01 up to 0.09 wt.% of the total weight.
2. MWCNT particles sonicated for 15 min using half of the used water as well as used superplasticizer for better dispersion under a temperature of 40 °C.
3. The geopolymer binder passing a sieve of 90 µm as represented in *Table 3* were hand mixed with the alkaline activator solution dissolved in the remaining used water for 10 min followed by a further 5 min using rotary mixer and mixed at medium speed (80 rpm) for another 30 seconds.
4. MWCNT and superplasticizer were then added and stirred with the mixture at high speed for additional 30 seconds.
5. Paste mixtures were cast into cubic-shaped moulds with 2.5 cm length, vibrated for compaction, sealed with a lid to minimize any loss of evaporable water, left to cure undisturbed under ambient temperature for 24 hrs, demolded and then subjected to curing at 40 °C with 100% relative humidity (R.H.) for 28 days [27].
6. All mixes were then immersed in 5% $MgCl_2$ solution [28], whereas the solution was replaced monthly, while their strength values were recorded, finally the crushed cubes were stopped for further hydration using acetone/methyl alcohol method (1:1) [29, 30], finally tightly conserved in container until examination time.

2.4 Exploration techniques

Chemical analysis was carried out using Axios (PW4400) WD-XRF Sequential Spectrometer (Panalytical, Netherland). Compressive strength tests were carried out using five tones German Brüf pressing machine with a loading rate of 100 kg/min determined according to [31]. X-ray diffraction (XRD) analysis was recorded on a Philips PW 1050/70 Diffractometer using a Cu-Kα source with a post sample Kα filter. XRD patterns were obtained from 0° to 50° 2θ (step size 0.02 °2θ and speed 0.4 °/min). Quartz silica was used as an internal standard. Data were identified according to the XRD software (pdf-2: database on CD-Release 2005). Bonding characteristics of the alkali activated specimens were analyzed using a Jasco-6100 Fourier transform infrared spectrometer FTIR. Test sample was ground and uniformly mixed with KBr at a weight ratio KBr: specimen=200:1. The mixture, 0.2 g was pressed to a disk of 13 mm in diameter for analysis at 8 t/cm². The wave number

Mix no.	Water cooled slag (WCS)/%	Metakaoline (Mk)/%	Silica fume (SF)/%	Waste glass (WG)/%	MWCNT/%	KOH/%	Na_2SiO_3/%	Superplasticizer (SP)/%	Water/binder%	SiO_2/Al_2O_3	Total M_2O/Al_2O_3	Total M_2O/SiO_2	Total W./M_2O
S0	50	40	10	–	0.00	10	5	0.80	0.16	2.73	0.712	0.153	6.64
S1	50	40	10	–	0.01	10	5	0.80	0.16	4.64	0.712	0.153	6.64
S2	50	40	10	–	0.03	10	5	1.00	0.16	4.64	0.712	0.153	6.64
S3	50	40	10	–	0.05	10	5	1.20	0.16	4.64	0.712	0.153	6.64
S4	50	40	10	–	0.07	10	5	1.40	0.16	4.64	0.712	0.153	6.64
S5	50	40	10	–	0.09	10	5	1.60	0.16	4.64	0.712	0.153	6.64
G0	50	40	–	10	0.00	10	5	0.80	0.26	2.60	0.800	0.18	9.54
G1	50	40	–	10	0.01	10	5	0.80	0.26	4.41	0.800	0.18	9.54
G2	50	40	–	10	0.03	10	5	1.00	0.26	4.41	0.800	0.18	9.54
G3	50	40	–	10	0.05	10	5	1.20	0.26	4.41	0.800	0.18	9.54
G4	50	40	–	10	0.07	10	5	1.40	0.26	4.41	0.800	0.18	9.54
G5	50	40	–	10	0.09	10	5	1.60	0.26	4.41	0.800	0.18	9.54

Table 3 Composition of the geopolymer mixes
3. táblázat A geopolimer keverékek összetétele

was ranging from 400 to 4000 cm^{-1} [32]. Thermogravimetry conducted using DT-50 Thermal Analyzer (Schimadzu Co-Kyoto, Japan), where the samples were crushed, transferred immediately to an alumina crucible, held under isothermal conditions for 60 min at 40°C to equilibrate in a nitrogen environment (N_2 flowing at 200 ml/min), and then heated to1000 °C at 10 °C/ min in the same gas environment.

3. Results and discussion

3.1 Fourier transform infra-red (FTIR)

FTIR spectra of 28 days (control) hybrid alkali activated composites incorporating 10 wt.% glass wastes or silica fume (*Fig. 2*) and having various ratios of multiwall carbon nano-tube (MWCNT) from 0.01 up to 0.09 wt.% indicates the growth of the asymmetric bands for amorphous geopolymer constituents for T-O-Si at about 1030 cm^{-1} in both mixes with increasing the MWCNT up to 0.07 wt.%, while decreasing with further increase in nanotube. It can be also noticed in glass waste mixes shifting of the previous main asymmetric band into lower wave number (980 cm^{-1}) as related to the increased amorphous geopolymer constituents than silica fume composites, where the increased fine structure (38 μm) of glass waste in addition to high alkalis within; facilitate and enhance geopolymer formation.

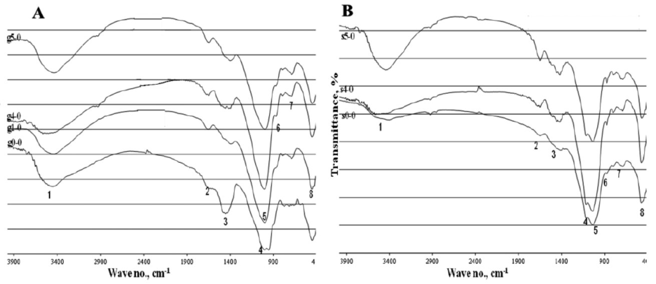

Fig. 2 FTIR spectra of 28 days alkali activated geopolymer specimens having various ratios of MWCNT, A) glass waste mixes; B) silica fume mixes. [1: Stretching vibration of O-H bond, 2: Bending vibrations of (HOH), 3: Stretching vibration of CO ,4: Asymmetric stretching vibration (Si–O–Si), 5: Asymmetric stretching vibration (T–O–Si), 6: Out of plane bending vibration of CO , 7: Symmetric stretching vibration (Si–O–Si), 8: Bending vibration (Si–O–Si and O–Si–O)]

2. ábra 28 napos alkáli aktivált geopolimer minták FTIR spektrumai, különböző arányú MWCNT tartalommal, A) üveghulladékkal keverve; B) szilikaporral keverve.

Another main featured band in both patterns is asymmetric stretching vibration (Si–O–Si) related to non-solubilized particles at about 1100 cm^{-1} which almost vanished with increasing MWCNT up to 0.07% reflecting the efficiency of nano-tube in enhancing anddissolving of unreacted constituents forming reactive amorphous geopolymer constituents. However, the intensity of previous band in silica fume mixes is higher than glass waste mixes reflecting the increased geopolymerization and activation of glass waste mixes than silica fume mixes. Increasing MWCNT ratios beyond 0.07% results in increasing O-H bands at about 3430, 1600 cm^{-1} which may be connected to the increased porosity with nano increase due to agglomeration of excess unreacted MWCNT, this note can be connected with the increased carbonate bands at about 1410 cm^{-1} as well as out of plane bending vibration band at 870 cm^{-1}. Another important note from both pattern is the increased O-H bands in glass waste mixes as compared with silica fume mixes where the lower grain size of glass waste acquire much water than silica fume as tabulated in *Table 3*, also reflects the increased of CSH in previous one as a results of its increased reactivity as compared with silica fume [32,14]. Another small bands at about 795, 690, and 448-468 cm^{-1} for symmetric stretching vibration of (Si-O-Si) attributed to α-quartz, symmetric stretching vibration (Si–O–Si), bending vibration (Si–O–Si and O–Si–O) associated with quartz [33], respectively, which increased with MWCNT up to 0.07% then decrease, as related to the activation and enhancement done by nano materials and their efficiency in enhancing geopolymerization reaction.

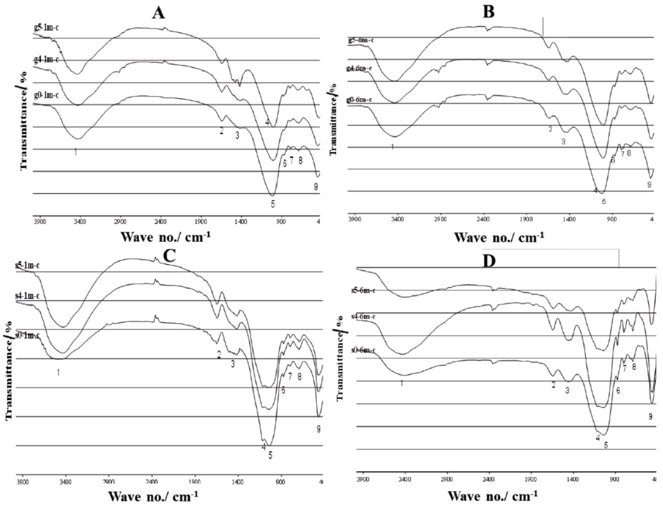

Fig. 3 FTIR spectra of alkali activated geopolymer specimens immersed in magnesium chloride solution and enhanced with various ratios of MWCNT: A) one month glass waste mixes, B) six month glass waste mixes, C) one month silica fume mixes, D) six month silica fume mixes. [1: Stretching vibration of O-H bond, 2: Bending vibrations of (HOH), 3: Stretching vibration of CO ,4: Asymmetric stretching vibration (Si–O–Si), 5: Asymmetric stretching vibration (T–O–Si), 6: Out of plane bending vibration of CO , 7: Symmetric stretching vibration (Si–O –Si) attributed to α-quartz, 8: Symmetric stretching vibration (Si–O–Si), 9: Bending vibration (Si–O–Si and O–Si–O)]

3. ábra Magnézium-klorid-oldatba merített és az MWCNT különböző aránnyal rendelkező alkáli aktivált geopolimer minták FTIR-spektrumai: A) egy hónapos üveghulladék keverékek, B) hat hónapos üveghulladék-keverékek, C) egy hónapos szilikapor keverékek, D) hat hónapos szilikapor keverékek.

FTIR of glass waste geopolymer mixes incorporating various ratio of MWCNT immersed in 5% magnesium chloride solution at one and 6 months, *Fig. 3* (A,B); showed an increased broadness in asymmetric band at about 1000 cm^{-1} with MWCNT up to 0.07% (G4) which consistent with both amorphous C–(A)–S–H structure formed by the activation of slag in alkaline media [34], and N–A–S–H gels formed in geopolymer binder systems derived from fly ash and metakaolin [35]. Further increase in nano-tube to 0.09% results in an increased intensity of asymmetric stretching vibration of (Si–O–Si) related to non-solubilized particles at about 1100 cm^{-1} where the increased MWCNT agglomerates and inhibit the dissolution and polymerization of geopolymer precursors. It can be seen that intensity of the carbonate at about 1430 cm^{-1} (ν C–O) splitted into two peaks with MWCNT increase to 0.09% as related to the distorted nature of CO_3 mineral and could be attributed to partial carbonation of C-S-H gel in air atmosphere [36]. One can notice a slight increase in carbonation bands at 870 and 1430 cm^{-1} with immersion time increase to 6 months, also the hydration bands at about 3430 cm^{-1} increased with MWCNT and with time increase where the dissolved constituents undergo hydration forming additional binding materials (CSH). The two patterns of glass waste mixes (*Fig. 3*(A,B)) showed little evidence of Friedel's salt formation where the last phase formed at about 3640 cm^{-1}, 3480 cm^{-1} (νOH), 1621 cm^{-1} (δH_2O), 785 cm^{-1}, 620 cm^{-1}, and 532 cm−1 (vibration of M–O ir M–O–H bands) are characteristic of Friedel's salt [37], where all bands except one at 532 cm^{-1} were overlapped by other bands, so only this peak shows the formation of Friedel's salt after 3 months of immersion in chloride solution. However the increased content of MWCNT leads to agglomeration, so more sodium cations are available for carbonation as clearly will be seen in *Fig. 6*.

On the other hand, silica fume based mixes immersed in chloride solution at 1 and 6 months (*Fig. 3*(C,D)) showed the same behavior with respect to the added MWCNT, whereas the main difference in those mixes are the presence of the shoulder at about 1100 cm^{-1} for non-solubilized silica which is inversely proportional with the asymmetric band of T-O-Si at about 1000 cm^{-1} where their increase reflect the deficiency in dissolving and polymerize the constituents of the geopolymer. Also, the hydration bands in silica fume decreases with time up to 6 months, as well as carbonate bands with time giving an indication about the continuous consumption of free alkalis and incorporation in geopolymer formation in spite the mix of 0.07% MWCNT acquired the highest content of hydration bands as reflected on the increased combined water content in the geopolymer network as well as the formed CSH and CASH phases. Another difference is the absence of the shoulder at about 1100 cm^{-1} for non- solubilized silica in glass waste mixes where high reactivity if glass waste enhance their dissolution and incorporation in geopolymerization reaction, however in silica fume there are still some unreacting constituents which not incorporated in the reaction.

FTIR spectra of geopolymer mixes incorporated glass waste and silica fume immersed in 5% magnesium chloride solution up to 6 months, and enhanced by 0.07% MWCNT (*Fig. 4* (A,B)). The pattern of both mixes exhibit an increased intensity in the amorphous geopolymer constituents as represented by asymmetric stretching vibration of T-O-Si at about 1000 cm^{-1} with slight shifting to lower wave number with time. Also, there is an increased dissolution of unreacted slag materials with curing time up to 6 months as illustrated from the decreased asymmetric band at about 1100 cm^{-1} for non-solubilized particles as well as symmetric vibration of α-quartz at about 797 cm^{-1}, confirming the activation and nucleating efficiency increase by MWCNT [38]. The band at 690 cm^{-1} is attributed to the symmetric vibration mode of the Si-O-Si or Al-O-Si bonds. This band corresponds to C-A-S-H type phases, and the zeolites forming in these systems, as identified by XRD (*Figs. 5, 6*). This band has also been observed in unreacted slag [39], and has been attributed to gehlenite. All infrared band assignments follow references [40-42].

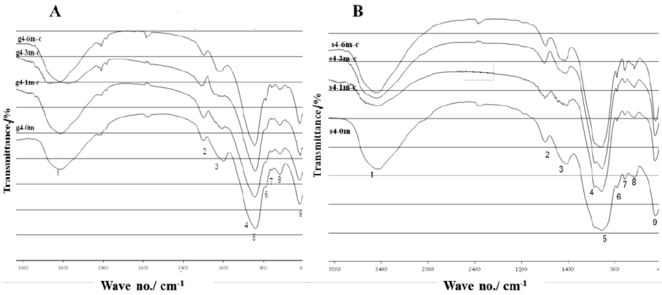

Fig. 4 *FTIR spectra of alkali activated Geopolymer specimens enhanced with 0.07% MWCNT immersed in magnesium chloride solution up to six months, A) glass waste mixes; B) silica fume mixes. [1: Stretching vibration of O-H bond, 2: Bending vibrations of (HOH), 3: Stretching vibration of CO ,4: Asymmetric stretching vibration (Si–O–Si), 5: Asymmetric stretching vibration (T–O–Si), 6: Out of plane bending vibration of CO , 7: Symmetric stretching vibration (Si–O –Si) attributed to α-quartz, 8: Symmetric stretching vibration (Si–O–Si), 9: Bending vibration (Si–O–Si and O–Si–O)]*

4. ábra *Legfeljebb hat hónapig magnézium-klorid-oldatba merített 0,07% MWCNT tartalmú alkáli aktivált geopolimer minták FTIR-spektrumai A) üveghulladék keverékek; B) szilikapor keverékek.*

There is a decrease in the carbonation bands observed with MWCNT and time, where the carbonate constituents in slag materials lead to the growth of the carbonate band as discussed above, showing that the carbonates identified in this raw material do not react significantly under alkaline activation conditions [43]. The CO_3^{2-} vibration band decreases with time as attributed to the fact that the increased nucleation of MWCNT increase the formation of geopolymer structure and decrease the availability of free Na^+ species which will be subjected to carbonation.

3.2 X-ray diffraction (XRD)

XRD patterns of six months alkali-activated geopolymer mixes based on glass waste and silica fume incorporating various ratio of MWCNT (0, 0.07, 0.09 wt.%), immersed in magnesium chloride solution are shown in *Fig. 5* (A,B). The pattern of glass waste mixes (*Fig. 5A*) illustrate mostly absence of hump in the region of 17° to 35° 2θ which characterize glassy phases, this region considered as vital key in geopolymer characterization, where any increase in this hump will be reflected on the performance and efficiency of the resulting geopolymer gel. Also, there is sharp peak for Friedel's salt at 11.20 (2θ) ($C_3A.CaCl_2.10H_2O$) reflecting the susceptibility for this mix for chloride attack.

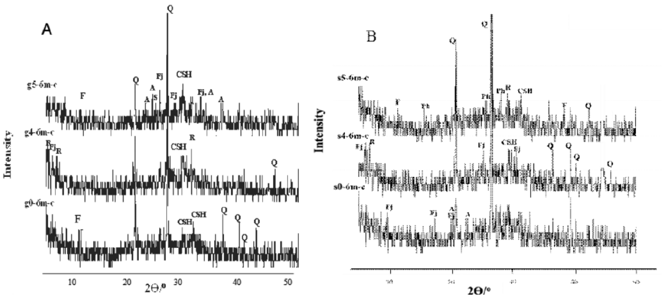

Fig. 5 *XRD pattern of six months immersed alkali activated geopolymer specimens in magnesium chloride solution; A) glass waste mixes, B) silica fume mixes. [Q:Quartz, A:ZeoliteA, Fj: Faujasite, F: Friedel's salt, R: Reversedite, CSH: Calcium silicate hydrate]*

5. ábra *Hat hónapig magnézium-klorid-oldatba merített alkáli aktivált geopolimer minták XRD ábrái; A) üveghulladék keverékek; B) szilikapor keverékek.*

It can be seen an increased broadness of this hump up on increasing MWCNT to 0.07% with the increase of CSH as well as reversedite phases ($C_3S_2H_3$) which is one of the calcium hydrate phases that add additional strengthening as well as nucleating sites for geopolymer formation and accumulation [44], the increased intensity of this hump favors the activation done by MWCNT resulting in enhancement of geopolymer reaction. Further increase in nano results in an agglomeration, forming weak points within the matrix which hinder geopolymer propagation leading to formation of short zeolite chains as confirmed by the increased intensity of zeolite phases (faujasite, zeolite A, sodalite) on the expense of the amorphous geopolymer structure. This decrease in the amorphous geopolymer phases made the matrix more prone to chloride attack as indicated by the appearance of Friedel's salt, but its intensity still much lower than control mix which suggests the ability of MWCNT even in high dose to suppress the chloride attack.

The behavior of silica fume based mixes almost similar to those of glass waste mixes (*Fig. 5B*), except the decreased hump in the region from 17- 35 ° (2θ) related to the amorphous content as well as the hump in the region 6-10° (2θ) for aluminosilicate gel where the increased reactivity of glass waste than silica fume favors the increased hump broadness in glass waste mixes than that of silica fume. The main remark in silica fume mixes also is the increased zeolite content as related to its lower reactivity which favor the zeolite formation than amorphous geopolymer constituents especially up on using high MWCNT dose while accompanied by the increased intensity of Friedel's salt.

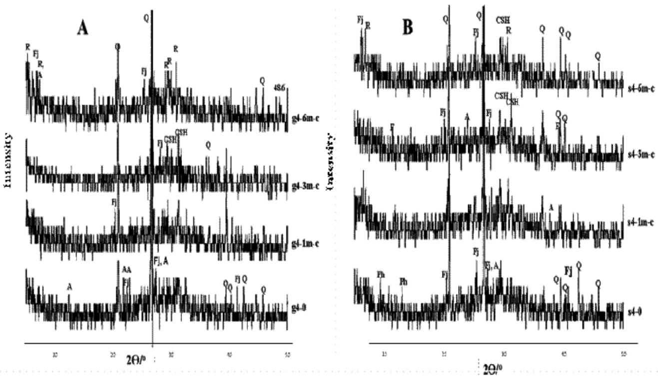

Fig. 6 *XRD pattern of alkali activated Geopolymer specimens enhanced with 0.07% MWCNT immersed in 5% magnesium chloride solution up to 180 days. A) glass waste mixes, B) silica fume mixes. [Q:Quartz, A:ZeoliteA, Fj: Faujasite, R: Reversedite, CSH: Calcium silicate hydrate, Ph : Phylipsite]*

6. ábra *Legfeljebb hat hónapig 5%-os magnézium-klorid-oldatba merített 0,07% MWCNT tartalmú alkáli aktivált geopolimer minták XRD ábrái A) üveghulladék keverékek; B) szilikapor keverékek.*

On examining the effect of immersion time up to 6 months on the optimum mixes incorporating 0.07% MWCNT in glass waste and silica fume mixes as illustrated in *Fig. 6*, there is continuous growth in amorphous geopolymer hump with time in addition to the increased CSH-phases as attributed to the effect of the NaOH alkaline solution during processing as discussed in a previous investigation [45]. The carboxylate based superplasticizer was effective in dispersing MWCNTs at 0.07 wt.% and lower, where most of MWCNT interact and activate the geopolymerization reaction forming three dimensional networks. Another main concluded remark was the increased faujasite phase in silica fumes mixes up to 3 months whereas in glass waste mixes there is continuous growth and crystallization of CSH. The increased zeolite phases in silica fume mixes made the matrix more prone to chloride attack especially at 3 months as represented by peaks due to Friedel's salt, while beyond this age the progress of geopolymer formation results in increasing the medium alkalinity which will destabilize the formed Friedel's salt leading to lowering in its intensity [46,47].

It is likely that a significant proportion of Na^+ species is consumed in the activation of binding constituents to form a sodium aluminosilicate-type gel, reducing the availability of Na^+ species in the pore solution [48] and, therefore, reducing the alkalinity from the high levels which would favor zeolite growth, even with the higher alkali dosage added to these samples. It can be noticed also the absence of calcite phases mostly in all mixes as well as with immersion time which reveals the absence of free alkalis as they are mostly consumed in geopolymer formation. This observation come in accordance with FTIR pattern where the intensity of carbonate bands are very small while in XRD there are no carbonates as the XRD tool concerned about crystalline content of the minerals which can detect only more than 3%, which means that calcite phases are too small in the matrix.

3.3 Differential thermo-gravimetric analysis (DTG)

Differential thermogravimetric curves for geopolymer composites incorporating various ratio of MWCNT are represented in *Figs. 7-10*. The pattern of one month glass waste and silica fume geopolymer composites having 0, 0.07 and 0.09% MWCNT represented in differential thermograms (*Figs. 7, 8*), showed a characteristic two endotherms at temperature lower than 68 °C as well as endothermic band lower than 149 °C; the first associated with the loss of freely evaporable water present in large pores of the aluminosilicate type product (geopolymer gel) for Mk–geopolymer [26,49], while the second associated with the dehydration of a C-S-H gel [50], as this is the main reaction product identified in GBFS-rich blended binders [40,51]. In addition to another endothermic peak at temperatures at about 590, 615, 725 °C, this attributed to the presence of calcium carbonates of varying crystallinity as has been observed in previous studies of alkali-activated slag using a similar precursor [50] as a consequence of weathering of the slag before sample preparation. Another endothermic peak can be distinguished in some mixes in the range 309–331 °C attributed to dehydroxylation by condensation of the bound silanol groups in zeolite of Faujasite, which is completed at 500 °C [51].

Fig. 7 illustrate the growth in the intensity of endothermic peak at about 62 °C with MWCNT increase to 0.07%, with sharp increase in the endothermic peak for CSH at about 149 °C which reflect the increased efficiency of MWCNT in activating and enhancing geopolymer formation as well as CSH, as coincide with XRD and FTIR observations. However, increasing MWCNT to 0.09% lead to a decreased intensity of endothermic peak at 62 °C as well as growth of endothermic peak at about 310 °C for zeolite dehydroxylation. Another main notice in this figure is the absence of endothermic peak for Friedel's salt at all MWCNT's ratios at 360-370 °C [52,53].

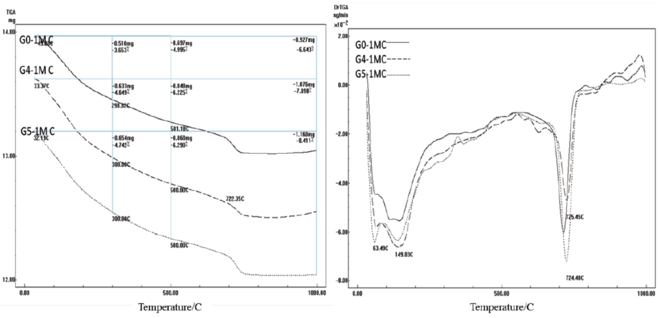

Fig. 7 *Differential thermo-gravimetric pattern of one month alkali activated glass waste geopolymer specimens enhanced with various ratios of MWCNT and immersed in 5% magnesium chloride solution.*

7. ábra *Egyhónapos 5% -os magnézium-klorid-oldatba merített alkáli aktivált üveghulladék geopolimer minták termo-gravimetrikus mérési eredményei, különböző MWCNT arányok esetén,*

With respect to the carbonate which mentioned in previous studies of alkali-activated slag using a similar precursor [50] as a consequence of slag weathering before sample preparation. Considering that samples were cured and stored under controlled sealed conditions, a significant extent of carbonation is not expected to occur in the specimens assessed. The figure showed the lowest intensity of carbonation endotherm at 0.07% as confirmed by the dense structure of this matrix. None of the samples show significant weight loss above 725 °C.

Total weight loss for one month immersed glass waste geopolymer mixes in magnesium chloride solution varied with MWCNT giving ~6.643, ~7.898 and ~8.411% for 0, 0.07 and 0.09%, respectively. The total weight loss reflected the increased the amorphous aluminosilicate content with nano materials up to 0.07%, while the increase in total weight loss with further nano increase related mainly to the increased zeolite formed (as seen from the endothermic at about 310 °C for dehydroxylation of zeolite as mentioned before) as a result of agglomeration of excess nanotube leading to the decrease in the amorphous geopolymer constituents and forming short crystalline zeolite chains.

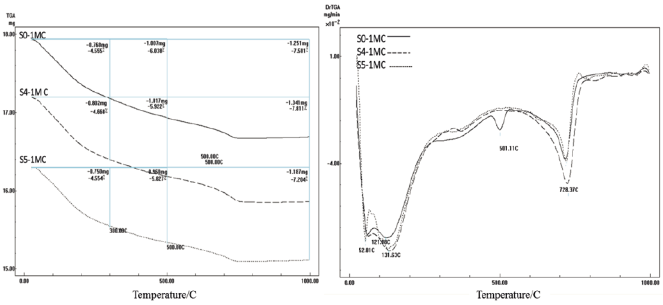

Fig. 8 *Differential thermo-gravimetric pattern of one month alkali activated silica fume based geopolymer specimens enhanced with various ratios of MWCNT and immersed in 5% magnesium chloride solution.*

8. ábra *Egyhónapos 5% -os magnézium-klorid-oldatba merített alkáli aktivált szilikapor alapú geopolimer minták termo-gravimetrikus mérési eredményei, különböző MWCNT arányok esetén,*

In case of silica fume geopolymer mixes (*Fig. 8*), the same behavior with respect to MWCNT addition except that the endothermic peak for freely evaporable water in geopolymer shifted to lower temperature (52 °C) indicating the lower matrix density of those mixes as compared with glass waste mixes and the free water of geopolymer is not tightly bound as the previous mixes. Also, the CSH shifted to lower temperature to 131 °C as the formed CSH binding materials are not of dense structure as compared with previous mixes, whereas the carbonate peaks are almost equal in intensity.

Total weight loss for one month immersed silica fume geopolymer mixes in magnesium chloride solution varied with MWCNT giving ~7.501, ~7.811and ~7.204% for 0, 0.07 and 0.09%, respectively. The total weight loss reflected the increased the amorphous aluminosilicate content with nano materials up to 0.07%, while its decrease as compared with glass waste related to the absence of zeolite peak at about 310 °C in silica fume mixes. On the other hand, prolonged immersion of glass waste geopolymer and silica fume mixes incorporating 0.07% MWCNT in magnesium chloride solution up to six months (*Fig. 9, 10*), there is a continuous increase in the amorphous aluminosilicate content at about 60 °C, with the almost vanishing of zeolite dehydroxylation peak at 310 °C as a resulted of continuous geopolymerization reaction, however at 6 months of immersion there is a new formed peak for zeolite dehydroxylation at about 87 °C. Also, a noticeable increase in the peaks related to CSH at about 149 °C with the shifting to lower temperature of 133 °C as resulted from the difference in the nature of water bonded to the structure than in geopolymer gel, such as C–S–H gel [49], these observations come in accordance with XRD and FTIR illustrations as mentioned before.

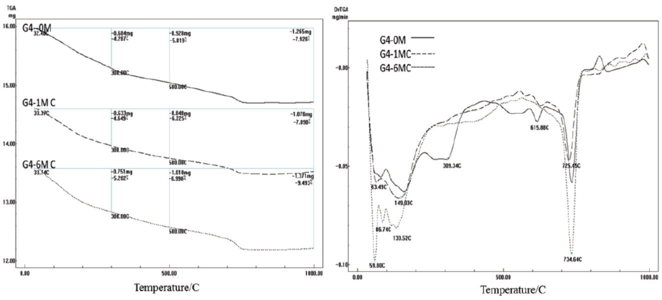

Fig. 9 *Differential thermo-gravimetric pattern of alkali activated glass waste geopolymer specimens enhanced with 0.07% MWCNT and immersed in 5% magnesium chloride solution up to six months*

9. ábra *Legfeljebb hat hónapig 5% -os magnézium-klorid-oldatba merített, 0,07% MWCNT tartalmú alkáli aktivált üveghulladék geopolimer minták termo-gravimetrikus mérési eredményei*

On investigating the figure of silica fume mix, nearly there was symmetry with glass waste mix up on immersion in chloride solution except the absence of peak due to zeolite at about 87 °C in addition to the increased broadness of the carbonate peaks at various temperatures from 590 to 730 °C as attributed to the presence of calcium carbonates of varying crystallinity, whilst in glass waste, the calcite peaks are narrow at 725 °C. Total weight loss for glass waste as well as silica fume geopolymer mixes incorporating 0.07% MWCNT immersed in magnesium chloride solution up to 6 months increased with time giving ~7.93, ~7.90 and ~9.49% for 0, 1 and 6 months, as well as ~6.90, ~7.81, ~10.43%, at 0, 1 and 6 months, for glass waste and silica fume mix, respectively. This increase in the total loss attributed to the growth in the amorphous aluminosilicate content as well as CSH with time even under immersion in aggressive chloride solution.

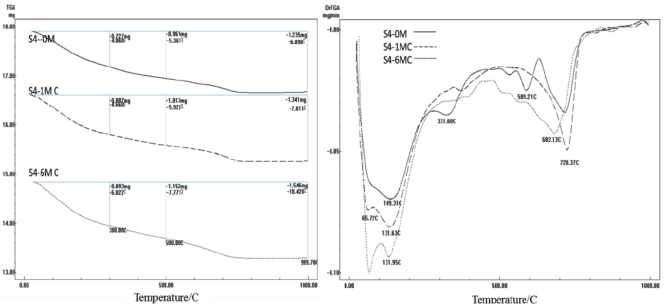

Fig. 10 *Differential thermo-gravimetric pattern of alkali activated silica fume geopolymer specimens enhanced with 0.07% MWCNT and immersed in 5% magnesium chloride solution up to six months*

10. ábra *Legfeljebb hat hónapig 5%-os magnézium-klorid-oldatba merített, 0,07% MWCNT tartalmú alkáli aktivált szilikaport alapú geopolimer minták termo-gravimetrikus mérési eredményei*

3.4 Compressive strength

Fig. 11 shows the compressive strength of glass waste as well as silica fume geopolymer composites enhanced with various ratios of MWCNT; immersed in 5% magnesium chloride solution up to 6 months. The results showed the increase of strength in all composites in spite of their immersion in the aggressive magnesium chloride solution, and reaching the maximum at 0.07% MWCNT while decreases with further increase in the carbon nanotube.

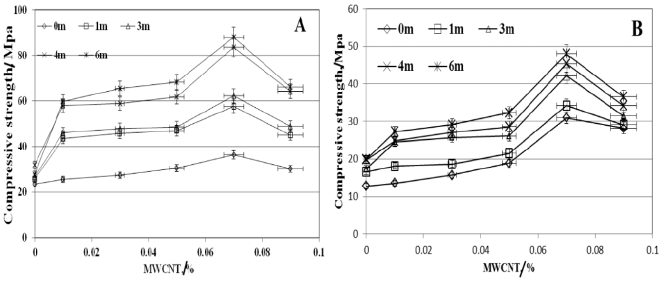

Fig. 11 *Compressive strength of alkali activated geopolymer specimens enhanced with various ratios of MWCNT and immersed in magnesium chloride solution up to 6 months, A) glass waste mixes, B) silica fume mixes*

11. ábra *Alkáli aktivált geopolimer minták nyomószilárdsága, különböző MWCNT arányok esetén és magnézium-klorid-oldatba merítve 6 hónapig; A) üveghulladék keverékek; B) szilikapor keverékek.*

As known the main deleterious effect up on immersion in magnesium chloride solution is the formation of Friedel's salt ($C_3A.\ CaCl_2.\ 10H_2O$) which known by its softening characteristics as well as their formed by-product magnesium hydroxide which known by its lower pozzolanic activity as well as its essential effect in lowering the pH of the medium which is the main driving force for the geopolymer reaction as well as its lower solubility which in turn results in hindering the propagation of hydration reaction as seen from the following equations:

$$3Ca(OH)_2 + Al(OH)_4^- \rightarrow C_3A + 3H_2O \quad (1)$$

$$Ca(OH)_2 + MgCl_2 \rightarrow CaCl_2 + Mg(OH)_2 \text{ (low solubility)} \quad (2)$$

$$CaCl_2 + C_3A + 10H_2O \rightarrow C_3A.CaCl_2.10H_2O \text{ (Friedel's salt)} \quad (3)$$

Magnesium ions with its lower solubility decrease medium pH forming M-S-H instead of C-S-H; which is known by its non-cementitious properties and leads to softening on prolong exposure time leading to destabilization of the hydration materials [53,54].

In our case, optimization of the strength values for geopolymer composites containing 0.07% MWCNT ascribed to its spreading throughout the geopolymer matrix with a uniform density. Where, The good dispersion of MWCNTs was also attributed to the effect of the NaOH alkaline solution during processing as discussed in an earlier publication [45] and hydrophilic groups (-COOH) in carboxylate based superplasticizer forming covalence-modified CNTs to improve interfacial interactions within composites, in which the -COOH groups form strong coordinate bonds with Ca^{2+} ions in geopolymer matrix, thus enhancing the formation of three dimensional geopolymer in addition to CSH [39, 55]. However, The carboxylate based superplasticizer was ineffective in dispersing MWCNTs in ratios more than 0.07%, where most of MWCNT were agglomerated in the alumino-silicate gel and hinder the propagation of the three dimensional network.

Incorporated MWCNTs increase the geopolymerization rate after addition to the same system; therefore, the MWCNTs inhibit the retardation effect caused by aggressive chloride solution as reflected on the decreased intensity of the formed zeolite as well as Faujasite phases at the optimum MWCNT dose as seen from XRD, DTG and FTIR patterns. The activation effect done by MWCNT and their efficiency in resisting aggressive media can be explained by their ability to work as nucleation-sites in the system, where the functionalized MWCNTs provide different reaction sites for the crystal growth of geopolymer products [56].

The negative effect of MWCNT overdose than 0.07% was confirmed by the increased zeolite as well as Faujasite with the increased MWCNT, as the geopolymer network was terminated forming the crystalline zeolitic structures with lower reactive characteristics which facilitate the ingress of aggressive chloride solution as confirmed by slight peak at 0.09% in XRD pattern (*Fig. 5*) for Friedel's salt. Also, the intensity of the formed Friedel's salt in glass waste mixes is lower than that of silica fume mixes due to variation in reactivity of both as can be seen from their compressive strength values, where strength values for optimum MWCNT (0.07%) after six months of immersion reaches about 88MPa while for silica fume mix at the same ratio reaches about 48 MPa. Zeolite formation is also well known to take place in KOH-activated geopolymer, similar to their NaOH-containing counterparts. However, crystallization is less rapid in KOH/metakaolin geopolymer compared to the NaOH/metakaolin system [57,58] which confirmed the lower intensity in DTG for zeolite phases and lower intensity detected in XRD.

4. Conclusions

1. Hybridization of various aluminosilicate precursors including either glass wastes or silica fume produce sustainable building materials with superior resistivity to aggressive magnesium chloride solution.
2. Addition of various ratios of MWCNT to alkali activated hybrid composite increases and offers an extra nucleation sites for alkaline composite formation and accumulation.
3. MWCNT possess an extra enhancement in the stability of the produced alkali activated composites reaching to the optimum at 0.07%.

4. XRD, FTIR and DTG emphasized the absence of chloride bearing compounds (Friedel's salt) even at later ages except weak peaks in the control as well as mixes incorporating 0.09% MWCNT.
5. Glass wastes incorporating mixes encounter better resistivity to the aggressive solution than silica fume incorporating mixes due to the variation in their reactivity. Where the optimum mix (0.07% MWCNT) in glass waste group acquired compressive strength of about 88 MPa after 6 months of immersion, while optimum silica fume mix at the same ratio acquired about 48 MPa.

References

[1] Duxson, P.; Fernandez-Jimenez, A.; Provis, J.L.; Lukey, G.C.; Palomo, A.; van Deventer, J.S.J., "Geopolymer technology: the current state of the art", J Mater Sci., 2007;42(9):2917–33.

[2] Duxson, P.; Provis, J.L.; Lukey, G.C.; van Deventer, J.S.J., " The role of inorganic polymer technology in the development of green concrete", Cem Concr Res., 2007;37(12):1590–7.

[3] Habert, G.; d'Espinose de Lacaillerie, J. B.; Roussel, N., "An environmental evaluation of geopolymer based concrete production: reviewing current research trends', J. Cleaner Prod., 2011; 19: 1229.

[4] Rashad, A.M.; "Alkali-activated metakaolin: a short guide for civil engineer – an overview",Constr.Build.Mater., 2013; 41:751–765.

[5] Autef, A.; Joussein, E.; Gasgnier, G.; Rossignol, S., "Role of the silica source on the geopolymerization rate", J.Non-Cryst. Solids, 2012; 358:2886–2893.

[6] Aly, Z.; Vance, E.R.; Perera, D.S., "Aqueous dissolution of sodium aluminosilicate geopolymers derived from metakaolin", J.Nucl. Mater.,2012; 424:164–170.

[7] Khalaj, G.; Nazari, A., "Modeling split tensile strength of high strength self-compacting concrete incorporating randomly oriented steel fibers and SiO2 nanoparticles", Compos.B:Eng., 2012; 43:1887–1892.

[8] Khalaj, G.; Hassani, S.E.S.; Khezrloo, A.; Haratifar, E.-A.-D., "Split tensile strength of OPC-based geopolymers: application of DOE method in evaluating the effect of production parameters and their optimum condition", Ceram.Int.., 2014; 40:10945–10952.

[9] Jin, F.; Park, S., "A review of the preparation and properties of carbon nanotubes- reinforced polymer composites", Carbon Lett., 2011; 12:57–69.

[10] Saafi, M.; Andrew, K.; Tang, P.L.; Ghon, D.M.; Taylor, S.; Rahman, M.; Yang, S. ; Zhou, X., "Multifunctional properties of carbon nanotube/fly ash geopolymeric nanocomposites", Constr.Build.Mater.,2013; 49:46–55

[11] Tyson, B.; Al-Rub, A.; Yazdanbakhsh, A.; Grasley, Z., " Carbon nanotubes and carbon nanofibers for enhancing the mechanical properties of nanocomposites cementitious materials",J.Mater.CivilEng., 2011; 23: 1028–1035.

[12] Maeva, I.S.; Yakovlev, G.I.; Pervushin, G.N.; Buŕyanov, A.F.; Korzhenko, A.; Machyulaitis, R., "Modification of Anhydrite Compositions with Multilayer Carbon Nanotubes. Stroitel'nye materialy", Construction Materials, 2010; 7: 25–27.

[13] Kholmberg, K.; Iensson, B.; Kronberg, B.; i dr. Poverkhnostno- aktivnye veshchestva i polimery v vodnykh rastvorakh "Surfacants and polymers in aqueous solutions", M.: BINOM. Lab. znanii, 2007. 528 p. (in Russian).

[14] Khater, H.M.; Abd el Gawwad, H.A., "Characterization of alkali activated geopolymer mortar doped with MWCNT", Construction and building materials, 2015; 102 (2016) :329–337.

[15] Khater, H.M.; Abd el Gawwad, H.A., "Effect of firing temperatures on alkali activated Geopolymer mortar doped with MWCNT", Advances in nano research "Techno press", 2015; 3(4) :225–242,

[16] Farag, A.B.; Ramadan, A.M.; Osman, T.A.; Khater, H.M.; Yosri, K., "Physicomechanical Characteristic of Slag Geopolymer Mortar Enhanced with Multiwall Carbon Nano-tube", International Journal of Engineering Trends and Technology (IJETT), 2015; 21(1): 52-60.

[17] Morsy, M.S.; Alsayed, S.H.; Aqel, M., "Hybrid effect of carbon nanotube and nanoclay on physicomechanical properties of cement mortar", Constr. Build.Mater., 2011; 25:145–149.

[18] Lio, H.; Baomin, W.; Yu, H.; Jun, Q.; Zhiqiang, G., "The influence of carbon nanotubes/ silica fume on the mechanical properties of cement –based composites", Rom.J.Mater., 2015;45:29–34.

[19] Hunashyal, A.M.; Tippa, S.V.; Quadri, S.S.; Banapurmath, N.R., "Experimental investigation on effect of carbon nano tubes and carbon fibres on the behavior of plain cement mortar composite round bars under direct tension", Int. Sch. Res. Not.Nanotechnol., 2011; 201:1–6.

[20] Barnes, P.; Bensted J., "Structure and Performance of Cements", Second edition, Spon Press Taylor & Francis Group, 2008.

[21] Yubin Jun; Seyoon Yoon ; Jae Eun Oh, "A Comparison Study for Chloride-Binding Capacity between Alkali-Activated Fly Ash and Slag in the Use of Seawater" , journal Appl. Sci. 2017; 7:971.

[22] Khater, H.M., "Influence of electric arc furnace slag on characterisation of the produced geopolymer composites", építôanyag , Journal of Silicate Based and Composite Materials, Sept. 2015; 67(3), 82-88, https://doi.org/10.14382/epitoanyag-jsbcm.2015.13.

[23] Khater , H.M.; Abd el Gawwad, H.A., " Synthesis and characterization of MK/Slag geopolymer composites enhanced by various ratios of nano kaolin" , építôanyag § Journal of Silicate Based and Composite Materials, August 2017; 69(2) :40–48, https://doi.org/10.14382/epitoanyag-jsbcm.2017.8.

[24] Han B; Yu X; Ou J.,"Multifunctional and smart carbon nanotube reinforced cement-based materials", Nanotechnology in Civil Infrastructure, Springer, 2011; 1:47.

[25] Collins, F.;Lambert, F.; Duan,W.H., "The influence of admixtures on the dispersion, workability, and strength of carbon nanotube–OPC paste mixtures", Cem Concr Compos., 2012; 34(9):1067–74.

[26] Weitzel, B; Hansen, MR; Kowald, TL;Müller, T; Spiess, HW; Trettin, HFR, "Influence of Multiwalled Carbon Nanotubes on the Microstructure of CSH-Phases" , In proceeding of 13th congress on the Chemistry of Cement, 3-8 july 2011, Madrid, Spain.

[27] El-Sayed, H. A.; Abo El-Enein, S. A.; Khater, H. M.; Hasanein, S. A., "Resistance of alkali activated water cooled slag geopolymer to sulfate attack", Ceramics – Silikáty, 2011; 55: 153–160.

[28] ASTM C1152, "Standard Test Method for Acid-Soluble Chloride in Mortar and Concrete", Annual Book of ASTM Standards; ASTM International: West Conshohocken, PA, USA, 2008.

[29] Saikia, N.; Usami, A.; Kato, S.; Kojima, T. "Hydration behavior of ecocement in presence of metakaolin", Resource Progressing Journal, 2004; 51: 35–41.

[30] Taha, A. S.; El-Didamony, H.; Abo.EL-enein, S. A.; Amer, H. A. "Physicochemical properties of supersulphated cement pastes", Zement-Kalk-Gips, 1981; 34:351–353.

[31] ASTM C109M "Standard Test Method for Compressive Strength of Hydraulic Cement Mortars", Annual Book of ASTM Standards; ASTM International: West Conshohocken, PA, USA ,2016.

[32] Alexandre Silva de Vargas; Denise.C.C. Dal Molin; Ângela.B. Masuero; Antônio.C.F. Vilela; Joao Castro-Gomes; Ruby M. Gutierrez, "Strength development of alkali-activated fly ash produced with combined NAOH and CA(OH)2 activators", cement and concrete composites, 2014; 53, 341-349.

[33] Bakharev, T., "Durability of geopolymer materials in sodium and magnesium sulfate solutions", Cement and Concrete Research, 2005; 35: 1233-1246.

[34] Puertas, F.; Palacios, M.; Manzano, H.; Dolado, J.S.; Rico, A.;Rodríguez, J., "A model for the C–A–S–H gel formed in alkali-activated slag cements". J Eur Ceram Soc., 2011; 31(12):2043–2056

[35] Garcia-Lodeiro, I.; Palomo, A.; Fernández-Jiménez, A.; Mac- Phee, D.E., "Compatibility studies between N–A–S–H and C–A–S–H gels. Study in the ternary diagram Na_2O– CaO–Al2O3–SiO2–H_2O", Cem Concr Res., 2011; 41(9):923–931.

[36] Rees, C.A.; Provis, J.L.; Lukey, G.C.; van Deventer, J.S.J.,"Attenuated total reflectance Fourier transform infrared analysis of fly ash geopolymer gel aging", Langmuir, 2007; 23(15):8170–8179.

[37] Kalinkin, A. M.; Politov, A. A.; Boldyrev, V. V.; Kalinkina, E. V.; Makarov, V. N.; Kalinnikov, V. T., "Study of Mechanical activation of Diopside in a CO_2 Atmosphere", J. Mater. Syn. Proc., 2002; 38: 163–167.

[38] Dai,Y.; Qian,G.; Cao, Y.; Chi, Y.; Xu, Y.; Zhou, J., "Effective removal and fixation of Cr(VI) from aqueous solution with Friedel's salt", J. Hazard. Mater., 2009; 170: 1086-1092.

[39] Jiang, X.; Kowald, T.; Staedler, T.; Trettin, R., “Carbon nanotubes as a new reinforcement material for modern cement-based binders”, RILEM Proceedings, 2nd International Symposium on Nanotechnology in Construction,2005; 209-213.

[40] Bernal, S.A.; Provis, J.L.; Rose, V.; Mejía de Gutiérrez, R., “Evolution of binder structure in sodium silicate-activated lag metakaolin blends”, Cem. Concr. Compos.,2011; 33(1):46–54.

[41] Huang, C. K.; Kerr, P. F., “Infrared study of the carbonate minerals”. Am. Mineral., 1960; 45: 311.

[42] Farmer, V. C., “The Infrared Spectra of Minerals”. London: Mineralogical Society,1974.

[43] Bernal, S.A.; Rodríguez, E.D.; de Gutiérrez, R.M.; Provis, J. L.; Delvasto, S., “Activation of Metakaolin/Slag Blends Using Alkaline Solutions Based on Chemically Modified Silica Fume and Rice Husk Ash”, Waste Biomass Valor,2012; 3:99–108.

[44] Rees, C. A. ; Provis, J. L.; Lukey, G. C., van Deventer, J. S. J., “The mechanism of geopolymer gel formation investigated through seeded nucleation”, Colloids Surf. A, 2008; 318: 97–105.

[45] Heister, E.; Lamprecht, C.; Neves, V.; Tîlmaciu, C.; Datas, L.; Emmanuel Flahaut, E., “Higher dispersion efficacy of functionalized carbon nanotubes in chemical and biological environments”. ACS Nano, 2010; 4(5):2615–26.

[46] Brown, P.W.; Bothe, J.V.,“The stability of ettringite”, Adv. Cem. Res.;1993; 5: 47–63.

[47] Famy, C., “Expansion of heat-cured mortars”, PhD Thesis, Univ. of London, 1999; 256p.

[48] Duxson, P.; Provis, J. L.; Lukey, G. C.; van Deventer, J. S. J. ; Separovic, F.; Gan, Z. H.,“39K NMR of Free Potassium in Geopolymers,” Ind. Eng. Chem. Res., 2006; 45 (26): 9208–10.

[49] Alarcon-Ruiz, L.; Platret, G.; Massieu, E.; Ehrlacher, A, “The use of thermal analysis in assessing the effect of temperature on a cement paste”, Cem. Concr. Res.,2005; 35(3): 609–613.

[50] Buchwald, A.; Tatarin, R.; Stephan, D., “Reaction progress of alkaline-activated metakaolin-ground granulated blast furnace slag blends”,J Mater Sci., 2009; 44:5609–5617.

[51] Engelhardt, G.; Felsche, J.; Sieger, P., “The Hydrosodalite System Na6+x[SiAlO4]6(OH)x.nH2O: Formation, Phase Composition, and De- and Rehydration Studied by 1H, 23Na, and 29Si MAS-NMR Spectroscopy InTandem with Thermal Analysis, X-ray Diffraction, and IR Spectroscopy,” J. Am. Chem. Soc., 1992;114: 1173–82.

[52] Luo, R.; Cai, Y.; Wang, C.; Huang, X., “Study of chloride binding and diffusion in GGBS concrete”, Cement and Concrete Research,2003; 33:1 –7.

[53] Khater, H.M.,“Influence of Metakaolin on Resistivity of Cement Mortar to Magnesium Chloride Solution”, J. Mater. Civ. Eng., 2011; 23(9): 1295-1301.

[54] Bonen, D., “A micro structural study of the effect of produced by magnesium sulfate on plain and silica fume-bearing Portland cement mortars”, Cement and Concrete Research, 1993; 23:541–553.

[55] Peyvandi, A; Soroushian, P.; Abdol, N, “Surface-modified graphite nanomaterials for improvedreinforcement efficiency in cementitious paste”, Carbon, 2013; 63: 175-186.

[56] Temuujin, J.; van Riessen, A.; Williams, R., “Influence of calcium compounds on the mechanical properties of fly ash geopolymer pastes”, J. Hazard. Mater., 2009; 167, (1–3), 82–88.

[57] Li, Y; Wang, P.; Zhao, X., “Mechanical behaviour and microstructure of cement composites incorporating surface-treated multi-walled carbon nanotubes”, Carbon, 2006; 43: 1239-1245.

[58] Duxson, P.; Mallicoat, S. W.; Lukey, G. C.; Kriven, W. M.; Van Deventer, J. S. J., “ mechanical properties of metakaolin-based geopolymers”, Colloids and Surfaces A – Physicochemical and Engineering Aspects,2006; 292:8–20.

Ref.:

Khater, H. M.– **El Nagar**, Abdeen: *Evaluation of chloride resistance of silica fume and glass waste MWCNT- geopolymer composite*
Építőanyag – Journal of Silicate Based and Composite Materials, Vol. 73, No. 2 (2021), 44–53. p.
https://doi.org/10.14382/epitoanyag-jsbcm.2021.8

Thermal conductivity of wood-plastic composites as insulation panels: theoretical and experimental analysis

Hadeel Mahmood MUSSA ▪ Mustansiriyah University, College of Engineering, Iraq
▪ hadeelmussa52@gmail.com
Tawfeeq Wasmi M. SALIH ▪ Mustansiriyah University, College of Engineering, Iraq
▪ tawfeeqwasmi@uomustansiriyah.edu.iq

Érkezett: 2020. 08. 30. ▪ Received: 30. 08. 2021. ▪ https://doi.org/10.14382/epitoanyag-jsbcm.2021.9

Hadeel Mahmood MUSSA
Is a university postgraduate student in Mustansiriyah University, Iraq. She is studying for a master degree in Engineering of Materials.

Tawfeeq Wasmi M. SALIH
Is a university teacher in Mustansiriyah University, Iraq. He has a Ph.D. in Mechanical Engineering. He teaches Insulation Materials and Heat Transfer and has many researches in renewable energies and energy efficient buildings.

Abstract

The aim of this study is evaluating the thermal performance of wood plastic composites (WPCs) as insulation panels depending on the values of thermal conductivity (k). Three types of wood flour taken from (pine, oak and walnut) trees with concentrations (10, 20, 30 %), and two types of thermoplastics; high density polyethylene (HDPE) and polypropylene (PP), have been selected for the evaluation. Theoretical work uses mathematical relations in the calculation of thermal conductivity of WPCs. Experimental work includes the manufacturing of the specimens, the measurements of k-values. The results show that the increasing in wood content leads to a reduction in k-values for WPCs by 6-8.5% for each 10% addition of wood. The k-values of WPCs tend to increase, when temperatures rise from 25-75 °C, by 20-25% for HDPE-wood composites, and by 15-20% for PP-wood composites. Furthermore, 10 % of water content will increase the k-value by 10-20%.

Keywords: wood, plastic, composite, thermal conductivity, insulation
Kulcsszavak: fa, műanyag, kompozit, hővezető képesség, szigetelés

1. Introduction

There are many technical solutions to decrease energy consumption and reduce greenhouse emissions, which is necessary also because of the need for the energy balance improving [1]. Thermal insulation is an essential part in the residential building to prevent heat transfer between outside and inside. Most of insulation materials are synthetic materials which consume extra sources of raw materials, and spend a lot of money and effort. Recently, many investigations have been developed to invest the natural materials or recycled materials. Wood plastic composites (WPCs) are relatively new family of composites and environmentally friend materials, where they can be manufactured from recycled plastics and waste woods. The wooden materials are usually: wood fiber, flour fiber, kenaf hemp and sisal. While, the plastics are usually: polyethylene (PE), polypropylene (PP), polyvinyl chloride (PVC) [2]. Wood contents in WPCs may reach 50% of the composition. The wood and thermoplastics are usually compounded above the melting temperature of the thermoplastic polymers and then further processed to make various products. WPC can be manufactured in a variety of shapes and sizes, and with different surface textures depending on the processing method [3]. Factors attributes to mechanical and thermal properties of WPCs depend on [4]: wood content, type of polymer, type of additives and processing temperature. Studies conducted in PWCs show that the presence of wood contents increases the thermal properties, i.e. thermal resistance [5]. On the other hand, the mechanical properties, i.e. tensile strengths, decrease with the increasing of wood fibers for a certain range [6].

Researchers have been looking for the development of plastics with natural wooden materials as reinforcement. In this context, wood is usually used as flour or fiber in the composition of composite material. Several promising studies [7-24] have taken place in the evaluation of thermal properties of wood plastic composites (WPCs), for several wood types, wood contents, and polymer types as well as additives contents. Most of the studies were experimental investigations, while some others were theoretical and numerical studies or models. The major outcome of the previous works, which related to thermal properties, had focused on the thermal stability of WPC material or the variation in phase change zone and the corresponding melting point, temperature of crystallization and glass transition temperature. Less concentration had taken place for the effect of wood content on the thermal conductivity. Hence, the present study focuses on the thermal conductivity as a preferable parameter in thermal resistance calculation. The present study includes both: theoretical and experimental works. The plan suggested three types of wood flour in different concentrations (10, 20 and 30 %) with two types of thermoplastics, high density polyethylene (HDPE) and polypropylene (PP).

2. Theoretical analysis

The coefficient of thermal conductivity is the most important property of any material which indicates whether it is an insulator or not. Material with relatively low thermal conductivity, less than 0.2 W/m.K, consider as a thermal insulator [25]. The reciprocal of thermal conductivity called thermal resistivity, which is a measure of material resistance to the heat transfer. The other thermal properties are: heat reflectivity, heat capacity, coefficient of thermal expansion, thermal stability and phase-change points.

Although several theoretical works have been conducted to determine the thermal conductivity of composite materials, there is still some inaccuracy in the predicted values due to several important parameters like: operational conditions (temperature and water content), particle features (size and distribution) as well as interface quality (adhesion). For this reason, some of these effects will be discussed through numerical simulations. The effective thermal conductivity of a composite material k depends on the thermal conductivities of both: the reinforcement kr and the matrix km, as well as concentration ϕ of each material. The simplest model assumes that the particles are placed in series manner with respect to the heat flow direction. This gives [26];

$$k = k_r \O_r + k_m \O_m \tag{1}$$

The coefficient of thermal conductivity mainly depends on: temperature, water content and some other thermo-physical properties of the material [27]. The thermal conductivity is measured in W/m.K. In general, the material with a small k-value is a good thermal insulator; on the other hand, the material with a large k-value is a good heat conductor.

2.1 Temperature rise effect

In the case of solid materials, the variation of thermal conductivity due to the change in medium temperature predominantly depends on electronic effect. The coefficient of thermal conductivity is affected by heat transport characteristics, where the microstructure of molecules affects the heat transfer. Thermal conductivity is proportional to the pore size; smaller pores will lead to lower heat conductivity [28].

In general, as temperature increases, both number of free electrons and lattice vibrations increase. Thus the thermal conductivity of the material is expected to increase. Many studies have shown that thermal conductivity of wooden materials increases with the temperature rise for a certain range, as shown in *Fig. 1* [29].

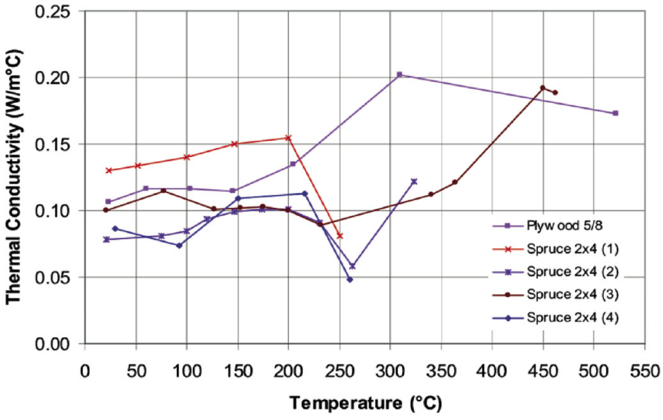

Fig. 1 *Variation of thermal conductivity with the temperature for some wooden materials [29]*

1. ábra *A hővezető képesség változása a hőmérséklet függvényében különböző faanyagok esetében [29]*

Prisco U. (2014) [14] has shown that, in wooden materials, the thermal conductivity has general linear increasing as temperature increases before degradations, as following;

$$k = k_o + 1.9 \times 10^{-4}\, T \tag{2}$$

Where ko refers to the initial k-value for the selected wood in the study in a limitation of temperature not exceeds 80 °C.

Heat conduction in polymers is considered as the propagation of anharmonic elastic waves through a continuum. The temperature dependent term is interpreted as the intrinsic thermal conductivity due to the Umklapp process (an anharmonic phonon–phonon scattering process), and the temperature independent term as conductivities due to the collective contribution of all point defect scattering terms. The conductivity decreases with temperature increase because "Anharmonic Umklapp" process becomes more frequent, and hence the phonon mean free path decreases [30]. Many recent investigations [30-32] indicated that, for crystalline polymeric materials, the thermal conductivity has reciprocating relation with respect to the temperature rise. The direct effect of temperature rise on the thermal conductivity of polymers is studied efficiently in reference [33], where the study presented the behavior of some polymers, as shown in *Fig. 2*. It can be concluded, from these studies, that the relationship between the thermal conductivity and the temperature may have the simple linear interpolation formula:

$$k = k_o - m\, T \tag{3}$$

Where, ko is the reference k-value at standard conditions. While, m is the index of variation and it has different values from polymer to another.

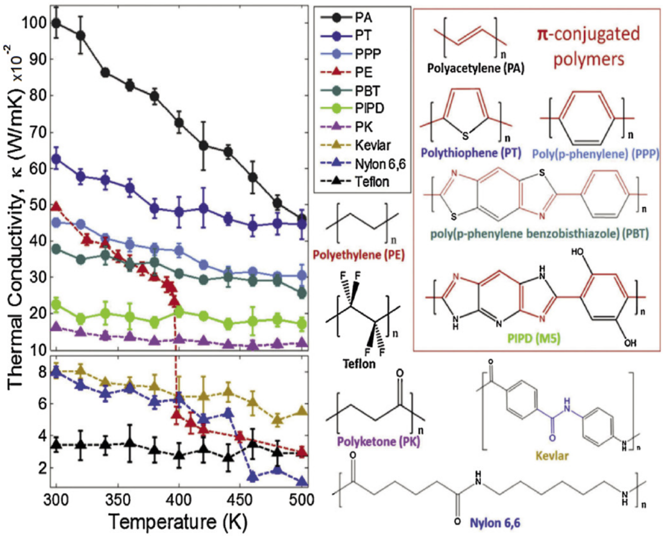

Fig. 2 *Variation of thermal conductivity with the temperature for some polymers [33]*

2. ábra *A hővezető képesség változása a hőmérséklet függvényében különböző polimerek esetében [33]*

2.2 Water content effect

In humid conditions, materials absorb moisture from the air, and that causes to crack, less resistance and failure [34]. When material absorbs moisture, heat begins to leak. It is noticed that the increasing of water content increases the density of the material, thus the thermal conductivity. This behavior has been extracted from many investigations [35-40]. A study conducted by Goss W. and Miller R. (1992) [39] to investigate the effect of water content on the thermal conductivity of wood has proposed the following formula;

$$k = k_o + 0.004\,w \qquad (4)$$

Where ko refers to the initial k-value for the selected wood in the study, while w is the water content up to 20% limit. This behavior is in line with a study carried out by Kawasaki T. and Kawai S. (2006) [40], where the increasing in the value of thermal conductivity for ply sandwich wood (PSW) with density range between 100–800 kg/m^3 was about 10-25% for a water content ranged between 5–10%.

3. Experimental work

In the current study, composite materials made of recycled wood and plastic, known as wood-plastic composites (WPCs), have proposed as thermal insulation materials. For this purpose, an experimental work has been done to manufacture and evaluate the thermal performance of WPCs as thermal insulations. The work includes collecting a group of materials (some woods and some plastics) and manufacturing a set of specimens with different mixing ratios, as well as different conditions. The tests include measuring the coefficient of thermal conductivity in room temperature and when temperature rises for certain ranges as well as water content.

3.1 Materials

A bunch of dried wood samples has been collected from the local market and this includes: Pine Wood (PW), Oak Wood (OW) and Walnut Wood (WW). It is worth noting that these samples of wood must be cut, spread, dried and grinded in order to obtain pure wood flour, as shown in *Fig. 3*.

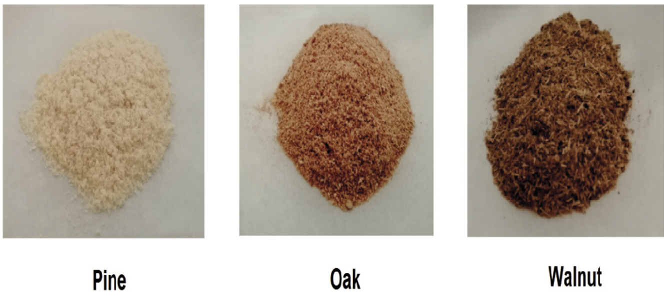

Fig. 3 Wood flour used in the study
3. ábra A tanulmányban használt fa őrlemények

Initially, some solid samples of the woods had taken to calculate their densities, by measuring both: volume (by ruler) and mass (by weight scale). These values have been compared with average values that taken from reliable sources [41-43], as shown in *Table 1*. The comparison indicates a slight percentage of variation and that is mostly due to the difference in the features of wood.

Wood type	Density (g/cm^3) as solid [41-43]	% Variation to the type used
Pine Wood (PW)	0.45	+11 %
Oak Wood (OW)	0.70	+6 %
Walnut Wood (WW)	0.78	+5 %

Table 1 Densities of woods
1. táblázat A vizsgált faanyagok sűrűsége

Other thermo-physical properties such as: specific heat, thermal conductivity and degradation temperature, are shown in *Table 2*.

Wood type	Specific heat (J/kg.K)	Thermal conductivity (W/m.K)	Degradation Temp. (°C)
Pine Wood (PW)	1500-1800	0.12-0.13	200-235
Oak Wood (OW)	2000-2400	0.14-0.16	200-220
Walnut Wood (WW)	2000-2400	0.17-0.19	200-225

Table 2 Some properties of woods from references [43-45]
2. táblázat A vizsgált faanyagok fontosabb tulajdonságai az irodalom alapján [43-45]

Thermoplastics that have melting point less than wood degradation temperature are commonly used with WPCs. Two types of thermoplastic materials have been purchased from the local market, which are: High Density Polyethylene (HDPE) and Polypropylene (PP). In order to ensure sufficient wood-plastic composites, granular raw materials of these plastics have been used, as shown in *Fig. 4*.

Fig. 4 Plastic grains used in the study
4. ábra A vizsgálat műanyag szemcsék

Initially, some solid pieces of these types of plastics were formed using the oven with certain dimensions, where their volumes and weights have been measured to calculate the density, as shown in *Table 3*. The average values that extracted from references [46-48] indicated an acceptance percentage of variation due to the difference in the features of plastics. Other thermo-physical properties, would be useful in the study, are shown in *Table 4*.

Plastic type	Density (g/cm^3) as solid [46-48]	% Variation to the type used
High density polyethylene (HDPE)	0.95	+1 %
Polypropylene (PP)	0.90	+2 %

Table 3 Densities of plastics
3. táblázat A vizsgált műanyagok sűrűsége

Plastic type	Specific heat (J/kg.K)	Thermal conductivity (W/m.K)	Melting point (°C)
High density polyethylene (HDPE)	2000-2500	0.44-0.48	140-160
Polypropylene (PP)	1500-2000	0.19-0.22	160-180

Table 4 Some properties of plastics from references [49-53]
4. táblázat A vizsgált műanyagok fontosabb tulajdonságai az irodalom alapján [49-53]

The variation in the thermo-physical properties of polymers is attributed to the features of type used which may be commercial or in accordance to a standard code. However, it is easy to recognize a certain type of polymer by comparing the values of several properties where there is similarity in the whole type used.

3.2 Manufacturing

The experimental work included manufacturing several specimens using different compositions of wood and plastic at different conditions. The work has conducted at Chemical Lab in Materials Engineering Department, Mustansiriyah University. Several devices and instruments have been used like, oven, thermometer, weight scale and molds. Some tools and auxiliaries have been used as well.

The majority of WPC researches suggested considering an amount of wood less than that of plastic to ensure sufficient bonding between the two components, thus the current study assumed a wood content not more than 30 % of the total weight. The wood was oven dried at 80 °C for 2 hours before processing to remove the moisture content (No more than 5%). However, WPC specimens prepared in the current study with their mixing ratios are shown in *Table 5*.

WPC type	Mixing ratio (%)	No. of specimens
HDPE	100	2
HDPE-PW	90-10, 80-20, 70-30	6
HDPE-OW	90-10, 80-20, 70-30	6
HDPE-WW	90-10, 80-20, 70-30	6
PP	100	2
PP-PW	90-10, 80-20, 70-30	6
PP-OW	90-10, 80-20, 70-30	6
PP-WW	90-10, 80-20, 70-30	6

Table 5 Mixing ratios of WPC specimens used in the study
5. táblázat A vizsgálatban használt WPC minták keverési arányai

For each WPC, two samples have manufactured for thermal conductivity test. Furthermore, four specimens have manufactured for temperature rise tests, and four specimens for water content tests. Besides that, three specimens have manufactured for pure wood evaluation. Thus, the total quantity reached to (51) specimens.

The desired quantities for each specimen components have weighted and combined in well mixing procedure, where two stages have proposed to ensure homogenous product as much as possible. In the first stage, some of the wood flour has mixed with the plastic grains in a bowl and then pour the mixture into a sheet of parchment paper to insert it easily to the oven for a period of time till the melting point. After that, the second stage of mixing is beginning by spreading the rest of the wood flour into the melted plastic and rolling it carefully. The oven used in the study is assigned for polymer melt-works which has the brand Jrad, with Italian thermostat operates up to 250 °C, as shown in *Fig. 5*.

Fig. 5 Oven used in the study
5. ábra A vizsgálatokhoz használt kemence

The period that the plastic grains spent in the oven to get melting, starting from room temperature, was ranged between 20-25 minutes at a constant rate of heat (10 °C/min). After that, the molten plastic-wood paste has ejected from the oven and inserted into the mold which has the dimensions: 5×5×1 cm^3. The paste of wood-plastic should be pressed in the mold using an appropriate cap which holds a weight of 2 kg and for a period of 10 minutes. The advantage of pressing is to strengthen the produced specimen during heat transfer process in the product to ensure sufficient WPC formation. Parchment paper or aluminium foil could be used in the base of the mold to extract the specimens easily. Finally, the specimens should be exposed to the still air for a period of 5 minutes for cooling.

Measurements of thermal conductivity require specimens have circular shapes of 42 mm diameter. Therefore, the manufactured specimens should be cut using a circular hole-saw. The final shapes of specimens are shown in *Fig. 6*.

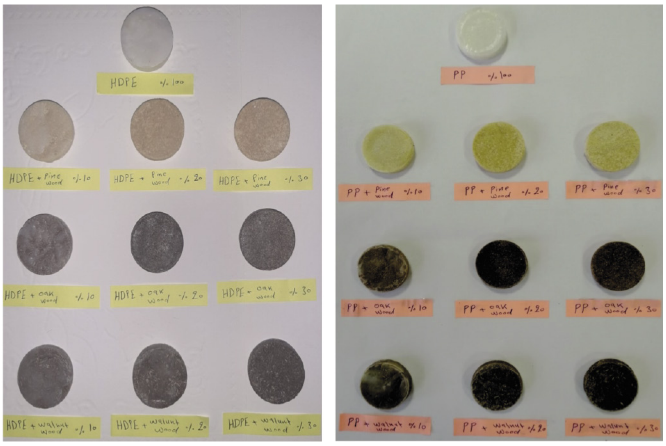

Fig. 6 Final shapes of WPC specimens (left: HDPE-wood; right: PP-wood)
6. ábra A WPC minták végső formája (balra: HDPE-fa; jobbra: PP-fa)

3.3 Measurements of thermal conductivity

The measurements of thermal conductivity for the specimens have conducted at the laboratory of Materials Research Department in Ministry of Science and Technology (MOST) according to ASTM C518 – 04, using Lee's disc apparatus, as shown in *Fig. 7*.

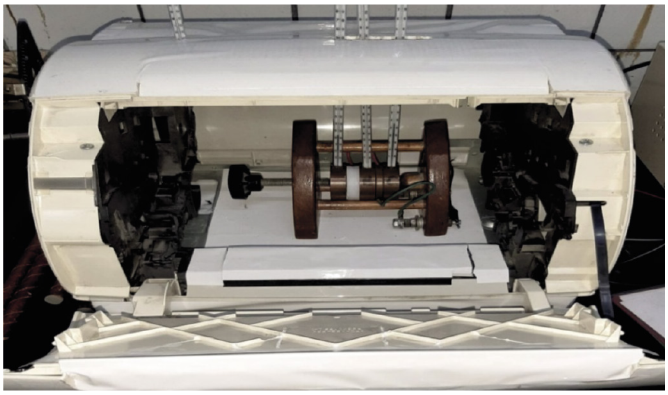

Fig. 7 Specimen is placed in the apparatus between hot and cold discs
7. ábra A készülékbe helyezett minták meleg és hideg lemezek között

The device consists of a chamber and a reader. The chamber has an electric heater, and there is a group of discs where the specimen should be placed between the hot and cold discs. The chamber has sufficient thermal insulation. The electric circuit was switched on until the equilibrium condition is reached. The reader recorded the temperatures across the specimen using sensors connected to a thermometer. The recorded values have compensated in a special equation approved for this device.

Since the produced WPC is assigned for residential applications (thermal insulation), thus the surface temperature on the hot side was limited not to exceed 80°C. It is important to refer here, that the thermal conductivity of pure solid wood specimens of (pine, oak and walnut) has measured as well in the same procedure. Furthermore, extra specimens of HDPE-PW and PP-PW, 10%, 20% and 30% wood content, have been selected for temperature rise tests. Moreover, four specimens of HDPE-PW and PP-PW, 30% wood content, have been selected for water content tests at 10% and 20% water content. For this purpose, the wood flour should be put in the water for certain period of time (several days) to insure increasing in wood mass due to water content by 10% or 20%.

4. Results and discussion

The thermal conductivity (k-value) is the property which indicates whether the material is a good insulator or not. The thermal conductivity of WPCs has been investigated in three situations; standard conditions, temperature rise effect and water content effect.

4.1 Standard k-values of WPCs

In general, the increasing in wood content leads to a reduction in k-value for WPC material because k-value of wood is less than that of polymer, thus the overall k-value of the composite tends to decrease. This decreasing was linear, as shown in *Figs. 8-13*. For HDPE-wood composites, it is noticed that there is a significant reduction in k-value when pine wood is used, due to the low k-value for pine wood (k=0.12 W/m.K) in compare to oak wood (k=0.15 W/m.K) and walnut wood (k=0.17 W/m.K). Theoretically, the reduction in k-value of HDPE-wood composite for every 10% addition of wood was about 8.5% when pine wood is used. On the other hand, it was 6.8% when oak wood is used. Furthermore, the using of walnut wood gave 6.2% reduction in k-value. This amount of increasing is going to be double when there is 20% addition of wood, or triple when there is 30% addition of wood. For PP-wood composites, the reduction in the k-value by the increasing of wood content was small (3-4%) due to the fact that k-value of pure PP raw material is basically low (k=0.22 W/m.K) compared to that of HDPE (k=0.48 W/m.K). Hence, the addition of wood to PP has less reduction in k-value. So, it is concluded that the technique of WPC is useful with plastics that have relatively high k-values (more than 0.3 W/m.K) such as; HDPE, LDPE and PA in order to get clear benefits of wood addition, thus reasonable results. The experimental k-values of HDPE-wood composite were lower than that calculated theoretically by a range of 1-6%, while for PP-wood composites they were higher by 1%. The difference between experimental and theoretical values is due to the inaccuracy of mathematical equation used, since it is a simple relation, as well as a percentage of error in experimental readings. However, the range of difference was slight.

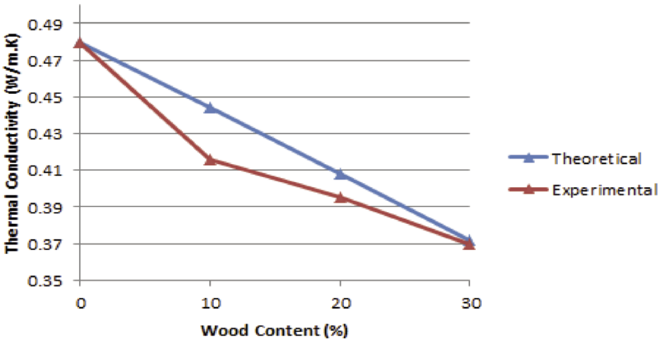

Fig. 8 Standard k-values for HDPE-PW
8. ábra A HDPE-PW szabványos k-értékei

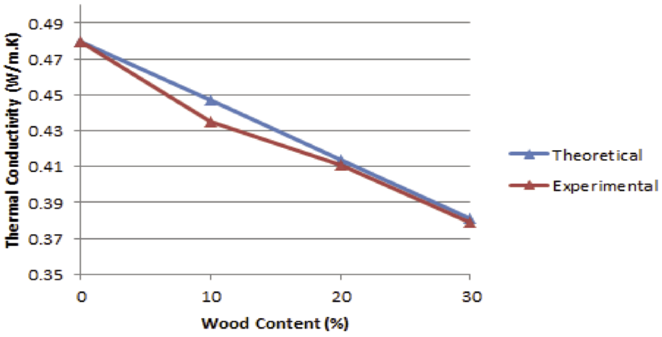

Fig. 9 Standard k-values for HDPE-OW
9. ábra A HDPE-OW szabványos k-értékei

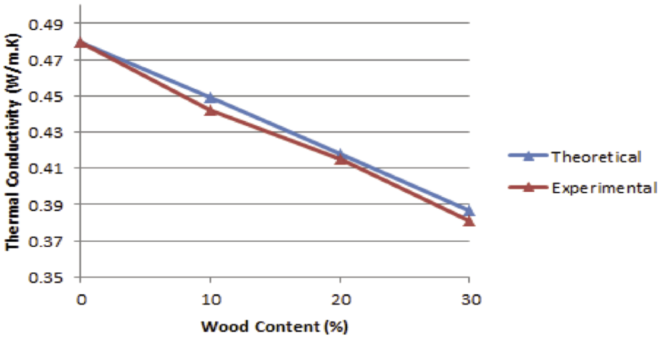

Fig. 10 Standard k-values for HDPE-WW
10. ábra A HDPE-WW szabványos k-értékei

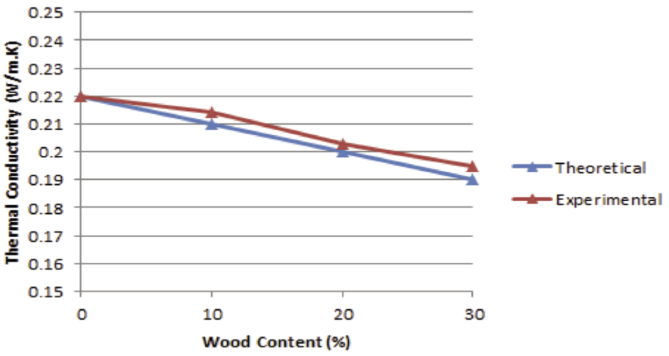

Fig. 11 Standard k-values for PP-PW
11. ábra A PP-PW szabványos k-értékei

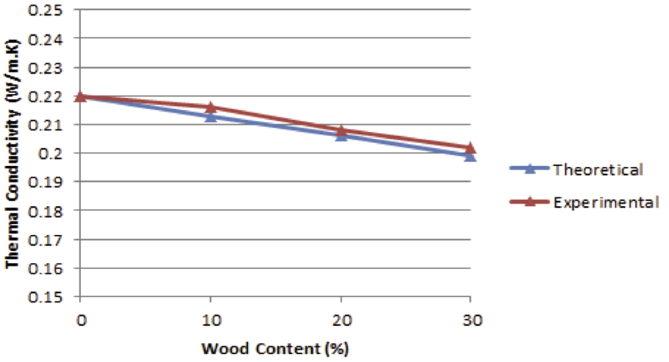

Fig. 12 Standard k-values for PP-OW
12. ábra A PP-OW szabványos k-értékei

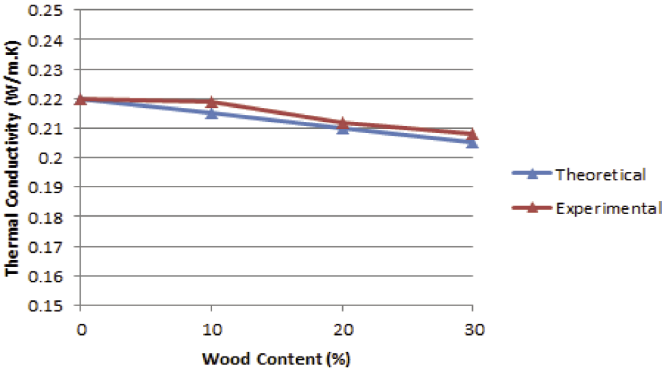

Fig. 13 Standard k-values for PP-WW
13. ábra A PP-WW szabványos k-értékei

4.2 Effect of temperature rise on k-valves

As mentioned theoretically, that the temperature rise has a negative impact on k-value of the wood and a positive impact on k-value of the polymer. Where k-value of wood increases proportionally when temperature rises for a certain range. On the other hand, k-value of polymer has a reciprocating relationship with temperature rise. Since the majority of the composition of WPC is polymer, hence the k-value of WPC tends to decrease with temperature rise. This theoretical behavior can be noticed clearly, as shown in *Figs. 14-19*, for HDPE-PW composites and PP-PW composites, where the temperature range was not exceeded 75 °C. The experimental results gave a contradictory behavior for the effect of temperature rise on k-value of WPCs. Where, the k-value of WPC tends to increase with temperature rise due to the presence of H_2O which evaporated from the wood and filled the cavities, where $k_{vapor} > k_{air}$, thus increasing in the overall k-value of the composite material without focusing on the side of the majority of the polymer in the composition of WPC. So, it is very important to modify the mathematical equation that describes the k-value of WPC by adding the temperature rise effect in the consideration. Experimentally, the temperature rise from 25-75 °C leads to an increase in k-value by 20-25% for HDPE-PW composites, and by 15-20% for PP-PW composites. These percentages are effective and may increase further if extra wood content is included, thus it is recommended (in high temperatures) to use relatively low amount of wood comparing to the polymer in the composition of WPCs, if there is no stabilizers or coupling agents used.

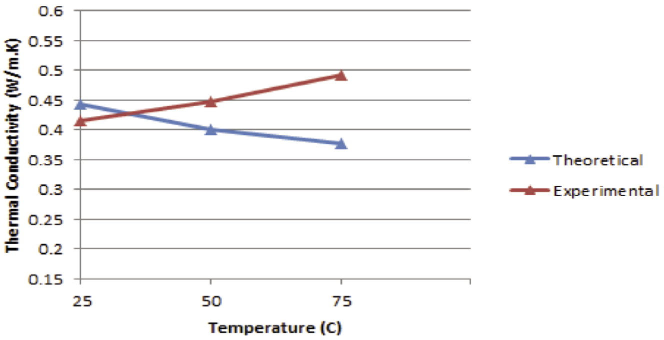

Fig. 14 Effect of temperature on k-values for HDPE-10%PW
14. ábra A hőmérséklet hatása a k-értékére HDPE-10%PW esetén

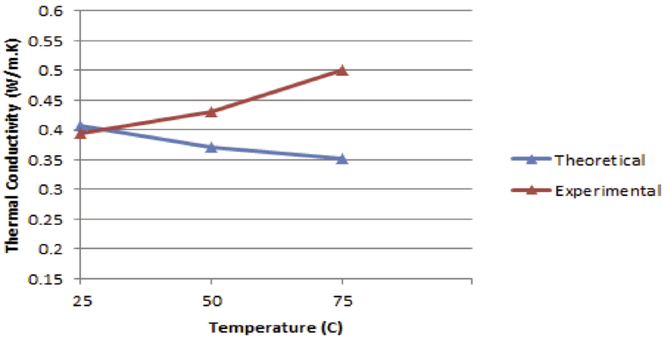

Fig. 15 Effect of temperature on k-values for HDPE-20%PW
15. ábra A hőmérséklet hatása a k-értékére HDPE-20%PW esetén

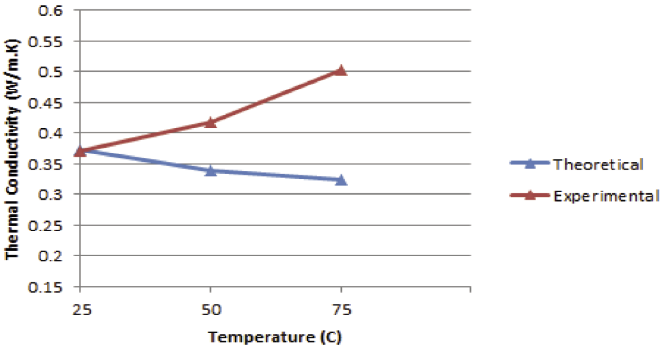

Fig. 16 Effect of temperature on k-values for HDPE-30%PW
16. ábra A hőmérséklet hatása a k-értékére HDPE-30%PW esetén

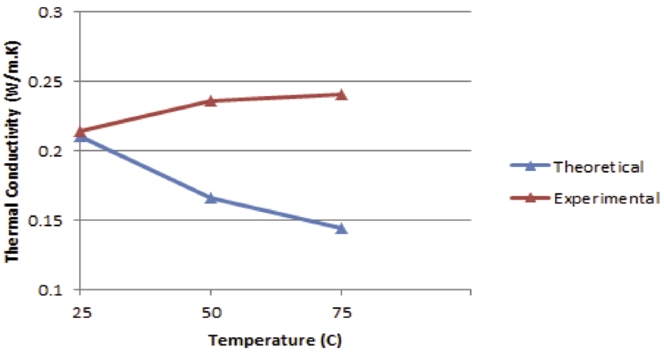

Fig. 17 Effect of temperature on k-values for PP-10%PW
17. ábra A hőmérséklet hatása a k-értékére PP-10%PW esetén

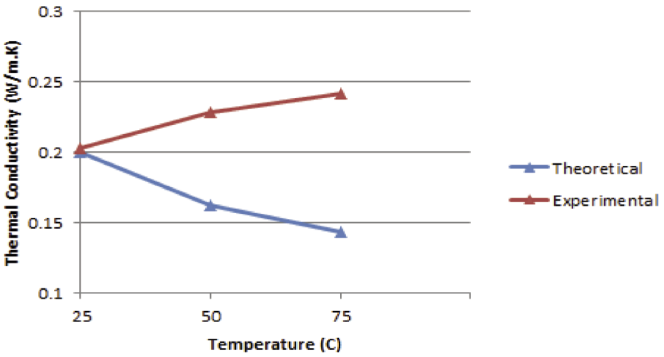

Fig. 18 Effect of temperature on k-values for PP-20%PW
18. ábra A hőmérséklet hatása a k-értékére PP-20%PW esetén

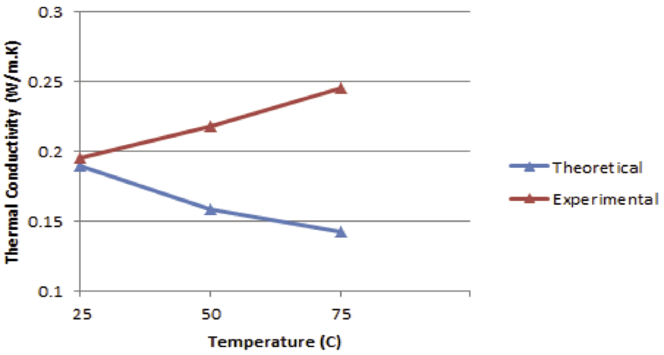

Fig. 19 Effect of temperature on k-values for PP-30%PW
19. ábra A hőmérséklet hatása a k-értékére PP-30%PW esetén

4.3 Effect of water content on k-values

The presence of water content in the wood will increase its k-value, because water molecules will fill the cavities, and since $k_{water} > k_{air}$ that means increasing in the overall k-value of the composite material. In this test, readings were taken at different percentages of water content (5, 10, 20%) in the pine wood mixed with either HDPE or PP. It is clearly that the increasing in the water content leads to increase the k-value of WPCs, as shown in *Figs. 20* and *21*. The increase in k-value of HDPE-PW composite was about 15-20% for each 10% addition of water content, and it was about 10-15% for PP-PW composite. The experimental results were relatively higher than the theoretical due to the fact that wet wood flour has spread over the entire WPC composition thus impacted more on the k-values. As a result, it is concluded that water content is undesired parameter because it has a negative impact on the k-value of WPC insulation panel.

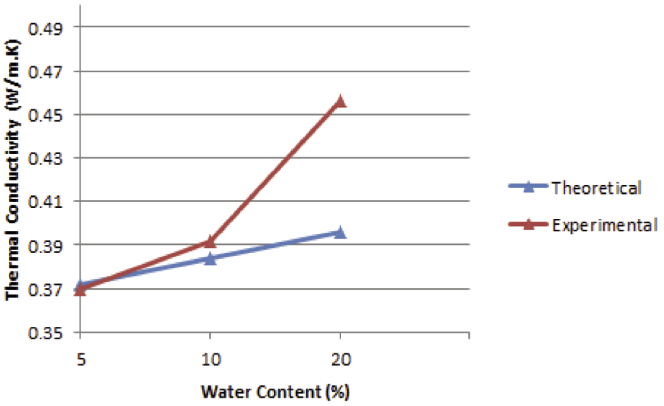

Fig. 20 Effect of water content on k-values for HDPE-30%PW
20. ábra A víztartalom hatása a k-értékére HDPE-30%PW esetén

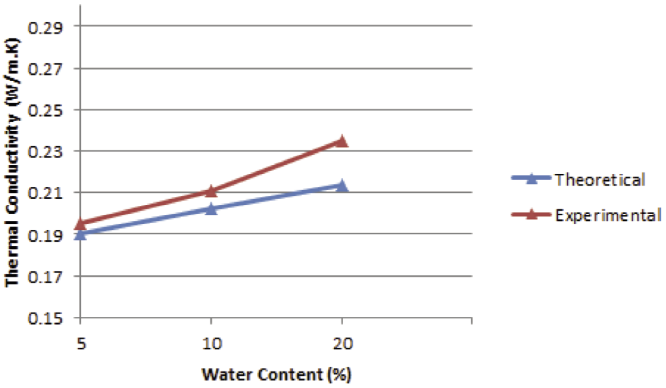

Fig. 21 Effect of water content on k-values for PP-30%PW
21. ábra A víztartalom hatása a k-értékére PP-30%PW esetén

5. Conclusions

Wood plastic composites (WPCs) that manufactured from waste wood and recycled plastics have possessed some advantages since they are renewable and environmentally fried, and present some desired thermo-physical properties. They are easy in manufacturing and can be produced as thermal insulation panels with a wide range of applications in the field of constructions, facilities and equipment. However, some specific points could be concluded from the recent study as following:

- The increasing in wood content leads to a decrease in k-value for WPC material because k-value of wood is less than that of polymer.
- The decrease in k-value of WPC was 6-8.5% for each 10% addition of wood.
- The k-value of WPC tends to increase with temperature rise due to the presence of H2O which evaporated from the wood and filled the cavities, thus increasing in the overall k-value of the composite material.
- The temperature rise from 25-75 °C leads to an increase in k-value by 20-25% for HDPE-PW composites, and by 15-20% for PP-PW composites. These percentages are effective and may increase further if extra wood content is included.

- It is important to modify the mathematical equation that describes the k-value of WPC by adding the temperature rise effect in the consideration.
- The presence of water content in the wood will increase its k-value, because water molecules will fill the cavities, and since $k_{water} > k_{air}$.
- The increase in k-value due to water content in HDPE-PW composite was about 15-20% for each 10% addition of water content, and it was about 10-15% for PP-PW composite.

Acknowledgments

Authors are grateful to all support given by College of Engineering, Mustansiriyah University for academically support.

References

[1] Komlós Ferenc, "Heat insulation and heat pump systems", Építőanyag – Journal of Silicate Based and Composite Materials, Vol. 60, No. 3, P.78–86, 2008. https://dx.doi.org/10.14382/epitoanyag-jsbcm.2008.14

[2] Tabarsa T., Khanjanzadeh H., Pirayesh H., "Manufacturing of wood-plastic composite from completely recycled materials", Key Engineering Materials, Vols. 471-472, Pages 62-66, 2011, https://doi.org/10.4028/www.scientific.net/KEM.471-472.62

[3] Adam T., Vikram Y., Karl R., David H., "Wood plastic composites - a primer", Washington State University, PB 1779, 2010

[4] Andre S., "Wood plastic composites (WPCs) as an alternative to solid lumber", Thesis, University of British Columbia, 2011

[5] João B., Carlos M., Fernando C., Raul F., "Influence of different thermoplastic polymer/wood ratios on the mechanical and thermal properties of composite materials", Procedia Engineering, 200, 480–486, 2017, https://doi.org/10.1016/j.proeng.2017.07.067

[6] Wolcott M., Englund K., "A technology review of wood plastic composites", 33rd International Particleboard/Composite Materials Symposium, Washington State University, Pages 103-110, 1999

[7] John Z., Qinglin W., Ioan I., "Surface and interfacial characterization of wood-PVC composites: Thermal and dynamic mechanical properties", Wood and Fiber Science, 36(4), Pages 500–510, 2004

[8] Alireza Kaboorani, "Effects of formulation design on thermal properties of wood/thermoplastic composites", Journal of Composite Materials, Vol. 44, No. 18, Pages 2205-2215, 2010, https://doi.org/10.1177/0021998309360938

[9] Song G., Qiu-yi L., Yi-wen Z., "Experimental research on the thermal insulation and flame retardancy performance of WPC wallboard made of paper-aluminum-plastics wastes", Applied Mechanics and Materials, Volumes 34-35, Pages 1676-1680, 2010

[10] Diene N., Laurent M., Sandrine M., Loıc V., Adams T., Jean-Luc G., "Thermal and mechanical properties of polypropylene/wood-flour composites", Journal of Applied Polymer Science, Vol. 119, Pages 3321–3328, 2011, https://doi.org/10.1002/app.32985

[11] Thanate R., Natchayapa T., Chatree H., "Mechanical and thermal properties of oil palm wood sawdust reinforced post-consumer polyethylene composites", ScienceAsia, 38, Pages 289–294, 2012

[12] Yiqun F., Qingwen W., Xiaoyan B., Weihong W., Paul A., "Thermal and burning properties of wood flour poly (vinyl chloride) composite", J Therm Anal Calorim, 109:1577–1585, 2012, https://doi.org/10.1007/s10973-011-2071-y

[13] Karim B., Bernard R., Denis R., "Effect of temperature on the thermal conductivity of wood-plastic composites", Polymers & Polymer Composites, Vol. 21, No. 7, 2013

[14] Prisco U., "Thermal conductivity of flat-pressed wood plastic composites at different temperatures and filler content", Sci Eng Compos Mater, 21(2), Pages 197–204, 2014

[15] Mazzanti V., Mollica F., El Kissi N., "Rheological and thermal properties of PP-based WPC", Times of polymers and composites, AIP Conference, Pages 274-277, 2014

[16] Hossain M., Shoumya N., Islam M., "Effect of types of wood on the thermal conductivities of wood saw dust particle reinforced composites", 10th International Conference on Mechanical Engineering, ICME 2013, Procedia Engineering, 90, Pages 46 – 51, 2014

[17] Rafel R., Josep P., José M., Jordi G., Francesc X., Gerard A., Pere M., "Orange wood fiber reinforced polypropylene composites: Thermal properties", Bioresources, 10(12), Pages 2156-2166, 2015

[18] Patrick Z., Elke M., Andre G., Torsten T., Antje L., "Synthesis of polyamide 6/11 copolymers and their use as matrix polymer in wood-plastic composites", Journal of Applied Polymer Science, 44155, Wiley, 2016, https://doi.org/10.1002/app.44155

[19] Alperen K., Turker G., Seyyed H., Nadir A., "Physical, mechanical and thermal properties of wood/zeolite/plastic hybrid composites", Maderas, Ciencia y tecnología, 19(3): 339 - 348, 2017

[20] Chung M., Park J., "An experimental study on the thermal performance of phase-change material and wood-plastic composites for building roofs", MDPI, Energies, 10 (195), 2017

[21] Shirley S., Leigh M., Tim G., Adrian K., "Properties of nylon-6-based composite reinforced with coconut shell particles and empty fruit bunch fibres", Plastics, Rubber and Composites, T&F, VOL. 47, NO. 2, Pages 77–86, 2018, https://doi.org/10.1080/14658011.2017.1418711

[22] Yong G., Shiliu Z., Yuxia C., Dagang L, "Thermal properties of wood-plastic composites with different compositions", Materials, MDPI, 12:881, 2019

[23] Xingli Z., Jinglan Z., Ruihong W., "Thermal and mechanical behavior of wood plastic composites by addition of graphene nanoplatelets", MDPI, Polymers, 11, 1365, 2019

[24] Jawad Lamyaa Abd Alrahman, Salih, Tawfeeq Wasmi M., "An investigation into practical values of sound transmission loss across natural luffa fibers", Építőanyag – Journal of Silicate Based and Composite Materials, Vol. 72, No. 3 (2020), P. 106–109 https://doi.org/10.14382/epitoanyag-jsbcm.2020.17

[25] Tawfeeq W. Salih, "Insulation materials", Bachelor Notes, University of Mustansiriyah, 2017

[26] Idicula M., Boudenne A., Umadevi L., Ibos L., Candau Y., Thomas S., "Thermophysical properties of natural fiber reinforced polyester composites", Comp. Sci. Tech., 66 (15), Pages 2719- 2725, 2006, https://doi.org/10.1016/j.compscitech.2006.03.007

[27] Zhang Z., "Effect of temperature on rock fracture", Rock Fracture and Blasting: Theory and Applications, Elsevier, Pages 111-133, 2016

[28] Hahn W., Özişik M., "Heat conduction", 3rd Ed., Wiley, 2012

[29] Benichou N., Sultan M., Maccallum C., Hum J., "Thermal properties of wood, gypsum and insulation at elevated temperatures", IR-710, NRC-CNRC, Canada, 2001

[30] Kingery W., McQuarrie M., "Thermal conductivity: I - concepts of measurement and factors affecting thermal conductivity of ceramic materials", J. Am. Ceramic Soc. 37 (2), 67, 1954

[31] Dos Santos W., De Sousa J., Gregorio R., "Thermal conductivity behaviour of polymers around glass transition and crystalline melting temperatures", Polymer Testing, 32, 987–994, Elsevier, 2013, https://doi.org/10.1016/j.polymertesting.2013.05.007

[32] Hongyu C., Valeriy G., Jian Y., Yunfeng Y., Wei L., Yan H., Libo D., Bin C., "Thermal conductivity of polymer-based composites: Fundamentals and applications", Progress in Polymer Science, Volume 59, Pages 41-85, 2016

[33] Zhang T., Wu X., Luo T., "Polymer nanofibers with outstanding thermal conductivity and thermal stability: fundamental linkage between molecular characteristics and macroscopic thermal properties", J Phys Chem C, 118:21148–59, 2014

[34] Gong B., Youping T., Yiyang Z., Ruihai L., Fuzeng Z., Zhuo X., Dong L., "Moisture absorption characteristics of silicone rubber and its effect on dielectric properties", Annual Report Conference on Electrical Insulation and Dielectric Phenomena, IEEE, 2013

[35] Shida S., Okuma M., "Dependency of thermal conductivity of wood based materials on temperature and moisture content (in Japanese), Mokuzai Gakkaishi, 26:112–117, 1980

[36] Zheng L., Zi L, Cheng L., Chen-jun G., Zhi-cheng G., Wang L., "Test & research of water absorption & water permeation of composite insulator HTV silicone rubber material", Shaanxi Electric Power, Vol. 40, No. 7, Pages. 14-18, 2012

[37] Jerman M. and Robert C., "Effect of moisture content on heat and moisture transport and storage properties of thermal insulation materials", Elsevier, Energy and Buildings 53, Pages 39–46, 2012, https://doi.org/10.1016/j.enbuild.2012.07.002

[38] Ochs F., Heidemann W. and Muller-Steinhagen H., "Effective thermal conductivity of moistened insulation materials as a function of temperature", Elsevier, International Journal of Heat and Mass Transfer, 51, Pages 539–552, 2008

[39] Goss W., Miller R., "Thermal properties of wood and wood products", Proceedings of the Thermal Performance of the Exterior Envelopes of Whole Buildings International Conference, Pages 193-203, 1992

[40] Kawasaki T., Kawai S., "Thermal insulation properties of wood-based sandwich panel for use as structural insulated walls and floors", The Japan Wood Research Society, J. Wood Sci, 52:75–83, 2006

[41] Henry M., A. Besnard, W. Asante, J. Eshun, S. Adu-Bredu, R. Valentini, M. Bernoux, L. Saint-Andre, "Wood density, phytomass variations within and among trees, and allometric equations in a tropical rainforest of Africa", Forest Ecology and Management, 260, Pages 1375–1388, 2010

[42] The Engineering ToolBox, "Density of various wood species", accessed on 15/11/2019 https://www.engineeringtoolbox.com/wood-density-d_40.html

[43] Glass S., Zalinka L., "The wood handbook: Wood as an engineering material, Chapter 4: Moisture relations and physical properties of wood", General Technical Report, USA, 2010

[44] Poletto M., Dettenborn J., Pistor V., Zeni M., Zattera A., "Materials produced from plant biomass, Part I: Evaluation of thermal stability and pyrolysis of wood", Materials Research, 13 (3), Pages 375-379, 2010, https://doi.org/10.1590/S1516-14392010000300016

[45] Poletto M., "Thermogravimetric analysis and kinetic study of pine wood pyrolysis", Brazilian Journal of Wood Science, 7(2), Pages 111-118, 2016

[46] Polymer Properties Database, accessed on 19/11/2019 http://polymerdatabase.com/polymer%20physics/Polymer%20Density.htm

[47] Scientific Polymers, Inc., accessed on 28/11/2019 https://scientificpolymer.com/density-of-polymers-by-density

[48] The Engineering ToolBox, "Polymers-Physical properties", accessed on 5/12/2019 https://www.engineeringtoolbox.com/polymer-properties-d_1222.html

[49] Dos Santos W., De Sousa J., Gregorio Jr., "Thermal conductivity behaviour of polymers around glass transition and crystalline melting temperatures", Polymer Testing, 32, Pages 987–994, 2013

[50] Bernd W., Michael H., Frank S., "Thermal conductivity, thermal diffusivity, and specific heat capacity of particle filled polypropylene", Composites Part A: Applied Science and Manufacturing, Volume 35, Issue 4, Pages 423-429, Elsevier, 2004

[51] Xue L., Lope G., Ikechukwuka N., Satyanarayan P., "Thermal diffusivity, thermal conductivity, and specific heat of flax fiber–HDPE biocomposites at processing temperatures", Composites Science and Technology, 68, Pages 1753–1758, 2008

[52] Mediha K., Kadir D., Yildirim A., "Thermophysical properties of blend of Poly (Vinyl chloride) with Poly (Isobornyl Acrylate)", International Journal of Science & Technology, Volume 3, No 1, Pages 37-42, 2008

[53] Mitsubishi Engineering-Plastics Corporation, "Thermal properties", Japan, 2018 www.m-ep.co.jp/en/pdf/product/iupi_nova/physicality_04.pdf

Ref.:

Mussa, Hadeel Mahmood – **Salih**, Tawfeeq Wasmi M.: *Thermal conductivity of wood-plastic composites as insulation panels: theoretical and experimental analysis*
Építőanyag – Journal of Silicate Based and Composite Materials, Vol. 73, No. 2 (2021), 54–62. p.
https://doi.org/10.14382/epitoanyag-jsbcm.2021.9

Effect of organoclay reinforcement on the mechanical and thermal properties of unsaturated polyester resin composites

Ibarra Miguel D. ABOBO ▪ Chemistry Department, College of Science,
De La Salle University, Manila, Philippines
Loida D. RODRIGUEZ ▪ Chemrez Product Solutions Inc., Quezon City, Philippines
Sonia D. SALVADOR ▪ D&L Industries Inc., Quezon City, Philippines
Henry C. SIY ▪ Chemrez Product Solutions Inc., Quezon City, Philippines
David P. PENALOZA Jr. ▪ Chemistry Department, College of Science,
De La Salle University, Manila, Philippines

Érkezett: 2020. 10. 18. ▪ Received: 18. 10. 2021. ▪ https://doi.org/10.14382/epitoanyag-jsbcm.2021.10

ABSTRACT

Unsaturated polyester resin (UPR) is a popular material of choice for composite materials, particular in glass fiber–reinforced plastics (FRP) and casting resins (non-reinforced). Our study presents the preparation of clay-based UPR composite materials employing various loadings of organo-modified montmorillonite clay as a filler to a UPR serving as the matrix material that resulted in enhanced thermal and mechanical properties compared to a bare UPR. Wetting behavior of the resulting composites was much better than UPR only. Such property enhancements were connected to the exfoliated morphology of the composite materials. Tensile measurements through universal testing machine was carried out to measure tensile strength while thermal stability was characterized using thermogravimetric analysis. Wetting behavior of the composite materials was evaluated using contact angle measurements. Evaluation of the structure and morphology of the composite materials as well as clay fillers was determined through scanning electron microscopy (SEM), Fourier transform (FTIR) infrared spectroscopy and x-ray diffraction (XRD) technique.

Keywords: unsaturated polyester resin, nanocomposite, organo-modified clay, montmorillonite, modification

Kulcsszavak: telítetlen poliészter gyanta, nanokompozit, szervesen módosított agyag, montmorillonit, módosítás

Ibarra Miguel D. ABOBO
MS Chemistry graduate of De La Salle University, Manila, Philippines

Loida D. RODRIGUEZ
Design and Development (D&D) manager, Chemrez Product Solutions Inc., Quezon City, Philippines

Sonia D. SALVADOR
Consultant, D&L Industries, Inc., Quezon City, Philippines

Henry C. SIY
General Manager, Chemrez Product Solutions Inc., Quezon City, Philippines

David P. PENALOZA Jr.
Associate professor in the Chemistry Department, College of Science, De La Salle University, Manila, Philippines. His research interests focus on self-assembled systems and nanostructured materials

1. Introduction

Unsaturated polyester resin (UPR) is a condensation product between the reaction of unsaturated acids or anhydrides and diols. UPR is usually dissolved in styrene which also serves as the crosslinking agent [1]. Addition of a small amount of an initiator, such as methyl ethyl ketone peroxide (MEKP), initiates the polymerization of styrene bridges bound to the unsaturated points of the polyester producing a highly crosslinked system. The presence of an unsaturated double bond provides the site for crosslinking making UPRs thermosetting polymers of major importance. UPRs are currently the most commonly used matrix for fiber-reinforced plastics. Among their applications are in construction, marine and land transportation industries, coatings, etc. To maximize the use of UPRs, modification methods of these resins are geared towards toughening and reinforcement, flame proofing and improving heat resistance [2-6].

One viable modification for UPRs is by clay reinforcement resulting in the preparation of clay-based polymer nanocomposites. Clay-based polymer nanocomposites are a class of inorganic-organic hybrids having a polymer matrix reinforced with a small loading (<10%) of nanometric-sized clay platelets. The term nanocomposite refers to a combination of two or more materials where one of the phases has one, two or three dimensions within the nanometer (10^{-9} m) range [7-11]. Due to the small size and the high surface-to-volume ratio of the inorganic filler at this length scale, the polymer nanocomposites have exhibited remarkable property enhancements and new properties compared to their unfilled polymer and conventional composites. The reinforcing material having at least one dimension in the nanometer length scale can be made up of particles, sheets or fibers. In the case of a clay-based polymer nanocomposite, the inorganic phase is a layered silicate clay. It has a layered structure consisting of stacks of silica platelets each having a thickness of about one nanometer [12-14].

One major drawback of preparing polymer/clay nanocomposites is the incompatibility of the inorganic clay with the organic polymer. This can be remedied by surface modification of the montmorillonite clay using organic intercalating agents to make it more compatible with the polymer matrix [15-18]. This will in turn allow for good dispersion and enhanced properties. Typical loading of clays is at <10% for optimum response.

The main objective of this study is to prepare an unsaturated polyester resin (UPR)/clay nanocomposite and to enhance the tensile strength with respect to the neat resin. Various characterization techniques such as contact angle determination, TGA and XRD, were conducted to verify the improvement brought to the UPR by the addition of montmorillonite clay.

2. Experimental

2.1 Materials

A commercial unsaturated polyester, Polycol 03 – 027PL (pre-added with a cobalt promoter), and an ammonium modified montmorillonite clay were provided by Chemrez, Inc.. Methyl ethyl ketone peroxide (MEKP) (Akzo Nobel) was used as received.

2.2 Clay loading of the unsaturated polyester resin (UPR)

Appropriate weights of Polycol 03 – 027PL, a commercial UPR from Chemrez, Inc., were weighed in five separate plastic containers. Then, various amounts of high purity long chain-alkyl ammonium modified montmorillonite was incorporated into the four containers to prepare 1%, 3%, 5% and 10% wt/wt clay with respect to the total mass of the UPR resin and the MEKP initiator). They were then hand mixed until no visible clay aggregates are present. The mixtures were set aside until ready to be cured. The fifth container only contained the resin (UPR only).

2.3 Curing of the unsaturated polyester resin (UPR) and its composites

One part of a free radical initiator, methyl ethyl ketone peroxide (MEKP), was added to each of the five containers. The contents were mixed for 1 minute and were subsequently poured into dog bone-shaped silicone molds. These were then allowed to polymerize for 15-20 minutes. Finally, the cured composites were post-cured at 70 ± 1°C in an oven for 3 hours. These were then set aside until ready to be tested.

2.4 Characterization

2.4.1 Tensile Strength Determination

The tensile strength of the prepared composites and bare UPR samples were measured using a universal testing machine (UTM). First, the width and thickness of the samples previously cured in silicone molds were measured. These data were used to obtain the cross-sectional area. Then, the force required to reach the breaking point was measured using a Multiensayo Electromechanical Universal Testing Machine (UTM). The tensile strength was calculated by dividing the force by the cross-sectional area. Appropriate unit conversions to report the obtained values in megapascals (MPa) was done. Finally, the tensile strength values were plotted against the amounts of clay in percent.

2.4.2 Contact Angle (CA) Determination

The contact angle was measured using Attension Contact Angle Machine. This was done by placing a drop of water with volume of 5.0 ± 0.1 μL in a stage and was imaged using a camera attached to a computer with the appropriate software. The left and right contact angles were measured and three trials were done for each. The average of the last measurement of the right and left ones were reported. This analysis was done to determine if there was an improvement in the hydrophobicity of the nanocomposites.

2.4.3 Thermogravimetric Analysis (TGA)

The thermal degradation of the UPR and nanocomposites was monitored using TGA55 (TA instruments). First, the instrument was calibrated for mass and temperature and was set to zero. Then, samples of the prepared composites, as well as the clay, (about 20-30 mg) were weighed in the platinum HT pan. Each of the samples was then subjected to a constant heating rate of 20 °C/minute from 25 °C to 1000 °C.

2.4.4 X-ray Diffraction (XRD) Analysis

The clay and the composite containing 1% clay (to represent various prepared samples), were powdered and subjected to X-ray diffraction analysis using Shimadzu XRD 6000. The radiation source is CuK$_\alpha$ with a generator voltage of 40 kV, a generator current of 30 mA, and a wavelength of 1.54 angstroms. The divergence is 1°, same with the scatter, with the receiving at 0.3 mm. Scanning was continous with a step of 0.02° and a speed of 2°/minute. The purpose of this analysis is to confirm the successful dispersion of the clay into the resin matrix via exfoliation.

2.4.5 Scanning Electron Microscopy (SEM)

Prior to the analysis proper, a small sample from the fractured portion of the UPR as-is, UPR with 3% and 10% montmorillonite clay, and montmorillonite clay itself were obtained and dried in an oven at 100 ± 1 °C for 1 hour. Then, they were stored in a dessicator until ready to be analyzed to ensure complete dryness. The samples were then mounted in an SEM pin holder and were gold coated for better conductivity. The holder was then placed in the sample chamber of JEOL JSM – 5310 scanning electron microscope. The samples were imaged using an accelerating voltage of 10 kV and different magnifications as per requirement (750-15,000x).

3. Results and discussion

3.1 Preparation of clay-UPR composites

This work describes the preparation of clay-UPR composites and the subsequent measurement of the tensile strength to see if there is any improvement that occured for the aforementioned property. In this method, the composites were prepared by: (1) incorporation of different amounts of clay (1%, 3%, 5%, and 10%) into the UPR matrix by simple hand mixing until no visible clay aggregates are present; (2) addition of free radical initiator (MEKP) and further hand mixing; (3) pouring of the mixture into the dog bone – shaped silicone mould to polymerize for 15 – 20 minutes; and finally, (4) post – curing at a 70 ± 1 °C oven for 3 hours.

The uncured composite samples exhibited a noticeable increase in viscosity compared to the neat resin as mixing these samples is more difficult than the latter. The increase in viscosity can be related to the added clay to the UPR. The mixtures though are stable and no noticeable phase separation was observed.

After curing in the dog bone-shaped molds, prepared composites showed no presence of clay aggregates and appeared homogeneous. The visual inspection is an evidence of good dispersion of the clay in the nanocomposite. However, as the amount of clay increases, the more hazy the resin becomes.

3.2 Tensile strength characterization of clay-UPR composites

Fig. 1 shows the plot of tensile strength as a function of clay amount in percent. The tensile strength of the neat UPR is at 26.45 MPa and it increased to 39.12 MPa (an increase of 44.04%) when 1% wt/wt clay was added. Furthermore, when the clay loading was increased to 3% wt/wt, the tensile strength increased to 47.94 MPa (+ 57.90%). However, at 5% wt/wt clay loading, the tensile strength decreased to 30.34 MPa and at the 10% wt/wt clay level, it was at 31.12 MPa. This shows that the tensile strength is improved at a certain level but will begin to decrease at higher loadings. In this particular study, the 3% wt/wt is the optimum clay loading for the composites that provides the highest increase in the tensile strength. At higher concentrations, the clay particles will start to aggregate once more and will take up more space within the polymer matrix. This will weaken the polymer network and consequently the tensile strength.

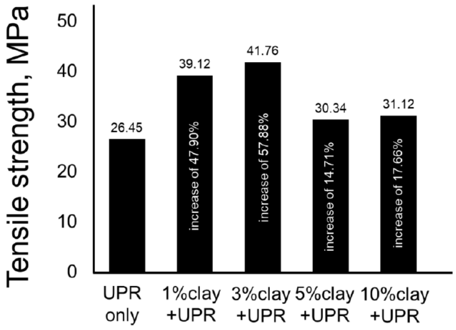

Fig. 1 Tensile strength as a function of clay amount. The composite with the 3% wt/wt clay + UPR has the highest tensile strength, with the trend going upwards from the bare UPR (0% wt/wt clay) then downwards to the one with 5% wt/wt clay + UPR. All composites have higher tensile strengths compared to the bare UPR.

1. ábra Húzószilárdság az agyag mennyiségének függvényében. A 3 tömeg% agyag + UPR kompozitnak van a legnagyobb a húzószilárdsága, a tendencia a tiszta UPR-től felfelé halad (0 tömeg% agyag), majd lefelé az 5 tömeg% agyag + UPR felé. Valamennyi kompozitnak nagyobb a húzószilárdsága a tiszta UPR-hez képest.

3.3 Wetting behavior of clay-UPR composites as measured in terms of contact angle

The contact angle curve as a function of the clay loading percentage is shown in *Fig. 2* with representative images of each sessile drop. Very much like the tensile strength profile, it has an optimum loading at 5% wt/wt with 84.01° (equivalent to 14.00% increase). The contact angle of the base resin is at 73.70° and it increased to 79.98° at 1% wt/wt and further increase to 82.75° at 3% wt/wt clay. However, it decreased to 82.29° at the 10% wt/wt loading of the clay. The possible explanation for this behavior is that as the amount of clay is increased, the amount of the organic modification attached to the clay is increased. Therefore, the composite becomes more hydrophobic. However, at a certain level, the clay particles will revert to its organized crystal structure and will form aggregates. Thus, the exposed long chain alkyl modification will decrease and the hydrophobicity will decrease. Consequently, the contact angle will also decrease.

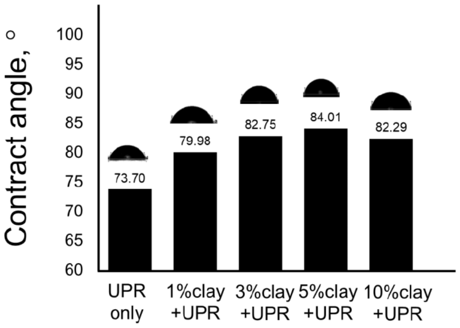

Fig. 2 Contact angle as a function of clay amount. The composite with the 5% wt/wt clay + UPR has exhibited the highest contact angle, with the trend going upwards from the bare UPR (0% wt/wt clay) then downwards to the one with 10% wt/wt clay + UPR. All composites have higher contact angles compared to the bare UPR. Inset: Representative sessile drops for each sample.

2. ábra Az érintkezési szög az agyag mennyiségének függvényében. Az 5 tömeg% agyag + UPR kompozitnak van a legnagyobb érintkezési szöge, a tendencia a tiszta UPR-től növekszik (0 tömeg% agyag), majd csökken a 10 tömeg%-os agyag + UPR irányába. Valamennyi kompozitnak magasabb az érintkezési szöge mint a tiszta UPR-nek.

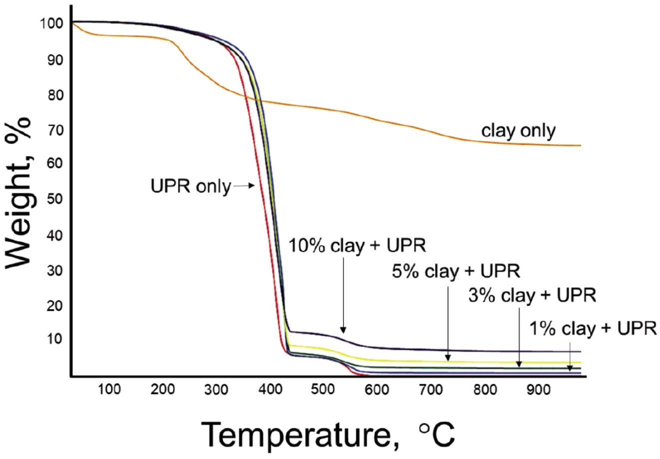

Fig. 3 TGA thermograms of the bare UPR, the clay only and the prepared composites. A clear shift in the thermal degradation profile was observed for all composites and the one with 1% wt/wt clay has the greatest shift (blue curve) from the neat UPR (red curve).

3. ábra A tiszta UPR, a tiszta agyag és az elkészített kompozitok TGA-termogramjai. A termikus bomlási profilban egyértelmű eltolódást figyeltünk meg az összes kompozit esetében, és az 1 tömeg% agyagot tartalmazónak van a legnagyobb eltolódása (kék görbe) a tiszta UPR-től (piros görbe).

3.4 Thermogravimetric analysis of clay-UPR composites

The thermogravimetric (TGA) plots of the UPR, clay, and the resulting composites are shown in *Fig. 3*. There is a very clear shift in the thermal degradation profile when clay is incorporated into the UPR, albeit the UPR and composites have the same trend. Moreover, the thermogram shows that the composites have three major components: the crosslinked UPR (degrades at around 224-424 °C), additives (degrades at around 424-524 °C) and the residue (the clay itself). The clay has a different profile compared to the UPR and the composites. Its first degradation is at a lower range (< 100 °C), most likely due to moisture. The second one is at around 224-324 °C, which most likely is the long chain alkylammonium modification. The clay residue is 70% of the total initial mass. The clay-UPR composites, on the other hand, have residues corresponding to the approximate clay loadings for each as can be noticed at the tail end of the thermogram.

3.5 X-ray diffraction characterization of the clay template and the clay-UPR composite

The clay and the 1% wt/wt clay-UPR composite were subjected to XRD analysis to confirm if there is exfoliation of the clay particles in the UPR matrix, that could be a reason for the observed increased in mechanical characteristic, wetting behavior and thermal property of the composites over the bare UPR. This is shown in *Fig. 4*. For the clay, the characteristic peak is shown at 4.16°, which corresponds to a d-spacing of 10.60 angstroms. This is the typical montmorillonite clay interlayer spacing. For the 1% wt/wt clay-UPR composite sample, the peak at 4.16° disappeared. This indicates the delamination of the clay layered structure, favoring the successful dispersion of the clay in the UPR matrix. It has been shown in the literature that exfoliation of previously organically-modified fillers in clay-based polymer nanocomposites have led to enhanced physical properties of the resulting composites materials over their bare polymer counterparts [7-9,16,18].

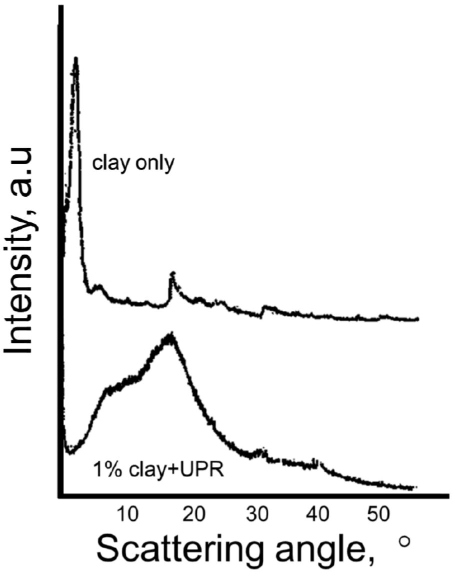

Fig. 4 XRD plots of clay only and 1% wt/wt clay + UPR. The distinguishing peak at 2θ = 4.16° for the clay only has disappeared in 1% wt/wt clay + UPR suggesting exfoliation of the clay in the UPR matrix.

4. ábra XRD ábrán a tiszta agyag valamint az 1 tömeg%-os agyag + UPR kompozit. A kiemelkedő csúcs 2θ = 4.16°-nál 1 tömeg%-os agyag + UPD kompozit esetén nincs jelen, ami az agyag leválására utal az UPR mátrixban.

3.6 Scanning electron microscopy of the bare UPR, the clay template, and the clay-UPR composites

The neat UPR, the clay and two composite samples containing 3% and 10% wt/wt clay were analyzed under scanning electron microscope (SEM) to confirm the dispersion of the clay in the UPR matrix. As shown in *Fig. 5*, flake-like and stacked morphology is evident for the montmorillonite clay image (*Fig. 5a*). The neat UPR also has a smooth appearance, which is to be expected as it is devoid of any filler material (*Fig. 5b*). However, upon addition of 3% wt/wt clay, it was very evident that some clay particles aggregated. However, most of them are present as individual primary particles that are smaller in size (*Fig. 5c*). As the amount was increased to 10% wt/wt, the clay flakes began to embed themselves in the UPR matrix (*Fig. 5d*). This is due to the sheer number of clay particles that are already present in the sample.

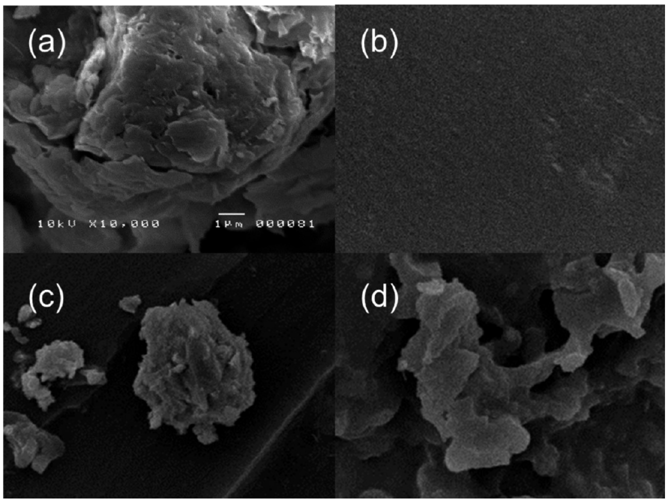

Fig. 5 SEM images of (a) clay only, (b) UPR only, (c) 3% wt/wt clay + UPR, and (d) 10% wt/wt clay + UPR. Note the flake – like and stacked morphology of the clay platelets in (a). The "clean" image of the neat UPR is very evident in (b). Few clay agglomerates were present in (c) with the smaller particles outnumbering them. Flakes were seemingly "embedded" in the UPR matrix in (d).

5. ábra SEM képek a) tiszta agyagról, (b) tiszta UPR-ről, (c) 3 tömeg%-os agyag + UPR kompozitról és (d) 10 tömeg%-os agyag + UPR kompozitról. Megfigyelhető az a) pontban említett agyaglemezek lemez-szerű és egybe tömörülő formája. A tiszta UPR homogén jellege jól látható a (b) ábrán. A (c) ábrán egy kevés agyag-agglomerátum látható, valmint több különálló kisebb méretű részecske. A (d) ábrán megfigyelhető, hogy az agyag lemezek látszólag „beágyazódtak" az UPR mátrixba.

4. Conclusions

We have successfully enhanced the tensile strength, wetting behavior and thermal property of a commercial UPR by incorporation of small amounts of long chain alkylammonium-modified montmorillonite clay. Tensile strength of the composites was measured with the incorporation of 1% and 3% wt/wt clay resulting in 47.94% and 57.90% improvement, respectively, of the resulting composites over the bare UPR sample. However, using 5% and 10% wt/wt clay loadings did not result in higher tensile strength but still improved the mechanical property of the prepared composites over the bare UPR. The hydrophobicity was also enhanced as exhibited by increased contact angles of the composites. It improved by as much as 14.00% at the 5% wt/wt clay loading. The TGA data supports that the addition of clay results in the thermal characteristic enhancement as there is a shift in the degradation profile at higher temperature exhibited by the composites versus the neat UPR with 1% wt/wt clay-UPR exhibiting the highest degradation temperature. XRD and SEM data confirm the successful exfoliation and dispersion of the added clay fillers in the UPR matrix.

Acknowledgements

The De La Salle University through its University Research Coordination Office (URCO) is acknowledged for the funding (URCO 28FU2TA15-3TAY16). Chemrez, Inc. and D&L Industries, Inc. are also thanked for their technical assistance.

References

[1] Yang, Y.S. – Lee, L.J. (1988): Microstructure formation in the cure of unsaturated polyester resins. Polymer Vol. 29, Issue 10, pp. 1793–1800, https://doi.org/10.1016/0032-3861(88)90393-X.

[2] Baley, C. – Busnel, F. – Grohens, Y. – Sire, O. (2006): Influence of chemical treatments on surface properties and adhesion of flax fibre-polyester resin. Composites Part A: Applied Science and Manufacturing, Vol. 37, Issue 10, pp. 1626–37, https://doi.org/10.1016/j.compositesa.2005.10.014.

[3] Kargarzadeh, H. – Mariano, M. Huang, J – Lin, N. – Ahmad, I. – Dufresne, A. – Thomas, S. (2017): Recent developments on nanocellulose reinforced polymer nanocomposites: a review. Polymer, Vol. 132, pp. 368–93, https://doi.org/10.1016/j.polymer.2017.09.043.

[4] Kamal, M.R. – Sourour, S. – Ryan, M. (2017): Integrated thermo-rheological analysis of the cure of thermosets, pp. 187–91.

[5] Singh, B. – Gupta, M. – Verma, A. (1996): Influence of fiber surface treatment on the properties of sisal-polyester composites. Polymer Composites, Vol. 17, Issue 6, pp. 910–18, https://doi.org/10.1002/pc.10684.

[6] Atiqah, A. – Maleque, M.A – Jawaid, M. – Iqbal, M. (2014): Development of kenaf-glass reinforced unsaturated polyester hybrid composite for structural applications. Composites Part B: Engineering, Vol. 56, pp. 68–73, https://doi.org/10.1016/j.compositesb.2013.08.019.

[7] Sinha Ray, S. – Okamoto, M. (2003): Polymer/layered silicate nanocomposites: a review from preparation to processing. Progress in Polymer Science (Oxford), Vol. 28, Issue 11, pp. 1539–1641, https://doi.org/10.1016/j.progpolymsci.2003.08.002.

[8] Alexandre, M. – Dubois, P. (2000): Polymer-layered silicate nanocomposites: preparation, properties and uses of a new class of materials." Materials Science and Engineering R: Reports, Vol. 28, Issue 1, pp. 1–63, https://doi.org/10.1016/S0927-796X(00)00012-7.

[9] Giannelis, E. P. (1996): Polymer layered silicate nanocomposites. Advanced Materials, Vol. 8, Issue 1, pp. 29–35, https://doi.org/10.1002/adma.19960080104.

[10] Penaloza, D.P. (2019): Enhanced mechanical, thermal and barrier properties of clay-based polymer nanocomposite systems. Epitoanyag – Journal of Silicate Based and Composite Materials, Vol. 71, Issue 3, pp.74–79, https://doi.org/10.14382/epitoanyag-jsbcm.2019.13.

[11] Paul, D. R. – Robeson, L. M. (2008): Polymer nanotechnology: nanocomposites. Polymer, Vol. 49, Issue 15, pp. 3187–3204, https://doi.org/10.1016/j.polymer.2008.04.017.

[12] Penaloza, D. P. (2019): Review on the preparation and properties of clay-based nanocomposites. Philippine Journal of Science, Vol. 148, Issue 4, pp. 827–38.

[13] Penaloza, D.P. – Seery,T.A.P. (2020): Utilizing exfoliated clay-poly (norbornene) nanocomposite prepared by metal-mediated surface-initiated polymerization as model end-tethered polymers on an organoclay substrate. Journal of Applied Physics, Vol. 127, Issue 16, 164702, https://doi.org/10.1063/1.5143825.

[14] Penaloza, D. P. – Sandberg, D. J. – Giotto, M. V. – Seery, T. A. P. (2015): An exfoliated clay-poly(norbornene) nanocomposite prepared by metal-mediated surface-initiated polymerization. Polymer Engineering and Science, Vol. 55, Issue 10, pp. 2349-2354, https://doi.org/10.1002/pen.24123.

[15] de Paiva, L.B. – Morales, A.R. – Valenzuela Díaz, F.R. (2008): Organoclays: properties, preparation and applications. Applied Clay Science, Vol. 42, Issue 1–2, pp. 8–24, https://doi.org/10.1016/j.clay.2008.02.006.

[16] Fu, X. – Qutubuddin, S. (2001): Polymer-clay nanocomposites: exfoliation of organophilic montmorillonite nanolayers in polystyrene. Polymer, Vol. 42, Issue 2, pp. 807–13, https://doi.org/10.1016/S0032-3861(00)00385-2.

[17] Penaloza, D. P. - Seery, T. A. P. (2018): Silylated functionalized montmorillonite clay for nanocomposite preparation. Epitoanyag – Journal of Silicate Based and Composite Materials, Vol. 70, Issue 5, pp.140–145, https://doi.org/10.14382/epitoanyag-jsbcm.2018.26.

[18] Ogawa, M. – Kuroda, K. (1997): Preparation of inorganic-organic nanocomposites through intercalation of organoammonium ions into layered silicates." Bulletin of the Chemical Society of Japan, Vol. 70, Issue 11, pp. 2593–2618, https://doi.org/10.1246/bcsj.70.2593.

Ref.:
Abobo, Miguel Ibarra D. – **Rodriguez**, Loida D. – **Salvador**, Sonia D. – **Siy**, Henry C. – **Penaloza** Jr., David P.: *Effect of organoclay reinforcement on the mechanical and thermal properties of unsaturated polyester resin composites*
Építőanyag – Journal of Silicate Based and Composite Materials, Vol. 73, No. 2 (2021), 63–67. p.
https://doi.org/10.14382/epitoanyag-jsbcm.2021.10

Rheological properties of a slip based on synthesized slavsonite and properties of ceramic materials based on it

G. V. LISACHUK ▪ National Technical University “Kharkiv Polytechnic Institute”, Ukraine ▪ lisachuk@kpi.kharkov
R. V. KRYVOBOK ▪ National Technical University “Kharkiv Polytechnic Institute”, Ukraine ▪ krivobok491@gmail.com
A. V. ZAKHAROV ▪ National Technical University “Kharkiv Polytechnic Institute”, Ukraine ▪ zakharovartem106@gmail.com
O. Yu. FEDORENKO ▪ National Technical University “Kharkiv Polytechnic Institute”, Ukraine ▪ fedorenko_e@ukr.net
V. V. VOLOSHCHUK ▪ National Technical University “Kharkiv Polytechnic Institute”, Ukraine ▪ valenty93vol@gmail.com
M. A. ZHADKO ▪ National Technical University “Kharkiv Polytechnic Institute”, Ukraine ▪ zhadko@gmail.com
V. V. SARAI ▪ National Technical University “Kharkiv Polytechnic Institute”, Ukraine ▪ nov_vitv@ukr.net

Érkezett: 2020. 10. 28. ▪ Received: 28. 10. 2020. ▪ https://doi.org/10.14382/epitoanyag-jsbcm.2021.11

George LISACHUK
Doctor of Sciences, full Professor. Specialist in material sciences of resource saving and energy-saving technologies, new structural ceramic materials and coatings. Head of Research department of NTU “KhPI”.

Ruslan KRYVOBOK
Ph.D, Senior researcher. Specialist in material sciences of new special-purpose ceramic materials and coatings. Deputy Head of Scientific and Research Part NTU “KhPI”

Artem ZAKHAROV
Ph.D, Deputy Head of Scientific and Research Part NTU “KhPI”. Fields of interests: development and physico-chemical properties of radiotransparent ceramic, functional materials.

Olena FEDORENKO
Doctor of Sciences, full Professor NTU “KhPI”. Fields of interests: chemical technology of functional ceramics and protective coatings

Valentyna VOLOSHCHUK
Ph.D. student, NTU “KhPI”, Department of technology of ceramics, refractories, glass and enamels. Specializes in the study of radiotransparent ceramic materials.

Maria ZHADKO
Ph.D., NTU “KhPI”, Department of materials science. Fields of interests: development of technology for creating thermally stable nanostructured materials by alloying with refractory metals

Volodymyr SARAI
Ph.D. student, NTU “KhPI”, Department of technology of ceramics, refractories, glass and enamels. Specializes in the study of radioabsorbing ceramic materials.

Abstract

The effect of thinning additives on the rheological properties of an aqueous slip based on the crystalline phase of slavsonite ($SrAl_2Si_2O_8$) has been studied. The influence of the properties of the slips under study on the performance characteristics of the created ceramics was established. The positive effect of the Dolapix PC 67 thinning additive in an amount of 0.1 wt. % has been shown. A decrease in the moisture content of the slip from 40% to 30%, and an improvement in the performance parameters of the developed ceramic materials is achieved.

Keywords: slavsonite, dense-sintered ceramics, slip, rheology, thixotropy,
Kulcsszavak: szlavszonit, sűrűn szinterezett kerámiák, öntő massza, reológia, tixotrópia

1. Introduction

The direction of research, part of which is described in this article, is the synthesis of the necessary crystalline phases with low dielectric properties and the technology of manufacturing products of complex geometric shape on their basis. In previous studies, a technology for the solid-phase synthesis of the required crystalline phase, namely slavsonite ($SrAl_2Si_2O_8$), at a reduced temperature was created [1,2]. The next stage is to establish the optimal technological conditions for casting products from an aqueous slip, which will make it possible to obtain dense sintering of a ceramic radio-transparent material.

In the study [3], it was found that heavy Sr^{2+} ions with close packing in the crystal lattice of anorthite weakly react to heating from room temperature to 1000°C and above in ultrahigh frequencies of electromagnetic radiation. Their insufficient participation in thermal ionic relaxation is expressed in low values of dielectric losses, therefore slavsonite is characterized by the following properties: dielectric constant $\varepsilon \le 6...8$, tangent of dielectric loss angle $tg\delta \le (1...50)\cdot 10^{-4}$, low TLEC $\le 3.8\cdot 10^{-6}$ K^{-1}; and also has a high melting point of 1654°C and high mechanical strength (E = 110...115 GPa) [4].

The relevance of the direction and study as a whole is to ensure a combination of low dielectric properties and high mechanical properties of slavsonite when obtaining a dense-sintered ceramic radio-transparent material by slip casting.

2. Analysis of literature data and problem statement

Today there are various options for forming ceramic products, but the most popular is casting. This method is based on the properties of materials to absorb and release water. Slip casting into porous molds is an individual method of formation, associated primarily with the different nature of the physicochemical interaction of materials with the liquid medium chosen for casting. For each material, it is necessary to select a liquid phase, the dispersion of the solid phase and methods of its grinding, stabilization conditions, stabilizers, and their ratio. Despite the peculiarities of slip casting into porous forms of many materials, the general technological scheme for manufacturing products using this method remains constant and consists of the following:

- making molds and preparing them for casting;
- preparation of the dispersed phase and dispersion medium;
- preparation of slip;
- casting;
- removal of the casting;
- drying of castings;
- firing or sintering.

In the production of many types of technical ceramics, the introduction of the clay component into the slip is not allowed. The dispersed phases of clayless slips generally differ from clay minerals in a lower dispersion, lower adsorption capacity, and hydrophilicity.

The main characteristics of slips are viscosity and the associated fluidity. Slip viscosity determines their ability to fill forms. All other things being equal, it can be adjusted by the ratio of the solid and liquid components in the slip, and it is also adjusted using thinning additives.

The effectiveness of stabilization and thinning of such slips is primarily determined by the value of the generated potential. The most common method for thinning such suspensions is to adjust their pH.

In suspensions of oxide materials that do not contain clay, structure formation is associated mainly with the partial dissolution of the solid phase. The properties of such suspensions are controlled by changing the pH of the medium and the introduction of surfactants [5]. Oxide particles, unlike clay particles, can form both negative and positive micelles. So, the minimum viscosity of the oxide suspension can be achieved by adding both acidic and alkaline electrolytes in a certain amount or by bringing the suspension to a certain pH value. For oxide suspensions, usually the lowest viscosity is obtained at pH = 2.5-4 with the addition of acid or pH = 10-12.5 with the addition of alkali. However, the introduction of alkali metal ions into oxide aqueous suspensions (slips) is almost always undesirable or even unacceptable, since their presence can reduce some properties of finished products, mainly electrophysical [6].

To give the necessary mechanical strength to cast and dried products, it is recommended to introduce up to 5% organic additives into the suspension [6]. The authors of [7] proposed a method for obtaining high-density aqueous slips with the addition of HCl or NH_4Cl as a stabilizer in the amount of 1.0-2.0 ml per 1 liter of slip, which leads to a decrease in the time of blank formation and a decrease in rejects when producing large-sized products.

The authors of the study [8] found that the introduction of complex SBFF (phloroglucinol furfural modifier) + STPP and SBFF + TPPN + NaOH additives into a ceramic slip promotes an increase in the density of finished products by 5-10% compared to samples containing additives C-3 + TPPN and reotan + TPPN. An increase in the mobility of a slip with the proposed complex additives indicates an increase in its aggregate resistance, which leads to a more uniform distribution of particles of the dispersed phase. This, in turn, contributes to the uniform distribution and reduction of the pore size in the sample, and affects the thermal conductivity coefficient.

Thus, it is advisable to study the properties of aqueous slips, adjusting them by the above methods, and to establish their effect on the characteristics of finished products.

3. The purpose and objectives of the study

The aim of the study was to establish the optimal technological conditions for casting slavsonite products from water slips, which would make it possible to obtain dense sintering of ceramic radio-transparent material.

To achieve the goal, the following tasks were set:

- to study the nature of fluidity and the level of thixotropy of slips;
- to study the influence of inorganic and organic thinning additives on rheological and technological properties (both under the condition of the individual action of thinning additives and with their complex use);
- to optimize slip properties (fluidity, thickening), which determine the quality of molding products by casting into porous forms;
- to produce prototypes, study their performance properties, which determine the quality of finished products.

4. Rationale for the choice of thinning additives for research

Dolapix PC 67 has a wide deflocculation range and counteracts thixotropy. Since the product is liquid and thus completely dissociates into ions, the deflocculating effect begins immediately after addition. This process is the result, on the one hand, of the cationic exchange of the additive with the slip, as well as the influence on this double electric layer of mineral particles. On the other hand, polymer chains attach to mineral particles and thus affect steric repulsion [9].

Stellmittel ZS prevents sedimentation, the optimal addition ranges from 0.05 to 0.3% dry weight, depending on individual working conditions. The most suitable way to add Stellmittel ZS is to thoroughly mix it in a slip shortly before casting the samples into molds [10].

Sodium tripolyphosphate (STPP) is the most common deflocculant in the polyphosphate class and has significant fluidizing properties. Polyphosphate anions are well adsorbed by slip particles, significantly increasing their negative charge. As a result, the viscosity of the ceramic suspension decreases [8]. The thikening effect occurs very quickly when very small amounts of solution are added. It is recommended to inject it into the slip in an amount of not more than 0.1% on dry matter – this is half or one teaspoon of the solution per 1 liter of slip. Tripolyphosphate is introduced into foundry masses only if absolutely necessary; it is better to use water glass or soda ash. A slip containing tripolyphosphate can be very liquid, but at the same time it slowly builds up the shard, and the product tends to “stick” to the wall of the mold [11].

5. Materials and methods

At the preliminary stage of research [12], the optimal composition of the masses was established and low-temperature synthesis of slavsonite was carried out; all subsequent studies were carried out using this synthesized powder. Slip preparation took place in a ball mill. Rheological properties (fluidity and thickening) were studied depending on the moisture content of the slip without additives and with thinning additives.

Depending on the type of ceramic, the rheological properties of the slip will have slightly different values, so the fluidity and thickening factor for porcelain slip – 10-15 s and 1.8-2.2 for semi-porcelain slip – 15-20 s and 1.9-23 s, and for faience – 15-25 s and 1.5-2.6 s [6]. The average runoff time for normally prepared slips is: for porcelain masses – 10 s, semi-porcelain masses – 15 s and earthenware masses – 20 s, and the thickening coefficient for high-quality slips used in fine ceramics is in the range of 1.8-2.2 [13]. For slips based on alumina, the optimal fluidity is within 4-10 s [14]. In view of the absence of these indicators for slavsonite ceramics, in the conditions of the pouring method, it was decided to focus on the average values – fluidity 15 - 25 s, thickening coefficient 1.7 – 2.5. The fluidity and thickening of the slips were determined using an Engler viscometer.

To reduce the fire shrinking of the samples, it is necessary to maximize the density of the slip while maintaining its rheological properties; therefore, the task was set to obtain a slip with better properties at a moisture content of 25 - 30%.

The samples were fired in a laboratory muffle furnace Nabertherm HTCT 01/16 at a temperature of 1350°C with a holding time of 2 hours.

The main characteristic, on the basis of which the degree of sintering can be estimated, is water absorption, and an important characteristic that makes it possible to evaluate the closed porosity is the apparent density. These characteristics, as well as open porosity, were investigated by the "express vacuumation" method according to ISO 5017:2014.

6. Research results

The results of determining the rheological properties of the slip are presented in *Table 1*.

Additive	Slip moisture, %	Slip fluidity, s	Slip thickening
No additive	40	7	-
	35	14	-
	30	-	-
Dolapix PC 67 (0.1 wt.%)	30	19	1.75
	28	22	1.67
	26	28	1.65
Stellmittel ZS (0.1 wt.%)	30	25	2.1
	28	27	1.84
	26	35	-
Sodium tripolyphosphate (0.1 wt.%)	30	20	1.73
	28	22	1.65
	26	30	1.61

Table 1 Rheological properties of the slip
1. táblázat Az öntő massza reológiai tulajdonságai

The performance properties of the samples were also determined, the slip was poured into pre-dried gypsum molds, and the appearance of the gypsum molds is shown in *Fig. 1*. In the absence of clay components in the slip and, accordingly, practically zero air shrinkage, at this stage, filter paper was laid in the gypsum molds. This made it possible to freely remove the workpiece from the mold after the set of the shard. There was also a low mechanical strength of the workpieces, which manifested itself in the form of chips under slight pressure. The fired ceramic samples were characterized by the absence of defects, and had significant porosity and low density.

Fig. 1 Plaster mold during casting
1. ábra Gipsz öntés során

From the data obtained, it can be seen that the slip without additive and at a moisture of 40% and 35% is characterized by high fluidity, and at a moisture of 30% the slip is too thick. According to the change in the properties of the slip, with the addition of the Dolapix PC 67 thinning additive, its positive effect is observed, the fluidity of the slip at a moisture of 30% is 19 s, the fluidity at a moisture of 28 and 26% is satisfactory, but the thickening coefficient is lower than the required values – 1.66 and 1.65, respectively, which indicates a narrow range of casting properties and, accordingly, the thixotropy of the slip. As for the expediency of using the Stellmittel ZS additive, it can be concluded from the experiment that this additive is better used as a slip stabilizer. Sodium tripolyphosphate, as a thinning additive, has less effect on the rheology of the slip (fluidity – 20 s, thickening capacity – 1.73). Since, under the same conditions, the slip with Dolapix PC 67 additive has better flow and thickening values, it is more expedient to use this additive.

After heat treatment, the performance properties of the samples were determined using industry-specific methods. The results of studies of the properties of samples cast from a slip with optimal properties are presented in *Table 2*.

Additive	Slip moisture, %	Firing shrinkage, %	Water absorption,%	Open porosity, %	Relative density, g/cm^3
No additive	40	24.8	11.6	23.0	2.03
	35	16.1	10.5	21.6	2.01
Dolapix PC 67 (0.1 wt.%)	30	12.5	10.2	21.5	2.11
	28	11.8	9.7	21.2	2.18
	26	11.2	8.8	19.6	2.23

Table 2 Properties of samples cast from a slip with optimal characteristics
2. táblázat Az optimális jellemzőkkel rendelkező öntvények tulajdonságai

For clarity, on the basis of the data obtained, a graphic interpretation of the properties of the obtained ceramic samples depending on the water content in the slip and the thinning additive was built (*Fig. 2*).

The data obtained indicate that a decrease in the moisture content of the slip from 30 to 26% improves the properties with a linear dependence. Water absorption and open porosity decrease from 10.2% to 8.8% and from 21.5% to 19.6%, respectively, and the apparent density increases from 2.11 to 2.23 g/cm^3.

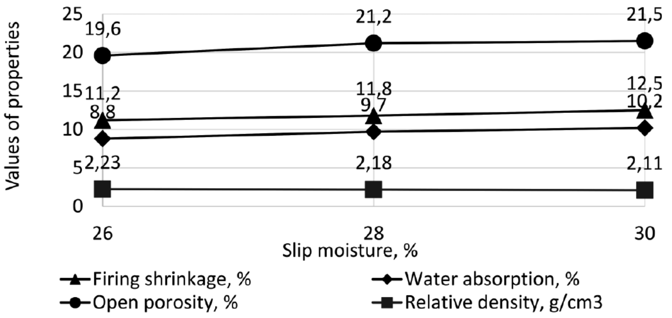

Fig. 2 Properties of the obtained samples of slavsonite ceramics after firing at a temperature of 1350°C depending on the moisture of the slip with the addition of Dolapix PC 67 thinner

2. ábra A szlavszonit kerámiaminták tulajdonságai 1350 °C hőmérsékleten történő égetés után, az öntő massza nedvességétől függően, Dolapix PC 67 hígító hozzáadásával

7. Discussion of the results

In this study, the main part of attention was directed to the development of technological parameters for obtaining an aqueous slip based on slavsonite with optimal rheological properties. The purpose of this decision was to establish the optimal technological conditions for casting products by studying the change in the moisture content of the slip and the use of thinning additives.

The choice of moisture content and the introduction of thinning additives made it possible to solve two problems. The first one is to achieve the required rheological properties of the slip while reducing the moisture content from 35% to 30%. The second one is to improve the properties of fired ceramic specimens: to reduce water absorption and increase the apparent density by 10%.

As a result of the experimental studies, it was possible to improve the rheological properties of the slip with a decrease in moisture, but it should be noted that indicators of water absorption and open porosity, as well as low values of the apparent density of the created ceramic samples have high values. This indicates a low density of the cast blank, and also negatively affects the mechanical characteristics of the cast products. Therefore, in subsequent studies on the rheology of the slip, it is planned to additionally conduct an experiment to determine the rate of gain and the strength of the shard. To reduce thixotropy, it is planned to additionally use stabilizing additives, and conduct casting on the vibrating table.

8. Conclusions

It has been experimentally established that a slip based on a slavsonite crystalline phase, even at a moisture of 40%, is characterized by a high level of thixotropy.

The influence of inorganic and organic thinning additives, namely Dolapix PC 67, Stellmittel ZS and sodium tripolyphosphate, has been investigated. Based on rheological and technological studies, it was established that Dolapix PC 67 in an amount of 0.1 wt. % imparts optimum properties to a slip with a moisture content of 30% (fluidity – 19 s, thickening – 1.75).

The resulting ceramic prototypes are characterized by the following parameters: water absorption – 10.2%, apparent density – 2.11 g/cm^3, fire shrinkage – 12.5%.

References

[1] Lisachuk, G. V. – Kryvobok, R. V. – Fedorenko, E. Y. – Zakharov, A. V. (2015). Ceramic radiotransparent materials on the basis of BaO-Al$_2$O$_3$-SiO$_2$ and SrO-Al$_2$O$_3$-SiO$_2$ systems Építőanyag – Journal of Silicate Based and Composite Materials, Vol. 67, No. 1, pp.20–23. http://dx.doi.org/10.14382/epitoanyag-jsbcm.2015.4

[2] Lisaschuk, G. V. – Kryvobok, R. V. – Zakharov, A. V., et al. (2019) Technological parameters of ceramics creation on the basis of slavsonite. Építőanyag – Journal of Silicate Based and Composite Materials, Vol. 71, No. 2, pp. 46–51. https://doi.org/10.14382/epitoanyag-jsbcm.2019.9

[3] Shchegoleva, N.E., – Sarkisov, P.D., – Orlova, L.A., et al. (2012). Physical-chemical and structural processes occurring during heat-treatment of strontium-aluminosilicate glass. Glass and ceramics, №.69, pp.117–121. https://doi.org/10.1007/s10717-012-9427-z

[4] Orlova, L.A. – Chainikova, A.S. – Alekseeva, L.A. – Voropaeva, M.V. (2015). Recent advances in radio transparent glass-ceramic materials based on high-temperature aluminosilicate systems. Russian Journal of Inorganic Chemistry, Vol. 60, № 13, pp 1692–1707 https://doi.org/10.1134/s0036023615130045

[5] Tombácz E. pH-dependent surface charging of metal oxides (2009). Periodica Polytechnica Chemical Engineering, № 53(2), pp. 77-86. https://doi.org/10.3311/pp.ch.2009-2.08

[6] Premachandran, R.S. – Malghan S.G. (1994) Dispersion characteristics of ceramic powders in the application of cationic and anionic polyelectrolytes Powder Technology, Vol. 79, Iss. 1, pp. 53-60. https://doi.org/10.1016/0032-5910(93)02793-A

[7] Pat. 2 366 637 RF, MPK S04V 33/28. Sposob poluchenija vysokoplotnyh vodnyh shlikerov na osnove litijaljumosilikatnogo stekla / E.I. Suzdal'cev, M.Ju. Rusin, D.V. Haritonov, patenetoobladatel' Federal'noe gosudarstvennoe unitarnoe predprijatie "Obninskoe nauchno-proizvodstvennoe predprijatie "Tehnologija". - № 2008102891/03; zajavl. 25.01.2008; opubl. 10.09.2009, Bjul. № 25.

[8] Pishh, I.V. – Klimosh, Ju.A. –Gabalov, E.V. (2013). Vlijanie razzhizhajushhih dobavok na reologicheskie svojstva keramicheskih shlikerov. Trudy BGTU Himija i tehnologija neorganicheskih veshhestv, № 3, pp 106–109. https://elib.belstu.by/handle/123456789/3018

[9] Gaydardzhiev, S. – Ay, P. (2006) Characterisation of aqueous suspensions of fumed aluminium oxide in presence of two Dolapix dispersants. Journal of Materials Science, vol. 41, pp. 5257-5262. https://doi.org/10.1007/s10853-006-0354-7

[10] Zschimmer&Schwarz. Ceramic auxiliaries: Suspension aids. – https://www.zschimmer-schwarz.com

[11] Piani L. and Papo A. Sodium Tripolyphosphate and Polyphosphate as Dispersing Agents for Alumina Suspensions: Rheological Characterization Journal of Engineering Volume 2013, Article ID 930832, 4 pages http://dx.doi.org/10.1155/2013/930832

[12] Lisachuk, G. – Kryvobok, R. – Zakharov, A., et al. (2017) Influence of complex activators of sintering on creating radiotransparent ceramics in SrO – Al$_2$O$_3$ – SiO$_2$. Eastern-European Journal of Eenterprise Technologies, Vol. 1, № 6 (85), pp 10–15. https://doi.org/10.15587/1729-4061.2017.91110

[13] Evcin A. (2011) Investigation the Effects of Different Deflocculants on the Viscosity of Slips. Scientific Research and Essays, № 6 (11), pp. 2302-2305. https://doi.org/10.5897/SRE10.686.

[14] A. Tsetsekou, C. – Agrafiotis, C.– Aggelos, M. (2001) Optimization of the Rheological Properties of Alumina Slurries for Ceramic Processing Applications Part I: Slip-Casting. Journal of the European Ceramic Society, № 21(3), pp. 363-373 https://doi.org/10.1016/S0955-2219(00)00185-0

Ref.:

Lisachuk, G. V. – **Kryvobok**, R. V. – **Zakharov**, A. V. – **Fedorenko**, O. Yu. – **Voloshchuk**, V. V. – **Zhadko**, M. A. – **Sarai**, V. V.: *Rheological properties of a slip based on synthesized slavsonite and properties of ceramic materials based on it*

Építőanyag – Journal of Silicate Based and Composite Materials, Vol. 73, No. 2 (2021), 68–71. p.

https://doi.org/10.14382/epitoanyag-jsbcm.2021.11

Shear behaviour of silicate-based structural adhesives for timber

Dániel CSANÁDY ▪ BME, Department of Construction Materials and Technologies
▪ csanady.daniel@emk.bme.hu
Olivér FENYVESI ▪ BME, Department of Construction Materials and Technologies
▪ fenyvesi.oliver@emk.bme.hu

Érkezett: 2021. 01. 28. ▪ Received: 28. 01. 2021. ▪ https://doi.org/10.14382/epitoanyag-jsbcm.2021.12

Abstract

In timber structures, many joints are constructed with polymer adhesives and industrial timber by-products also contain polymer resins in huge amount. Majority of these adhesives are artificial polymers with big environmental footprints and lots of them have a negative effect on human health. Some natural or silicate-based adhesives are available in the construction industry, but their heat or water resistance are poor. Some of these types of adhesives have evolved but compounds contain some artificial polymer, and the heat resistance is worse than silicate-based in general. In this article, water-resistance and heat resistance have been investigated in the case of silicate-based binders. In order to be a benchmark, a PVA based industrial timber adhesive (as reference) was also tested. The shear strength of the bonded joints was tested and compared under wet and hot conditions. Reference silicate-based binder was modified with other silicate, acids or alkalines. The effect of modifiers on the solubility of binders was also investigated.

As a result it was stated, that reference binder has a higher strength under normal conditions, but the modified silicate binders have better performance under wet and hot conditions. The modifiers can increase the shear strength, ductility, and water-resistance without decreasing the heat resistance and also makes the material quality more uniform. The silicate binders make a rough bond surface, which can pass the forces effectively between the components of specimens.

Keywords: shear behaviour, adhesives for timber, timber joints
Kulcsszavak: nyírószilárdsági viselkedés, faragasztó, ragasztott fakapcsolatok

Dániel CSANÁDY
Civil engineer k (BME 2017), PhD candidate, Department of Construction Materials and Technologi. Member of Hungarian Scientific Association of Silicate Industry. Main areas of interest: reaction to fire of building materials, development of new generation concretes and silicate binders, environmentally friendly building materials, biomimetics, thermal insulation, sound insulation, development of building materials.

Dr. Olivér FENYVESI
Civil engineer MSc (BME 2005), PhD (BME 2012), Specialized Engineer in Preservation of Building Heritage (BME 2017), Specialized Engineer in Corrosion (HCE 2018), assistant professor in BME, Department of Construction Materials and Technologies. Main research fields: early age shrinkage cracking in normal and lightweight concretes, fibre reinforced concretes, LWAC, building diagnostics, preservation of building heritage. Secretary of the Concrete Division and member of Stone and Aggregates Division of the Hungarian Scientific Association of Silicate Industry, member of the Hungarian Group of fib (International Federation for Structural Concrete), member of ACI (American Concrete Institute), member of the Hungarian Chamber of Engineers.

1. Research motivation

The application of timber in structures has revived in recent decades, as a result of which the amount of adhesive/binder used has increased. Most of these adhesives are high environment polluting, so the present research is concerned with developing a sustainable alternative. During the technological development of the nineteenth century, timber lost its leading role in the construction industry, and modern building materials, such as concrete and steel became dominant. Due to the extensive use of natural resources and the significant demand for invested energy, the construction industry has a huge environmental footprint today. In Europe today, the construction industry responsible for around 42% of total energy consumption generates 35% of total greenhouse gas emissions. Over the past two decades, the growing awareness of policymakers and society about the depletion of natural resources and climate change has had a strong impact on the construction industry, leading to an increase in the demand for sustainable and renewable building materials [1]. Wood is the best known renewable building material. Therefore, it has become important again, which has helped develop a new bond (glueing) technologies. This is well illustrated by the fact that the use of plywood in Europe almost doubled between 2007 and 2012 and is expected to increase further in the future [2] (*Fig. 1*).

Nowadays, the sustainable lifestyle, green thinking is dominant in all areas of life. As a result, many researches have been conducted to create possible, environmentally friendly alternatives to common adhesives. More than 70% of wood products are made with some kind of glued technology [3]. Wood adhesives have a significant share of the amount of adhesive used in the world. It is of paramount importance to reduce the amount of formaldehyde-containing adhesives used, which is currently used in the largest quantities to bond fibreboard and other by-product based boards (*Fig. 1*). The modern adhesive industry initially used large amounts of formaldehyde in almost all adhesives, which can significantly damage the health of workers, so the development of lower formaldehyde and formaldehyde-free adhesives began. Although modern adhesives are less harmful than their predecessors, in case most of them are worth using masks and skin and eye protection. In addition, their production is energy-intensive (mostly fossil-based) and produces large amounts of waste both during production and during use, which is currently difficult to dispose or recycle [4].

Environmentally conscious adhesives were initially made from natural polymers of plants and animals, animal blood, skin, casein, starch, soybeans, dextrin, or cellulose. However, they provided a weaker bond than synthetic adhesives and had low water and fire resistance. The growing interest in biopolymers from renewable sources such as wood, corn, and cereals has encouraged the R&D sector, for example, to use biopolymers as a sustainable adhesive [6]. Inorganic adhesives can have a similarly positive effect on reducing the environmental pollution in the same way as natural-based adhesives. The laboratory research section of this article deals with such inorganic adhesives. In the next chapter, the main classes of adhesives, the most important components and basic properties of these classes are briefly described and characterised.

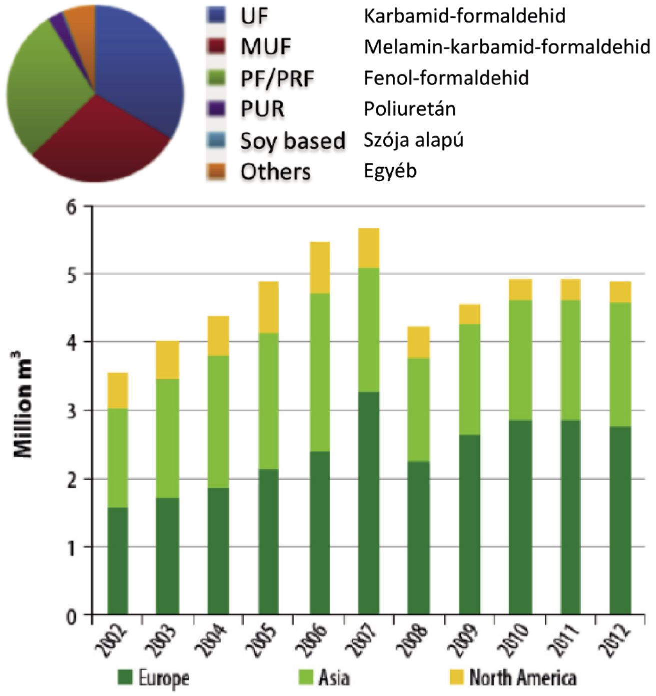

Fig. 1 Global market share of various adhesives [5] (above), Global consumption of plywood in recent years [2] (below)
1. ábra A különféle faragasztók globális piaci részesedése [5] (fent). A globális rétegelt ragasztott lemez felhasználás az elmúlt években [2] (lent)

2. Organic adhesives for the timber industry

Urea-formaldehyde was the first widespread synthetic adhesive introduced in the 1930s. Synthetic glue has resulted in rapid growth in the timber industry [7]. Subsequently, new synthetic adhesives for various special applications (not only for timber gluing) were continuously developed, and proven adhesives were further developed [8][9]. Synthetic adhesives fall into two categories: thermoplastics and thermosets. The two types differ in their chemical structure (linear and crosslinked polymers) [10].

2.1 Thermosetting adhesives

The setting (crosslinking) of thermosetting adhesives is an irreversible process. The curing process can be catalysed in most cases by an exothermic process and the introduction of external energy (heat, light) or chemicals (catalyst materials). The reaction results in a higher molecular weight and melting point. These adhesives provide a stronger bond than thermoplastics and are more resistant to thermal, mechanical and chemical effects. Thermosetting adhesives are often used to bond structural timber elements [11].

2.1.1 Dispersions based on polyvinyl acetate

The most common plastic-based adhesive is polyvinyl acetate. Most are white, viscous, water-based dispersions containing polyvinyl alcohol (PVA) as a protective colloid. After evaporation of the water, these types of plastic adhesives form a flexible film on the surface with good light resistance (UV) and durability. The film layer is sensitive to water, swells, decreases in strength, does not dissolve but regains a significant part of its strength after drying. Their advantage is that they show good compatibility with starch and gluten glues. As the temperature increases, their viscosity decreases, leading to incomplete film formation in porous materials. At low temperatures, the viscosity increases, which can cause bonding problems and prolong the setting time of the adhesive [12]. In the present study, polyvinyl acetate based adhesive was used as a reference to compare the test results.

2.1.2 Polyurethane adhesives

The advent of polyurethane-based (PUR) adhesives has been a major step forward. Due to their isocyanate content, they are sensitive to humidity and ambient temperature changes, and their use requires stable environmental parameters. These environmental parameters affect the setting time of the adhesive and the reactivity of the components, and thus also the properties of the crosslinked adhesive. Its crosslinking is initiated by the moisture content of the glued timber in the case of one-component glue, but there are also two-component variants. It is mainly used for plywood. Total solidification time is about 1-2 days. This type of bonding can ensure the highest load-bearing connections in the case of crosslinked synthetic resins [13].

2.1.3 Phenol formaldehyde

Phenol formaldehyde is used in a wide range of timber products. It bonds very well to timber and can be made of heavy-duty and durable contact even in dry and wet conditions. It is mainly used for products exposed to moisture and other weather conditions (chipboard or fibreboard, plywood, pressed laminated timber). Crosslinking is possible both hot and cold, in hot conditions without an initiator. In the cold, it crosslinks with the addition of initiator. Toxic, skin contact should be avoided, free skin should be protected during use, and a mask should be worn.

2.2 Thermoplastic adhesives

Their advantage is that the load-bearing bond is formed very quickly between the adhesive and the connected parts, significantly influenced by the instantaneous temperature of the glued elements. In the case of thermoplastic adhesives, the process of melting (plasticisation) and curing is reversible and can be repeated several times [15]. These adhesives are ideally suited for manufacturing technologies where high production speeds and early adhesion are particularly important, such as in the coating of the edges of timber products. Their main disadvantage is the limited thermal resistance, even a small temperature rise can significantly reduce the load-bearing capacity of the adhesive [16]. Their scope is limited, they cannot be applied to structural elements because they are not resistant to heat or fire. Thermoplastic adhesives are not used in timber construction. Therefore they are not relevant to the current dissertation topic, but they are closely related to timber as a material. [15]

3. Inorganic adhesives for the timber industry

Inorganic adhesives are based in most cases on the following compounds: sodium silicate, magnesium oxide chloride, lead oxide (litharide), sulphur and various metal phosphates. These materials form strong, though rigid bonds and are well suited for special conditions such as high temperatures, in which case they continue to be widely used. Increased use of synthetic organic polymer adhesives has resulted in a reduction in inorganic adhesives [17]. Nowadays, research on inorganic adhesives and organic-inorganic adhesive mixtures has come to the fore again, as it is generally true that the production of these adhesives and the waste generated from them are less harmful to the environment.

Water glass (aqueous sodium or potassium silicate) has long been used as a reliable, inexpensive adhesive for bonding various porous surfaces and materials such as paper, soil, mineral wool, and timber. Water glass is a colourless, odourless, non-flammable, highly alkaline, yet safe liquid. It's disadvantages are the hardened water glass is inelastic, and its water resistance is very poor. Zhang et al. studied the effect of polyvinyl alcohol (PVA) on the water glass. The adhesion, water and fire resistance of the adhesive made by mixing the two materials were investigated. Adhesion and water resistance have been shown to increase, but heat resistance decreases compared to pure water glass [18]. Peng et al. studied the properties of an adhesive/surface treatment agent made from a mixture of water glass and starch and found that the water resistance and flexibility of the mixture increased [19].

4. Force transfer in bonded connections

Timber is an anisotropic, porous material. Its cell cavities and dimples are large enough to provide a good way for liquid adhesives to penetrate. The adhesive penetration significantly influences the adhesion/bond of the glued timber elements into the pore system and the proportion of the open pores on the glued surface. [20] (*Fig. 2*). At this surface, the stresses in the bonded joints are transferred from the adhesive to the bonded base surface. If this is not just the result of adhesion but also a mechanical bond, the resulting bond will have higher strength.

These two components mainly determine the strength of bonded joints: the first is the internal strength of the bonded base material and the internal strength of the binder, so the cohesion and the second is the force acting at the interface of the base material and binder, this is the adhesion. In some cases, the mechanical interlock is also acting. In a good quality bonded joint, the adhesive forces are at least as high as the cohesive forces. This means, that when well-bonded pieces of material are subjected to a large force, the failure (tearing, breaking) occurs inside bonded material and not at the interface due to the separation of the binder [21]. With this simple model, the process of force transfer is more complicated in reality, and the layers of the connection cannot be so clearly divided. They can be divided into the following layers, which are chain-linked to each other (*Fig. 2*).

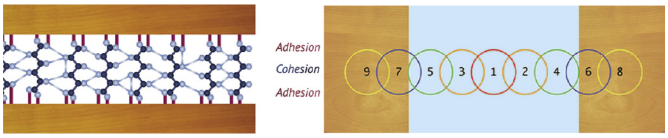

Fig. 2 Adhesion and cohesive forces in bonded timber joints (left) Chain analogy in force transfer of glued timber joints (right) [22]
2. ábra Adhéziós és a kohéziós erők működése a ragasztott fakapcsolatokban (balra) Lánc analógia ragasztott fakapcsolatok erőátadódásában (jobbra) [22]

1: Pure binder phase, which is not affected by the bonded base surface;

2-3: transition layer of binder no longer completely homogeneous affected by bonded base surface;

4-5: A boundary layer between the binder and the bonded surface, which ensures adhesion between the different materials, thus ensuring the connection by covalent or secondary chemical bonds;

6-7: In this layer, the binder enters in the surface pores and thus influences the properties of the base material, as well as provides mechanical interlock (*Fig. 3*) [3].

8-9: Pure timber material where glue does not enter

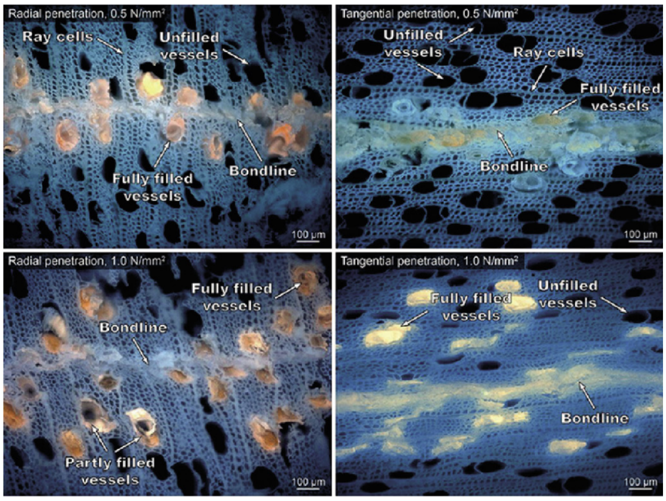

Fig. 3 The significance of adhesives penetrating the timber pore system. Lower strength at lower penetration (left), higher strength at higher penetration (right) [23]
3. ábra Faragasztók behatolása az anyag pórusrendszerébe. Kisebb szilárdság kisebb behatolás (balra), nagyobb szilárdság nagyobb behatolás (jobbra) [23]

5. Research objectives

Organic polymer-based adhesives have a high environmental impact, limited heat resistance and in many cases water/vapour resistance. Silicate-based adhesives have better thermal-resistance, but their performance under normal use generally lags behind organic polymers and is mostly sensitive to moisture. A basic goal is to select a silicate raw material that can be well developed and modified to improve the adhesive properties to approach the favourable properties of organic polymeric adhesives. The main goal is to increase moisture resistance and at least retention of thermal resistance. The developed binder is primarily recommended for bonding timber joints exposed to high temperatures.

6. Laboratory research

6.1 Materials

The adhesive-bonded specimens were made according to ASTM D906 and were 100 mm long, 25 mm wide, 4 mm thick, from C20 material class pine wood. The bonded connection was made on a surface with a nominal size of 30 mm × 25 mm for each specimen. The bonded surfaces of the specimens were ground to an absolute plane due to the proper connection of the bonded elements, and then the surfaces were dusted with high-pressure air. Each element was dried to constant weight at 60 °C in a drying oven before applying the binder.

A polyvinyl-acetate (Water resistance class D3 according to EN 205 [24]) adhesive was used for the reference specimens. The newly developed inorganic binder studied in this article was based on potassium silicate (signed as B1). To increase the binder strength and water resistance of this material, silicate derivatives (B2-B3) and acids or alkalis (B4-B6) were also used as additional materials to improve the properties of the binder. Among the modified silicate binder, B1-B5 are one-component, B6 is a two-component binder. The binders were applied in equal mass to each contact surface. It is important to note that after an initial pressing of 5-10 seconds, the B6 binder already had a minimum strength (i.e., crosslinking begins), in contrast to the other silicate-based binders tested.

To ensure that the load line passes through the adhesive layer and the centreline of the specimen, we checked the parallelism of the connected elements and marked the central axis of the elements so that it coincided with the central axis of the clamping jaws. Thus, all other possible stresses were excluded, the connection was loaded by pure shear stress (*Fig. 4*). The applied load was displacement controlled at a speed of 1 mm/min. The research matrix is summarised in *Table 1*.

Component	Organic/ Inorganic	Modifying agent	Test condition		
			normal	wet	high temp.
1	organic	-	x	x	x
1	inorganic	-	x	-	x
1	inorganic	x	x	x	x
1	inorganic	x	x	x	x
1	inorganic	x	x	x	x
1	inorganic	x	x	x	x
2	inorganic	x	x	x	x

Table 1 Research matrix
1. táblázat A kutatás kísérleti mátrixa

6.2 Test methods

6.2.1 Test under normal conditions

The bonded surfaces were designed according to ASTM D906 and, the reference adhesive was applied on specimens according to application instructions, left in laboratory air for the full cure time (24 hours) and then for 24 hours to ensure the same age of the different adhesives at the time of shear strength test. The specimens made by the silicate-based binder were cured in a 60 °C oven for 24 hours and then kept in laboratory air for 24 hours to be tested at the same moisture content as the reference adhesive.

6.2.2 Test under moisture load

B2 and B6 binder were tested under moisture load, as they performed best among silicate-based binders in the normal conditions test. In this case, the procedure was performed according to ASTM D-906 and D-1183too, the specimen was soaked in water at 24 °C for 48 hours, and then the shear test was performed in wet condition. The boiling test required by the standard was not performed because it is less relevant to the conditions of use.

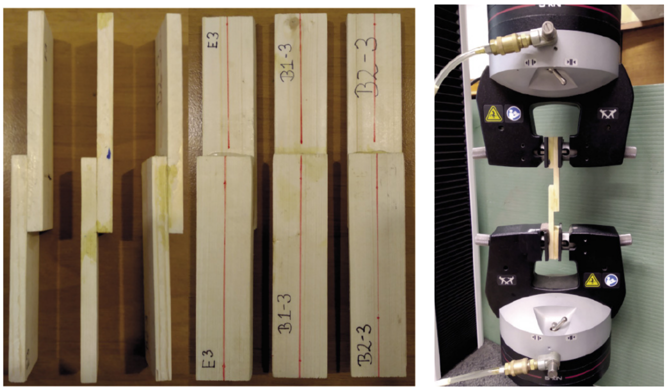

Fig. 4 Bonded specimens (left) and shear test (right)
4. ábra A ragasztott próbatestek kialakítása (balra) és a nyíróvizsgálat (jobbra)

In the case of silicate-based adhesives, water resistance is a common problem. It is an important parameter, so the water solubility of pure water glass was compared with the solubility of the modified silicate binder that achieved the best results in mechanical tests. A non-standard method was used for the study. For both types of binders tested, the same weight of waterglass was weighed into the formworks in every series (the water glass component was the same), so in the case of water glass mixed with silicate additive, the additive weight appeared as a surplus. This was necessary because it would distort the change in solubility of the base material if the weight of the additional material and its solubility were taken into account. The specimens were thin cylindrical plates with the same diameter and were tested by complete immersion in water. The specimens were dried to constant mass before and after the dissolution test, and the constant mass was reached at the same time for all specimens due to the initial same water content. The samples were submerged in silicone formworks (*Fig. 5*). The specimens were dissolved in distilled water. A quantity of water (water glass: water; 1:5) determined by the mass of dried water glass, so that any water saturation affected the results of the tests in the same way (the solution did not reach the saturated state in either case).

After drying, the mass of each specimen was weighted (on an analytical scales) and its integrity was visually inspected at the end of the dissolution cycle. Cycles were continued by type until the particular sample have its integrity, so did not disintegrate. The dissolution cycles were five hours long. Because silicate-based binders are sensitive to water, they can usually appear as an inner structural element.

Fig. 5 Parallel solubility test for adhesives B1 and B2
5. ábra Párhuzamos oldhatósági vizsgálat a B1 és B2 jelű ragasztók esetén

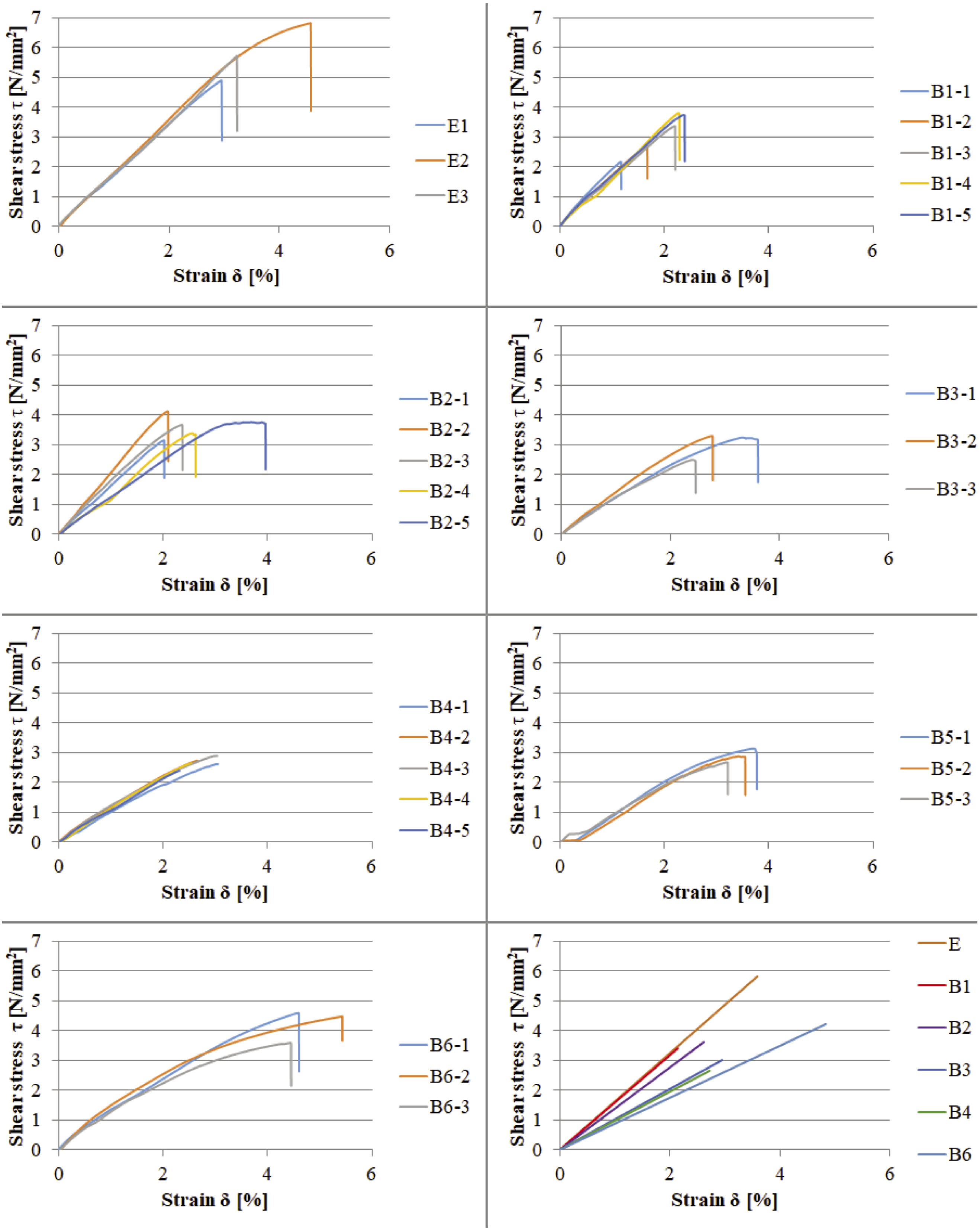

Fig. 6 *τ-δ diagrams of the connections with the tested binders in the case of air-dry condition and normal temperature. Approximation of the average results of the tested binders with a linear diagram of τ-δ (bottom right)*

6. ábra *A vizsgált ragasztókkal készített kapcsolatok τ-δ diagramjai légszáraz, normál hőmérsékletű esetben és a vizsgált ragasztók átlageredményeinek közelítése lineáris τ-δ diagrammal (jobbra lent)*

In this situation, water can only reach the inner structural elements in extreme situations, such as excessive leaking. In Hungary, the duration of such precipitation can be between 15 and 30 hours a month, so if such precipitation occurs weekly, the bonded structural contact may be exposed to moisture for approximately 5 hours [25][24][23]. Although in case of leaking "flowing" water loads the bonded joint, which can carry away the solution, with the weight ratio used and the potential for moisture exposure, the method used is quasi-equivalent to common environmental exposure.

6.2.3 Test under heat load

In this case, the reference, B2 and B6 binders were tested too. The shear specimens were tested according to ASTM D-2339-98 [26], so the specimens were kept at 105 °C for 6 hours and then tested in a heated condition. The specimens were kept at the appropriate temperature by being transferred from the furnace to the loading equipment as short as possible and insulating the loaded cross-section and its surroundings with loose (40 kg/m^3) mineral wool 105 °C.

7. Research results

7.1 Shear strength

7.1.1 Air dry, normal temperature case

The shear behaviour of all joints with the tested binder types can be modelled by a linearly elastic-perfectly rigid material model. Thus, the deformation-stress curves for the specimens can be properly approximated by linear lines, simplifying the averaging of the deformation-stress curves belongs to different adhesive types, and making their comparability illustrative (*Fig. 6*). The τ-δ curves for each binder are shown in *Fig. 6*. The highest shear stress results were achieved with the E (reference) binder as expected. Interestingly, in the case of B2 binder, the tensile strength and ductility were also increased compared to the adhesive B1 (pure waterglass). Although in most cases, the strength and ductility are inversely proportional to each other, which can be seen in the conventional types of investigated binders. In the case of binder B2, two-thirds of the strength of the reference binder was achieved. Although the best results were found by binder E, the failure occurs inside the timber in only one case, other cases on the bonded surface. This means the failure mode was not ideal in the case of the reference adhesive.

The explanation for this was verified by the bonded cross-section records (cut and polished) by scanning electron microscopy (*Fig. 7*). The section was made perpendicular to the direction of loading of the specimen (due to better sample preparation). Still, it can be assumed that the connection structure is also very similar in the parallel direction.

Silicate adhesives are more rigid, so they are more sensitive to tensile and shear loads than organic adhesives. On the other hand, their stiffness is higher than the timber specimens, so the stresses increase due to minor deformations in the bonded cross-section. Therefore, in general, the failure occurs in the glue cross-section or on the contact surface. Worthy of note again that in most tested silicate binders, the failure did not occur purely at the bonding contact surface, but partly inside the timber cross-section. It can be seen that in the case of the pure water glass adhesive B1, the failure occurred in the cross-section of the binder (*Fig. 8*), in contrast, in most of the modified binders B2-B6 the failure was partially in the timber cross-section (*Fig. 8*). In the B6 binder case, the complete failure typically occurred in the timber material (*Fig. 9*).

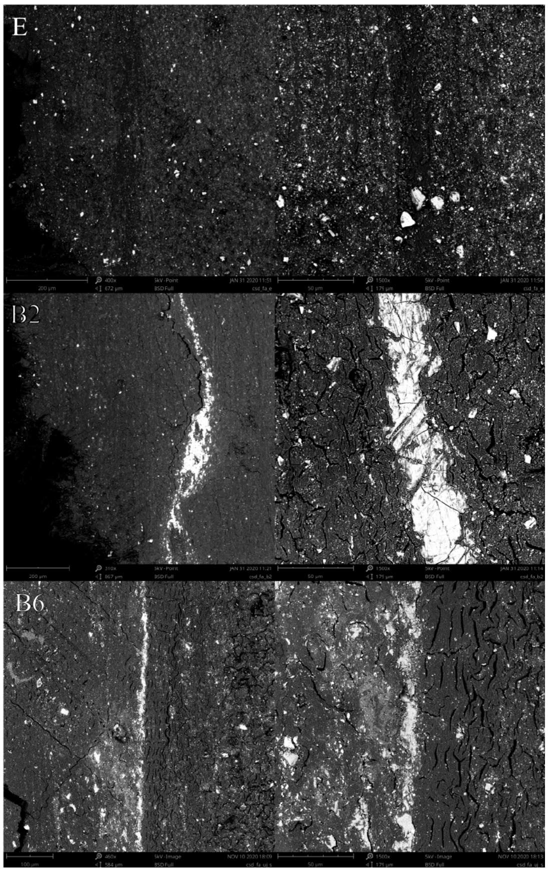

Fig. 7 *Typical cross-sectional view of E, B2 and B6 (top to down) adhesive joints after crack failure at 400 and 1500 magnification*

7. ábra *Az E, B2 és a B6 (fentről lefelé) ragasztóval készült kapcsolatok jellemző keresztmetszeti képe tönkremenetel után 400- és 1500-szoros nagyításban*

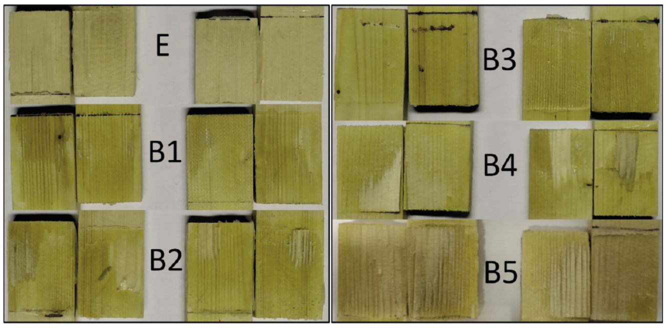

Fig. 8 *Typical failure surfaces of specimens are air-dry condition at room temperature*

8. ábra *Próbatestek jellemző tönkremeneteli felületei légszáraz, normál hőmérsékletű esetben*

It can be seen in *Fig. 7* that the line drawing of the connection surface with the binder E is more even, the cross-sectional thickness of the clear binder is smaller than in the case of the adhesive B2, the boundaries are blurred because it penetrates well into the nearby pores of the wood surface. In contrast, binder B2 has rough line drawing and variable-thickness layer, sometimes significantly thicker than binder E (despite the same amount of adhesive and pressing force applied). The reason for the rough line drawing and the contact surface is that the silicate adhesive contains inadequately dissolved portions of modifying material that penetrates in the surface and closing accordingly less evenly distributed. Increasing the binder layer thickness increases the chance of material defect sites appearing in the adhesive, making it more likely to result in a weaker contact strength. Microscopic images show that binder B6 could be applied to the surface in a thinner and more uniform layer, which is in line with the higher shear strength measured.

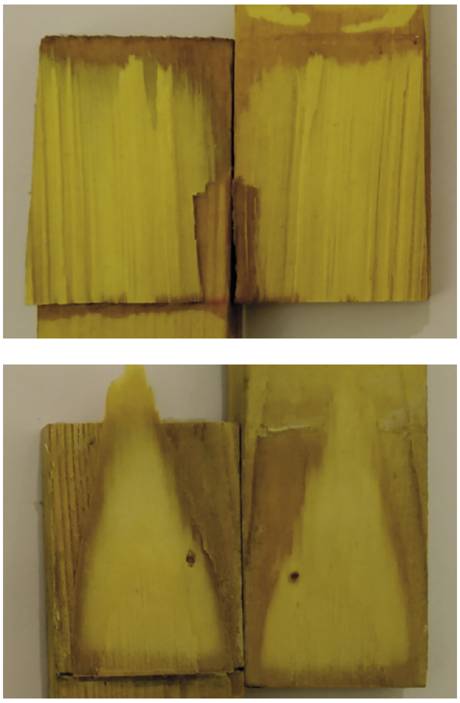

Fig. 9 B6 adhesive failure surfaces in air-dry (above) and wet condition (below) at room temperature

9. ábra A B6 jelű ragasztó tönkremeneteli felületei légszáraz (fent), illetve nedves (lent) normál hőmérsékletű esetben

The comparison of the internal structure is also instructive. The inner part of the binder E is solid and crack-free, while B2 is cracked and in some places detached from the surface. One of the reasons for these phenomena is shrinkage, which, due to the rigid nature of the material causes cracks, the other is the rigid behaviour during loading. The B6 typically contained fewer cracks (than other silicate binders) in the binder cross-section after failure, so the effect of shrinkage was reduced and the ductility of the material increased. It is important to note that the ductility of the adhesives increased steadily with each additional silicate adhesive mixture, but this accompanied only in two cases by an increase in strength (B2 and B6). When using the silicate binder, the structural joint is usually mechanical rather than chemical. The shear teeth are not sufficiently dense and / or sized, and the joint will quickly shear along the concatenated cracks material boundary. The effect of the shear teeth was more significant, the shear stress may have increased locally, failing the near-surface layers of the timber.

In the experiments, the joints bonded with the B2 binder achieved 62% of the strength of the joints formed with the PVA binder, which means this material is not an alternative of PVA under normal conditions of use. However, the B6 has already reached 75% of the strength of the PVA binder, which is forward-looking in the case of silicate adhesives. Future research should improve the flexibility of silicate adhesives and reduce their viscosity to penetrate deeper into the pores near the surface. The development of these properties can positively affect the shear strength of the joints tested in dry condition.

7.1.2 Moisture load at room temperature

After moisture loading, the specimens were examined prepared with binder E, B1, B2 and B6. The integrity of adhesives E, B2 and B6 was maintained after moisture loading, adhesive B1 was completely dissolved during soaking, so the bond could not be loaded. The shear strength results of the joints made with binder E and B2 got closer significantly to each other. While in the dry case, B2 reached only 62% of the reference adhesive strength in the wet case, this ratio was 115% (*Fig. 11*). The adhesives E and B2 softened, which did not cause failure in the bonded timber surface during load, and the elements of the specimens did not separate completely, but the joints could not reach higher bond strength. The B6 adhesive behaved unexpectedly, with a lower decrease in strength than any other type of binder tested. Besides, each of the three loaded specimens has partially failed in inside the timber. It should be noted that this mixture achieved 250% of the strength of the reference adhesive. Moisture and subsequent drying slightly increased the number of cracks in the bonding cross-section (*Fig. 12*). Thus, in the wet case, the modified silicate-based adhesive performed better although the potassium silicate adhesive containing no modifying agent was completely dissolved and thus could not be tested. It can be stated that the added modifier significantly increases the stability of the raw material against water and, as we have seen in the results of dry loading, the strength also increases. Worthy of note reference adhesive is waterproof according to the EN 205, but this standard requires 7 day of dry storing after moisture load and before the test. The examined case is different.

7.1.3 Heat load under dry condition

Tests under heat load were implemented on the joints formed with binder E, B1, B2 and B6. After six hours of heat exposure at 120 °C, all four types of adhesives maintained their integrity. Binder E reacted unfavourably to the elevated temperature, its strength decreased to 10% of its original value (compared to the normal temperature air-dry case) (*Fig. 13*). Its failure was a deformation rather than a strength failure, the bond surfaces slipped over each other, but the contact of the elements did not discontinue. After the stress exceeded the yield strength, the bonded surfaces began to slip, and the tension dropped and then continued to decrease as the area of the sheared surface decreased. This is a significant difference from the normal temperature case where there was no plasticisation. The bonded wooden surfaces are not damaged.

Adhesives B1, B2, and B6 lost their crystal water due to the high temperature (which can be seen from the adhesive discolouration), resulting in a decrease in inner strength (*Fig. 13*). As a result of the water loss, further shrinkage took place in the adhesive, which increased the number of microcracks, which could be more easily joined into macro cracks. However,

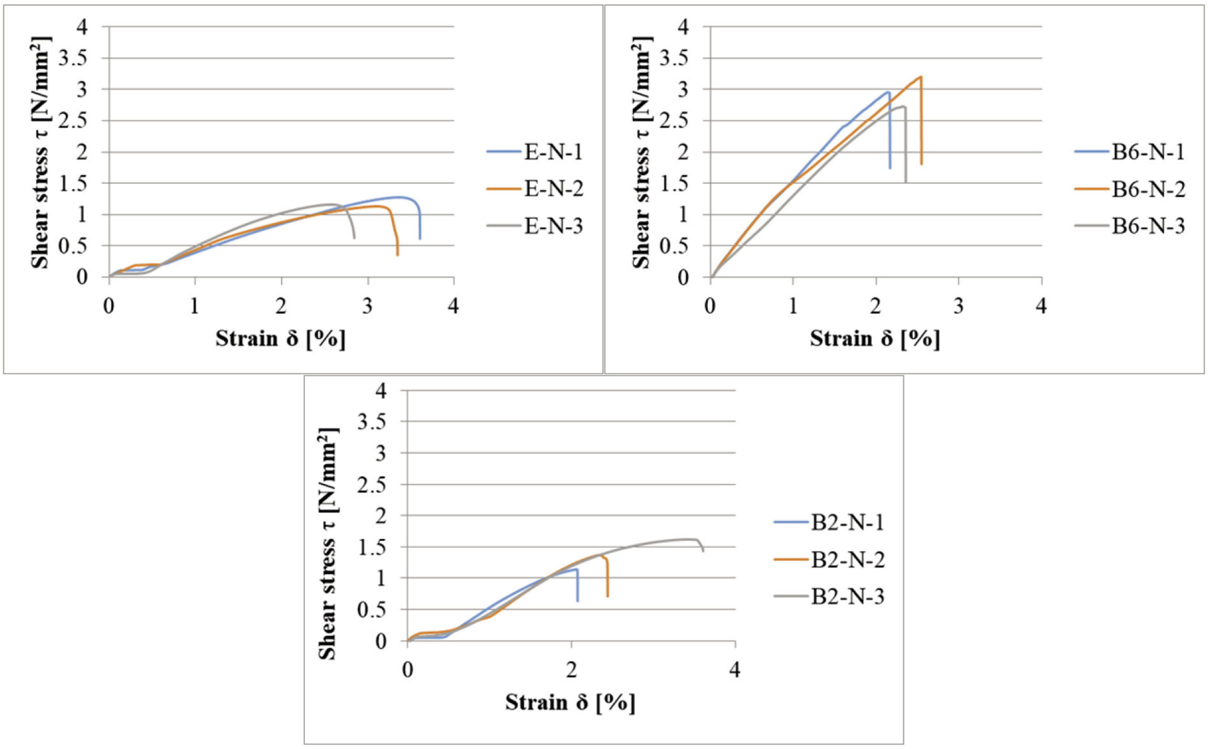

Fig. 10 τ-δ diagram of adhesives E (top left), B6 (top right) and B2 (below) after moisture loading
10. ábra Az E (balra fent), B6 (jobbra fent) és B2 (lent) jelű ragasztók τ-δ diagramja nedvességterhelés után

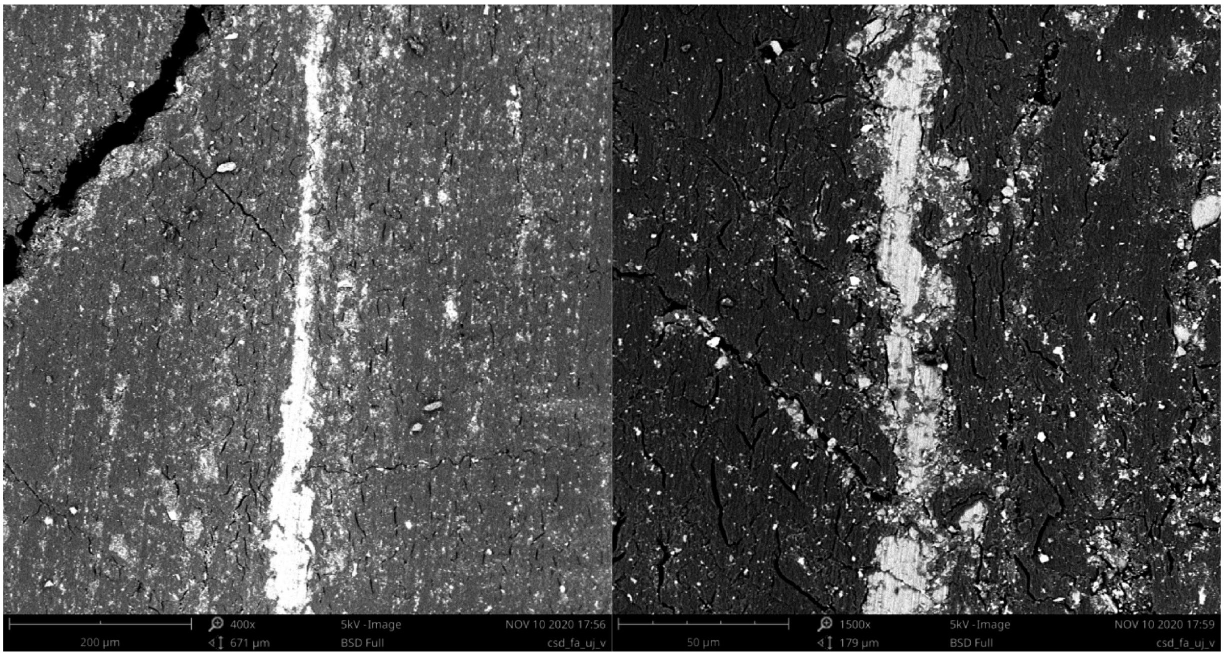

Fig. 11 The cross-section of adhesive B6 after moisture loading captured with SEM
11. ábra A B6 jelű ragasztó keresztmetszetének elektronmikroszkópos felvétele nedvesség terhelés után.

the ductility of the joint increased at a higher rate than the strength decreased. The strength of almost all silicate adhesives decreased to about 90%, compared to the normal temperature air-dry case. The failures happened inside the wooden cross-section in the case of almost every silicate-based adhesives, so the adhesion between the binder and the timber was strong. Compared to adhesive B1, the heat resistance of adhesives B2 and B6 did not decrease with the addition of modifiers.

7.2 Solubility test

The strength of PVA adhesives temporarily decreases under the influence of moisture until they dry again but do not dissolve in water. Thus, the solubility test was done with a comparison of three silicate-based adhesives, one of the pure potassium silicate (B1) from which the other adhesives were mixed, and the other two modified versions of it that performed best among the inorganic adhesives in the strength tests (B2, B6).

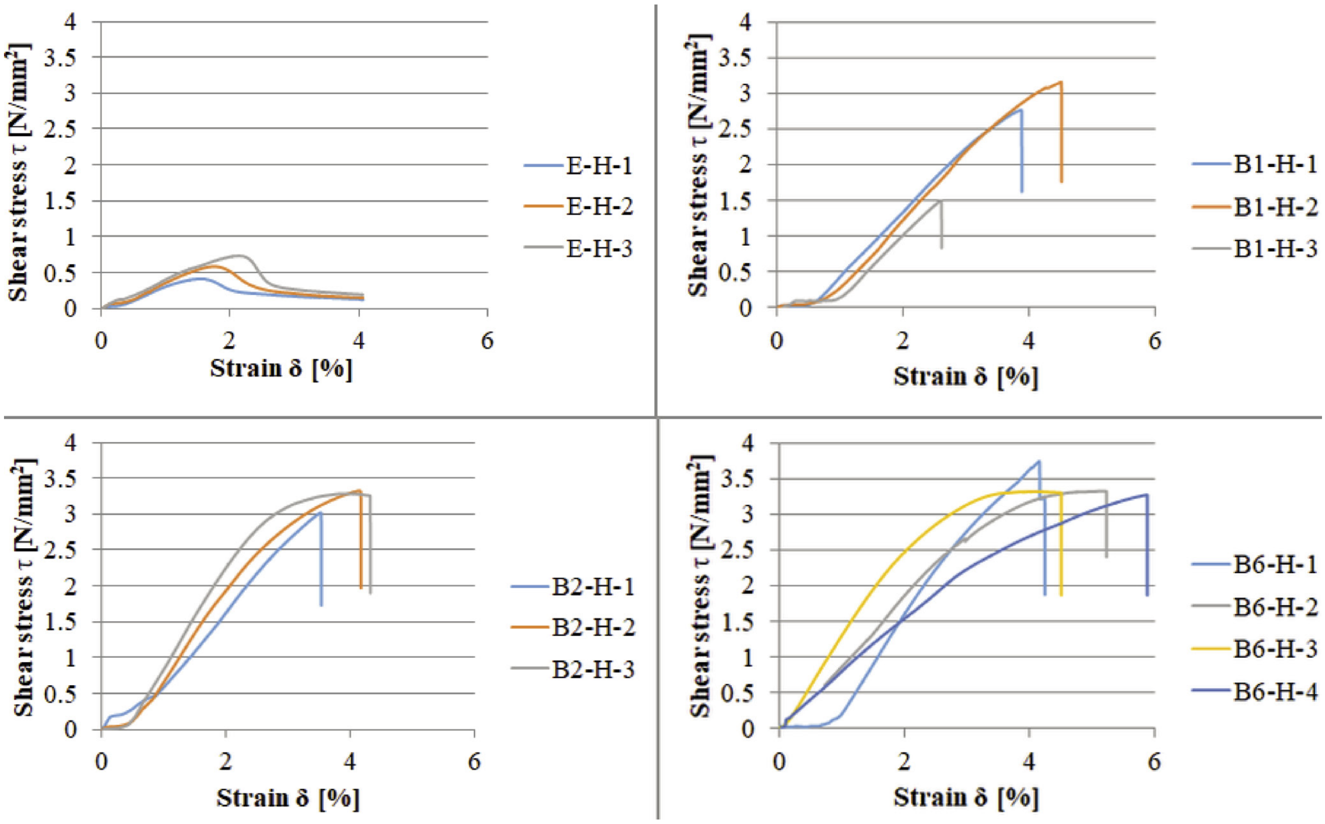

Fig. 12 τ-δ diagram of binders E (top left), B1 (top right) B2 (bottom left) and B6 (bottom right) during heat load
12. ábra Az E (balra fent), B1 (jobbra fent) B2 (balra lent) és B6 (jobbra lent) jelű ragasztók hőterhelés közbeni τ-δ diagramja

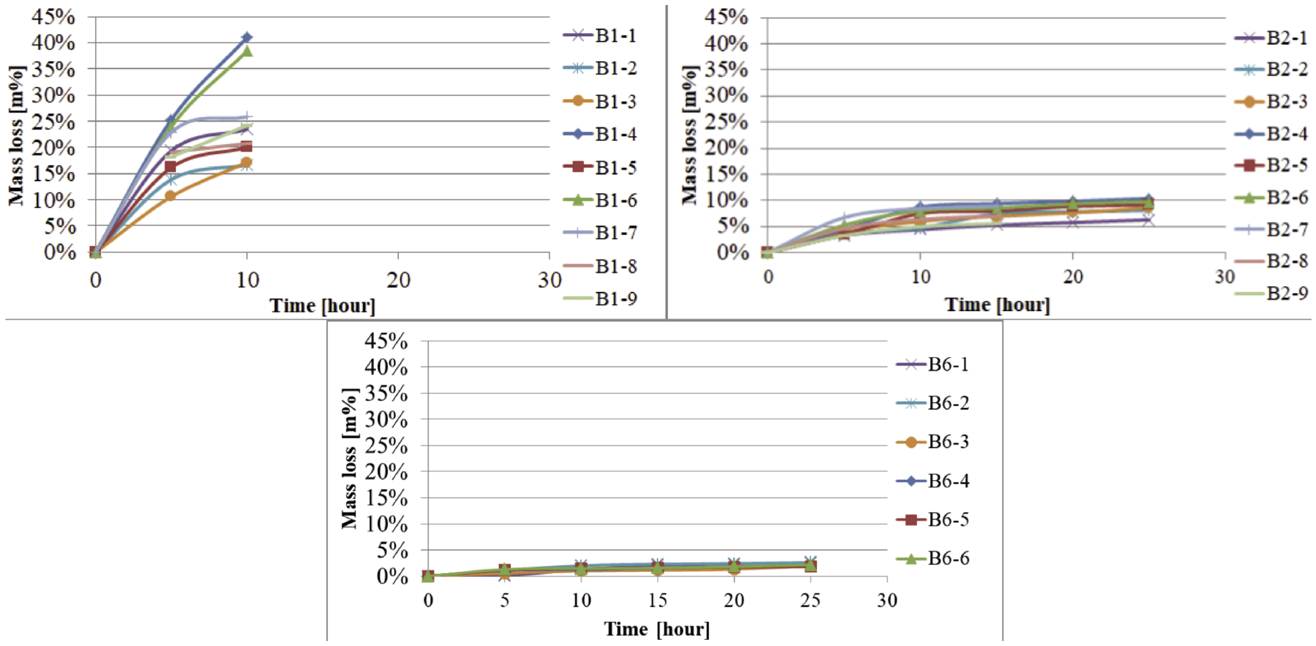

13. ábra A B1 (fent balra), B2 (fent jobbra) és B6 (lent középen) jelű ragasztók tömegvesztesége desztillált vízben való oldás során
Fig. 13 Weight loss of binders B1 (top left), B2 (top right) and B6 (bottom centre) on dissolution in distilled water

Pure potassium silicate adhesive could be tested in two cycles because, during the drying phase of the second cycle, all of the B1 samples lost their integrity. The reason for this can be seen from the mass loss-dissolution time diagram. A specimen lost more than 40% of its mass by the end of the second dissolution cycle (*Fig. 13*). On average, the B1 specimens had a 26% mass loss by this time. It can be clearly seen that the variance of the results is relatively large, so the material quality of the adhesive was not good even.

For the modified B2 binder, the dissolution was repeated in five cycles. Here a much lower mass loss was measured as a result of the unit-time dissolution, and the specimens maintained their integrity well. On average, the specimens lost 7% of their mass by the end of the last dissolution cycle (*Fig. 13*). It is worthy of note that the variance of the results is much smaller than for the B1 adhesive. Also, the proportion of dissolved potassium silicate decreases with an increasing number of cycles. From this, it can be concluded that the modifying agents are not completely homogeneously distributed in the sample but are present in a higher proportion in the inner parts of the cross-section. Here, the binder is properly stabilised, and the solubility of the binder increases as it moves away from the core. Once the more soluble outer layer dissolves, the mass of the binder is stabilised. The mass loss of the binder B6 also decreased compared to B2, and the material quality became even more uniform, as shown in *Fig. 14*. It is found that the outer shell is more soluble compared to the inner core.

8. Summary and conclusions

The research investigated the possibility of improving the properties of inorganic binders to approximate the strength of joints with PVA adhesives widely used in the wood industry today. Also, it was a priority to avoid the reduction of heat and water resistance of silicate adhesives. For this reason, the potassium silicate binder was modified with various other silicate-based materials as well as acids and alkalis. The shear strength properties of the silicate binders and the effect of the modifiers were investigated by forming bonded timber specimens, and shear strength was tested. Based on the experiments, the following conclusions can be drawn:

- Silicate adhesive cannot exceed the strength of organic polymer material under normal conditions. Silicate binder B6 achieved 75% of the shear strength of the joint formed with the reference adhesive, and binder B2 achieved 63%. The other silicate-based mixture performed significantly worse.
- Modifiers of silicate binder improve ductility and shear strength in small doses (B2, B6), but this phenomenon can be reversed (B3, B4). Overall, the ductility of the material increased to 225%, and its strength increased to 125% compared to the pure silicate adhesive used as a reference.
- It was a seemingly contradictory phenomenon that lower strength silicate binder mixtures (e.g., adhesive B5) caused a partial proportion of partial failure in the cross-section of the timber elements of the specimens. An explanation for this was found in the cross-sections examined by SEM. Silicate binders make an uneven bonding surface and, in some locations, dense shear teeth at the micro-level in the timber surface, causing local stress increases in the joint. Because of this, the failure happened in the timber material.
- Under the influence of moisture load, the shear strength results of binders E, B6 and B2 approached each other but decreased. The strength of the silicate adhesive B6 and B2 exceeded that of the PVA adhesive. B2 reached 115% and the adhesive B6 250% of the reference adhesive strength, so the used modifier can improve the water-resistance of the bonded joint.
- Under heat load, the strength of the PVA binder is significantly reduced. Timber joints showed deformation partly and partly strength failure, plastic behaviour appeared, while this was not observed at room temperature. The strength of the binder B2 and B6 decreased slightly because the silicate adhesive lost its crystal water due to the heat load, which increased the internal cracking of the adhesive.
- Under heat load, the shear strength of the bonded timber joint with modified silicate adhesive was higher than of PVA adhesive tested as a reference.
- Dissolution tests (B1, B2, B6) have shown that the addition of modifiers significantly reduces the solubility of potassium silicate and makes the material quality more uniform. Uniform material property, is not fully ensured within the cross-section, the modifying agents are oriented towards the inner layers/core of the sample and its stabilising effect appears here.

B2 and B6 performed better under moisture and heat load than the commonly used PVA binder among the silicate binders. Based on experimental results, it was stated that with modifiers, we could create an inorganic binder with a lower environmental footprint that is competitive with the binders currently used in structural timber elements.

References

[1] P. Glos, Holz - Potentiale des nachhaltigen Baustoffes, Informationsdienst Holz, 2008. https://informationsdienst-holz.de/fileadmin/Publikationen/3_Spezial/Spezial_Potenziale_des_nachhaltigen_Baustoffes_2008.pdf (accessed Feb. 07, 2020).

[2] Unece & Fao, (1944):, Forest products, Nature, vol. 153, number 3892, pp. 689–690, ISSN:00280836, ISBN:978-92-1-117081-8, https://doi.org/10.1038/153689a0.

[3] O. Ülker, Wood Adhesives and Bonding Theory. InTech, (2016):

[4] N. D. Lamontagne, (2014):, Making polyurethane foams more sustainable: Sustainability's a heavy topic even when talking about lightweight, energy-efficient PUR foams, Plastics Engineering, vol. 70, number 6, pp. 24–26, ISSN:00919578, https://doi.org/10.1002/j.1941-9635.2014.tb01190.x.

[5] Transparency Market Research, Wood Adhesives and Binders Market - Global Industry Analysis 2014 - 2020, 2014. http://www.transparencymarketresearch.com/wood-adhesives-binders-market.html (accessed Jan. 13, 2020).

[6] E. Norström, D. Demircan, L. Fogelström, F. Khabbaz, and E. Malmström, (2018):, Green Binders for Wood Adhesives, Applied Adhesive Bonding in Science and Technology, doi: 10.5772/intechopen.72072.

[7] A. Pizzi, K. Mittal, and F. Keimel, (2003):, Historical Development of Adhesives and Adhesive Bonding, Handbook of Adhesive Technology, Revised and Expanded, https://doi.org/10.1201/9780203912225.pt1.

[8] I. Skeist, (1977):, Handbook of adhesives., ISSN:00160032, https://doi.org/10.1016/0016-0032(62)90851-7.

[9] I. Skeist and J. Miron, (1990):, Introduction to Adhesives, Handbook of Adhesives, pp. 3–20, doi: 10.1007/978-1-4613-0671-9_1.

[10] A. NITTHIYAH, (2013):, Optimization and Characterizationof Melamine Urea Formaldehyde (Muf) Based Adhesive With Waste Rubber Powder (Wrp)As Filler.

[11] G. Zeppenfeld, (1991):, Klebstoffe in der Holz- und Möbelindustrie, pp. 49–51, ISBN:3871813591.

[12] M. L. Selbo, (1975):, ADHESIVE BONDING OF WOOD., Tech Bull US for Serv.

[13] U. Müller, S. Veigel, and J. Gabriel, (2009):, Performance of One Component Polyurethane in Comparison to Other Wood Adhesives, International Conference on Wood Adhesives 2009, pp. 196–202, doi: 9781617389863.

[14] G. Zeppenfeld, (1991):, Klebstoffe in der Holz- und Möbelindustrie, pp. 49–51, ISBN:9783871813597.

[15] A. Messmer, (2015):, Life cycle assessment (LCA) of adhesives used in wood constructions, number May, pp. 48, XXXI, [Online]. Available: https://www.researchgate.net/publication/279286317_Life_cycle_assessment_of_adhesives_used_in_wood_constructions.

[16] S. Cass, (1961):, A comparison of hot press interior plywood adhesives, Journal of Natural Products, vol. 11, pp. 285–287.

[17] M. L. Selbo, (1975):, Adhesive Bonding of Wood., Tech Bull US for Serv, number 1512.

[18] X. Zhang, Q. Chen, and J. Wang, (2016):, Optimization of conditions for preparation of poly (vinyl alcohol)-water glass adhesive by response surface methodology, https://doi.org/10.2991/icadme-16.2016.51.

[19] P. Peng, X. Zhou, and J. Ma, (2011):, Water glass compound starch used as surface sizing agent to improve the strength of linerboard, BioResources, vol. 6, number 4, pp. 4158–4167, ISSN:19302126, https://doi.org/10.15376/biores.6.4.4158-4167.

[20] F. A. Kamke and J. N. Lee, (2007):, Adhesive penetration in wood - A review, Wood and Fiber Science, vol. 39, number 2, pp. 205–220, ISSN:07356161.

[21] T. Czvikovszky, P. Nagy, and J. Gaál, (2000):, A polimertechnika alapjai, pp. 1–453, ISBN:963-420-621-2.

[22] O. Ülker, Wood Adhesives and Bonding Theory. (2016):

[23] I. Gavrilović-Grmuša, M. Dunky, M. Djiporović-Momčilović, M. Popović, and J. Popović, (2016):, Influence of pressure on the radial and tangential penetration of adhesive resin into poplar wood and on the shear strength of adhesive joints, BioResources, vol. 11, number 1, pp. 2238–2255, ISSN:19302126, https://doi.org/10.15376/biores.11.1.2238-2255.

[24] M. S. Testület, (2017):, MSZ EN 205:2017: Adhesives. Wood adhesives for non-structural applications. Determination of tensile shear strength of lap joints.

[25] L. Szentes, (2018):, A rövid idejű intenzív csapadékok statisztikai vizsgálata, pp. 56–60.

[26] W. Conshohocken, (2010):, Standard Test Method for Strength Properties of Adhesives in Two-Ply Wood Construction in Shear by Tension Loading 1, Library, vol. 98, number April 2004, pp. 12–14.

Ref.:
Csanády, Dániel – **Fenyvesi**, Olivér : *Shear behaviour of silicate-based structural adhesives for timber*
Építőanyag – Journal of Silicate Based and Composite Materials, Vol. 73, No. 2 (2021), 72–82. p.
https://doi.org/10.14382/epitoanyag-jsbcm.2021.12

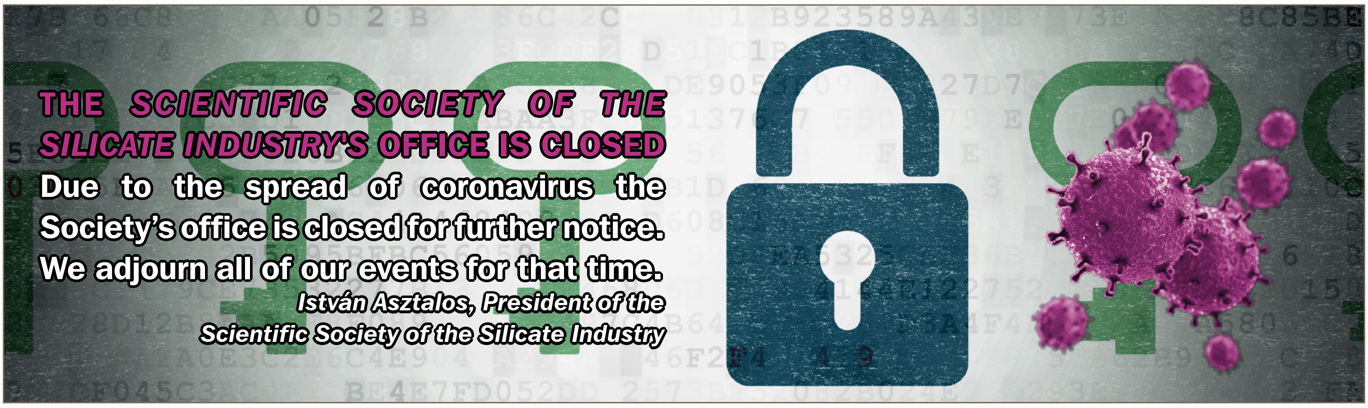

GUIDELINE FOR AUTHORS

The manuscript must contain the followings: title; author's name, workplace, e-mail address; abstract, keywords; main text; acknowledgement (optional)**; references; figures, photos with notes; tables with notes; short biography** (information on the scientific works of the authors).

The full manuscript should not be more than 6 pages including figures, photos and tables. Settings of the word document are: 3 cm margin up and down, 2,5 cm margin left and right. Paper size: A4. Letter size 10 pt, type: Times New Roman. Lines: simple, justified.

TITLE, AUTHOR

The title of the article should be short and objective.

Under the title the name of the author(s), workplace, e-mail address.

If the text originally was a presentation or poster at a conference, it should be marked.

ABSTRACT, KEYWORDS

The abstract is a short summary of the manuscript, about a half page size. The author should give keywords to the text, which are the most important elements of the article.

MAIN TEXT

Contains: materials and experimental procedure (or something similar), results and discussion (or something similar), conclusions.

REFERENCES

References are marked with numbers, e.g. [6], and a bibliography is made by the reference's order. References should be provided together with the DOI if available.

Examples:

Journals:

[6] Mohamed, K. R. – El-Rashidy, Z. M. – Salama, A. A.: In vitro properties of nano-hydroxyapatite/chitosan biocomposites. *Ceramics International.* 37(8), December 2011, pp. 3265–3271, http://doi.org/10.1016/j.ceramint.2011.05.121

Books:

[6] Mehta, P. K. – Monteiro, P. J. M.: Concrete. Microstructure, properties, and materials. *McGraw-Hill*, 2006, 659 p.

FIGURES, TABLES

All drawings, diagrams and photos are figures. The **text should contain references to all figures and tables**. This shows the place of the figure in the text. Please send all the figures in attached files, and not as a part of the text. **All figures and tables should have a title**.

Authors are asked to submit color figures by submission. Black and white figures are suggested to be avoided, however, acceptable.

The figures should be: tiff, jpg or eps files, 300 dpi at least, photos are 600 dpi at least.

BIOGRAPHY

Max. 500 character size professional biography of the author(s).

CHECKING

The editing board checks the articles and informs the authors about suggested modifications. Since the author is responsible for the content of the article, the author is not liable to accept them.

CONTACT

Please send the manuscript in electronic format to the following e-mail address: femgomze@uni-miskolc.hu and epitoanyag@szte.org.hu or by post: Scientific Society of the Silicate Industry, Budapest, Bécsi út 122–124., H-1034, HUNGARY

We kindly ask the authors to give their e-mail address and phone number on behalf of the quick conciliation.

Copyright

Authors must sign the Copyright Transfer Agreement before the paper is published. The Copyright Transfer Agreement enables SZTE to protect the copyrighted material for the authors, but does not relinquish the author's proprietary rights. Authors are responsible for obtaining permission to reproduce any figure for which copyright exists from the copyright holder.

Építőanyag – *Journal of Silicate Based and Composite Materials* allows authors to make copies of their published papers in institutional or open access repositories (where Creative Commons Licence Attribution-NonCommercial, CC BY-NC applies) either with:

- placing a link to the PDF file at **Építőanyag** – *Journal of Silicate Based and Composite Materials* homepage or
- placing the PDF file of the final print.

Építőanyag – *Journal of Silicate Based and Composite Materials*, Quarterly peer-reviewed periodical of the Hungarian Scientific Society of the Silicate Industry, SZTE.
http://epitoanyag.org.hu